

Antecedent Synoptic Environments Conducive to North American Polar/Subtropical Jet Superposition Events

Andrew C. Winters

Department of Atmospheric and Oceanic Sciences

University of Colorado Boulder

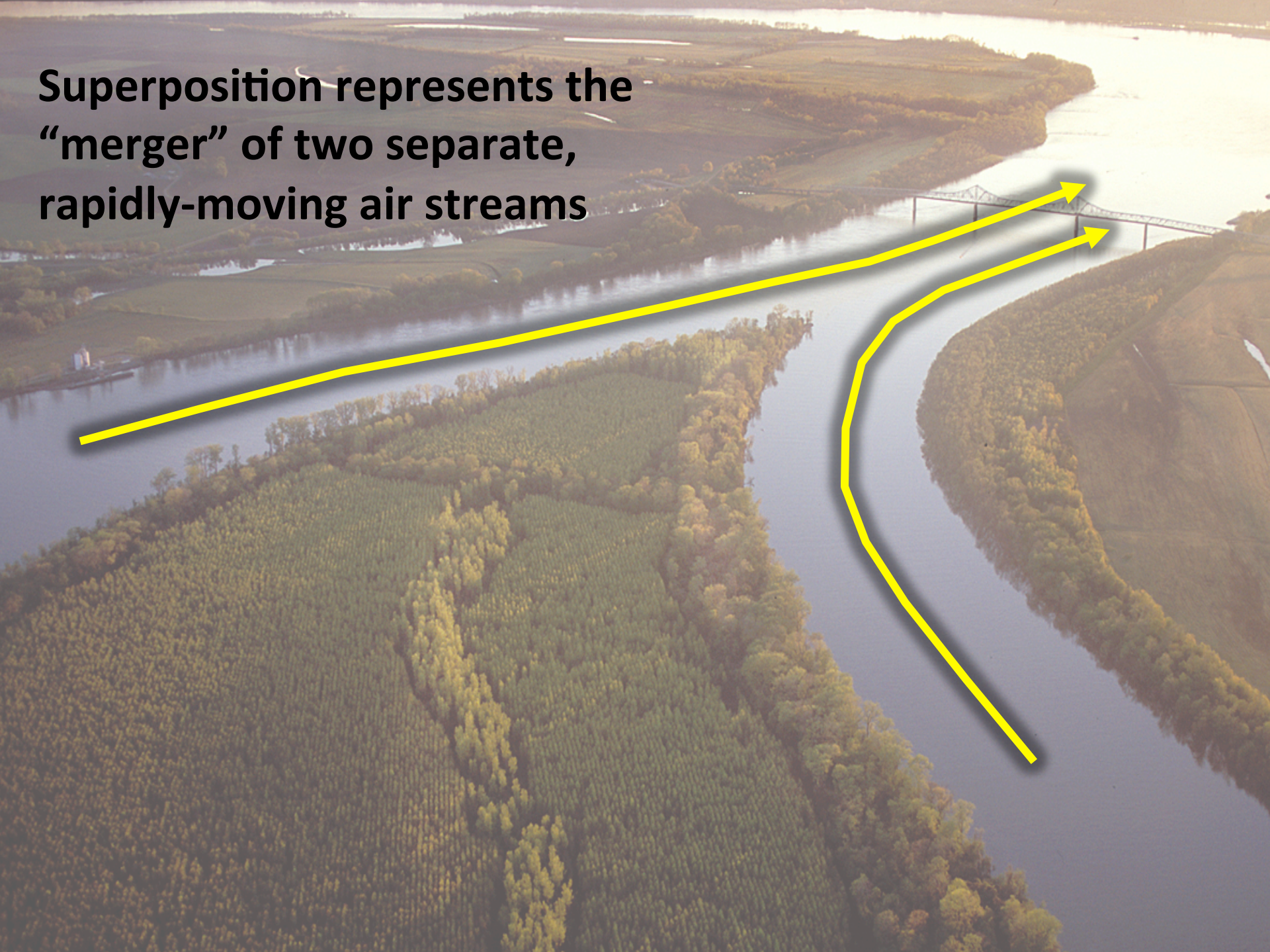
Boulder, CO

4 March 2019

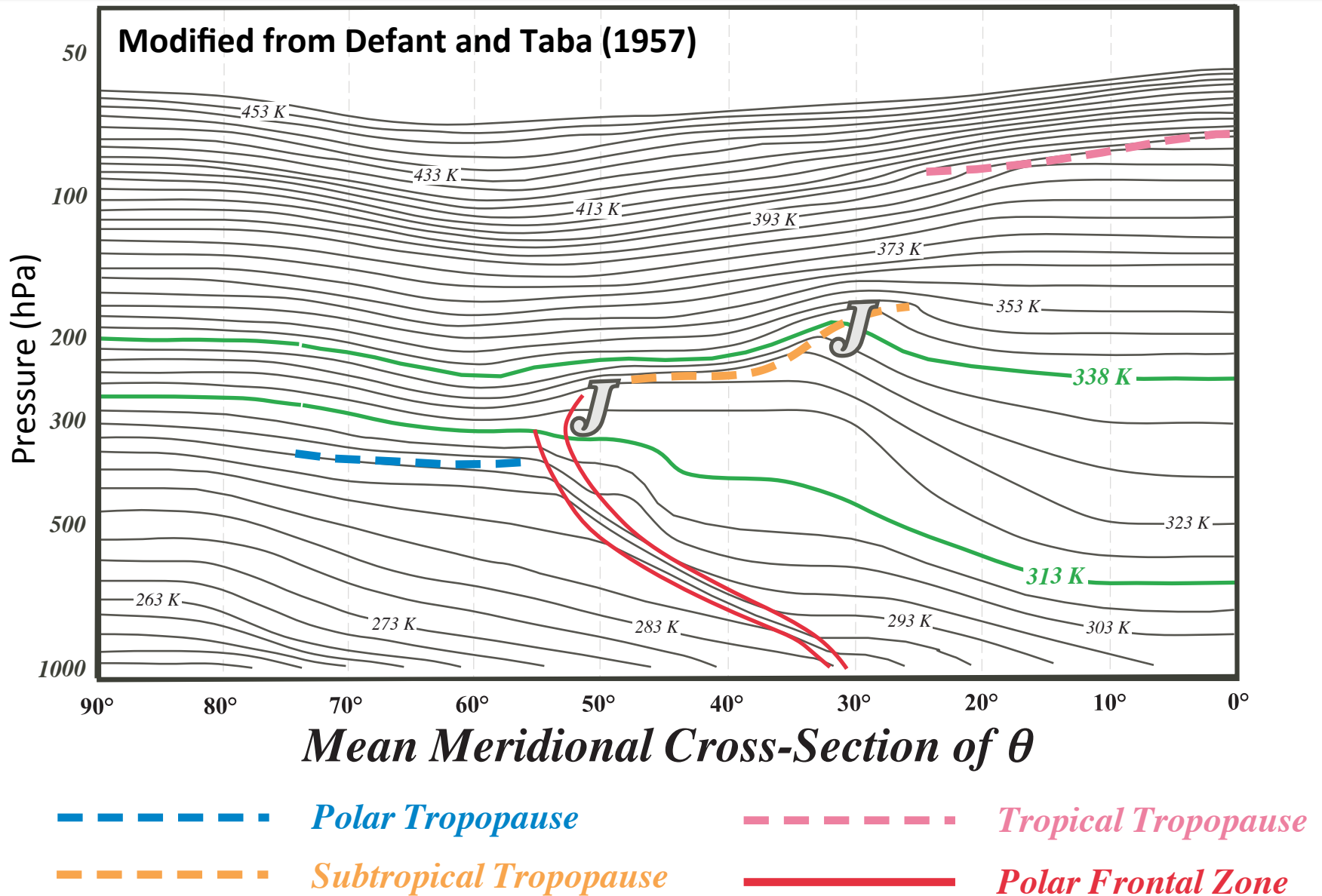


This work is funded by an NSF-PRF (AGS-1624316)

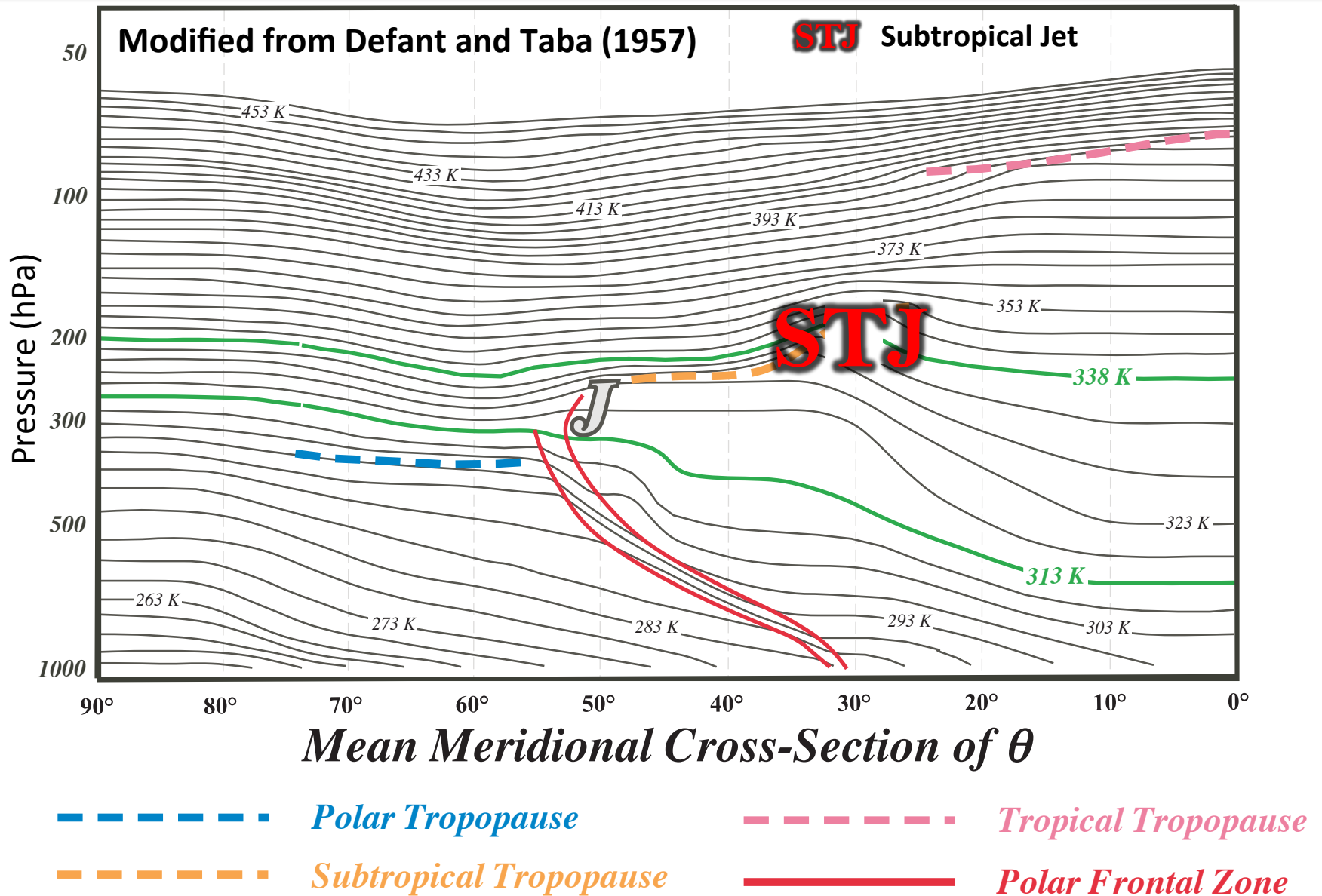
Superposition represents the “merger” of two separate, rapidly-moving air streams



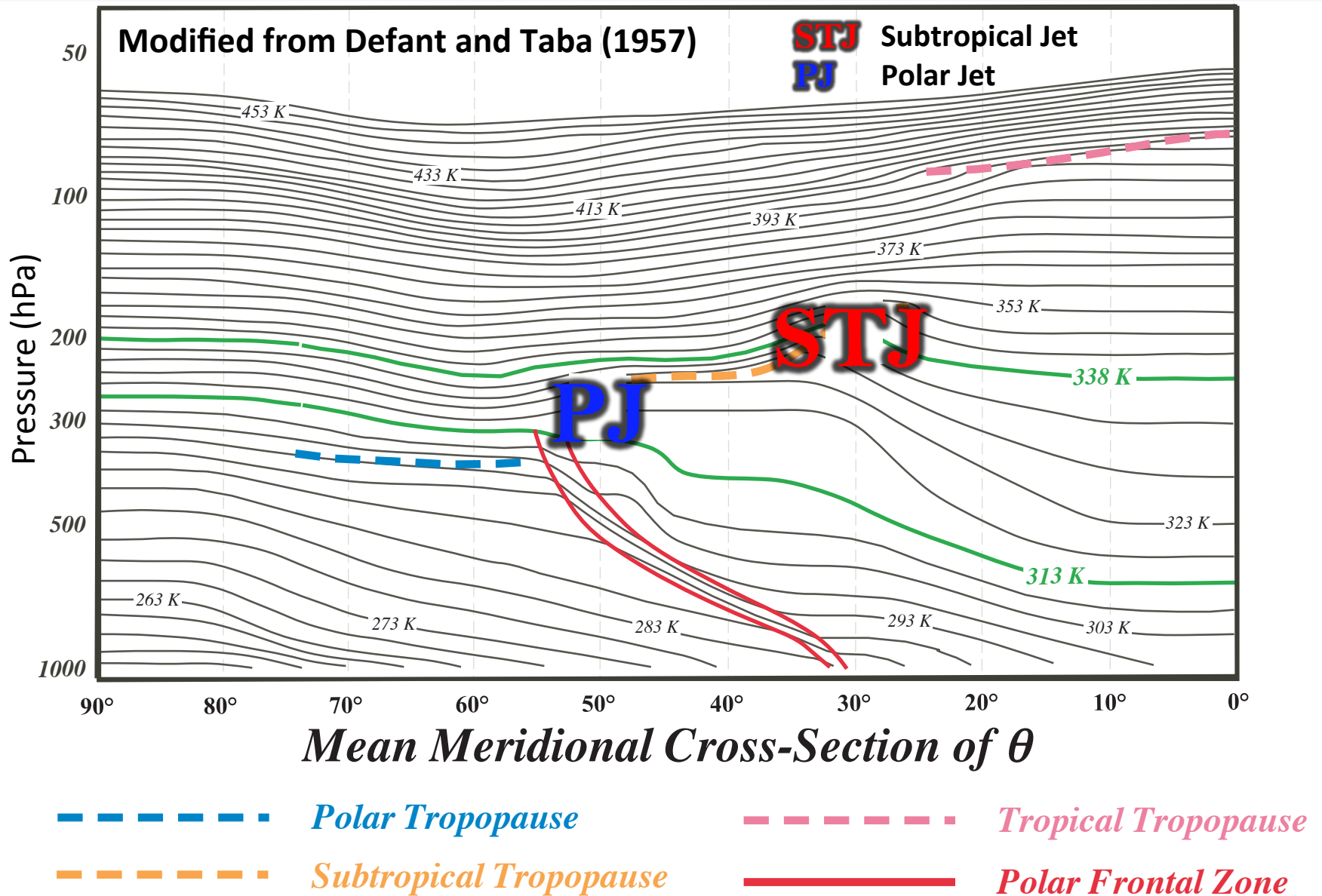
Background



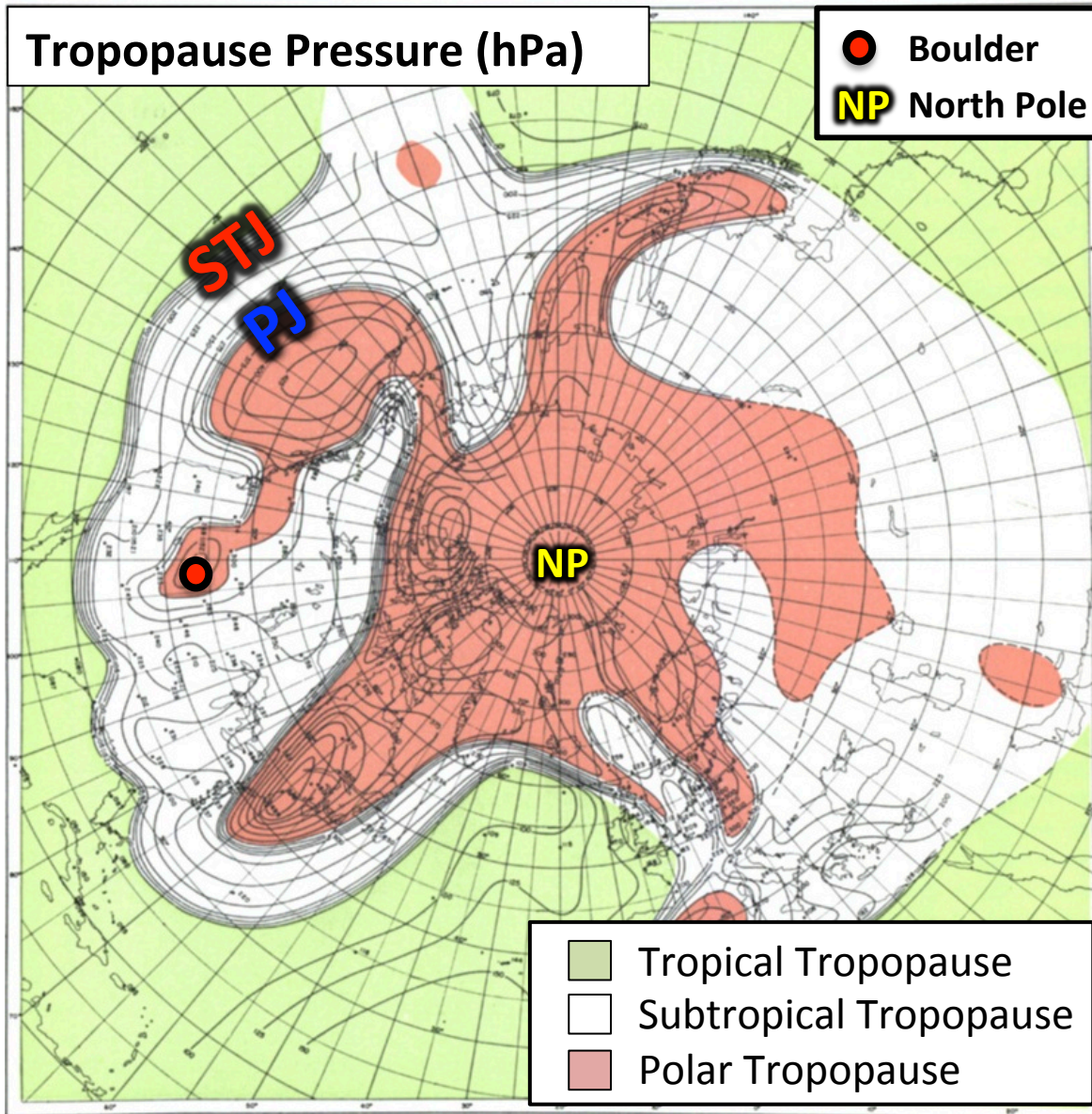
Background



Background



Background

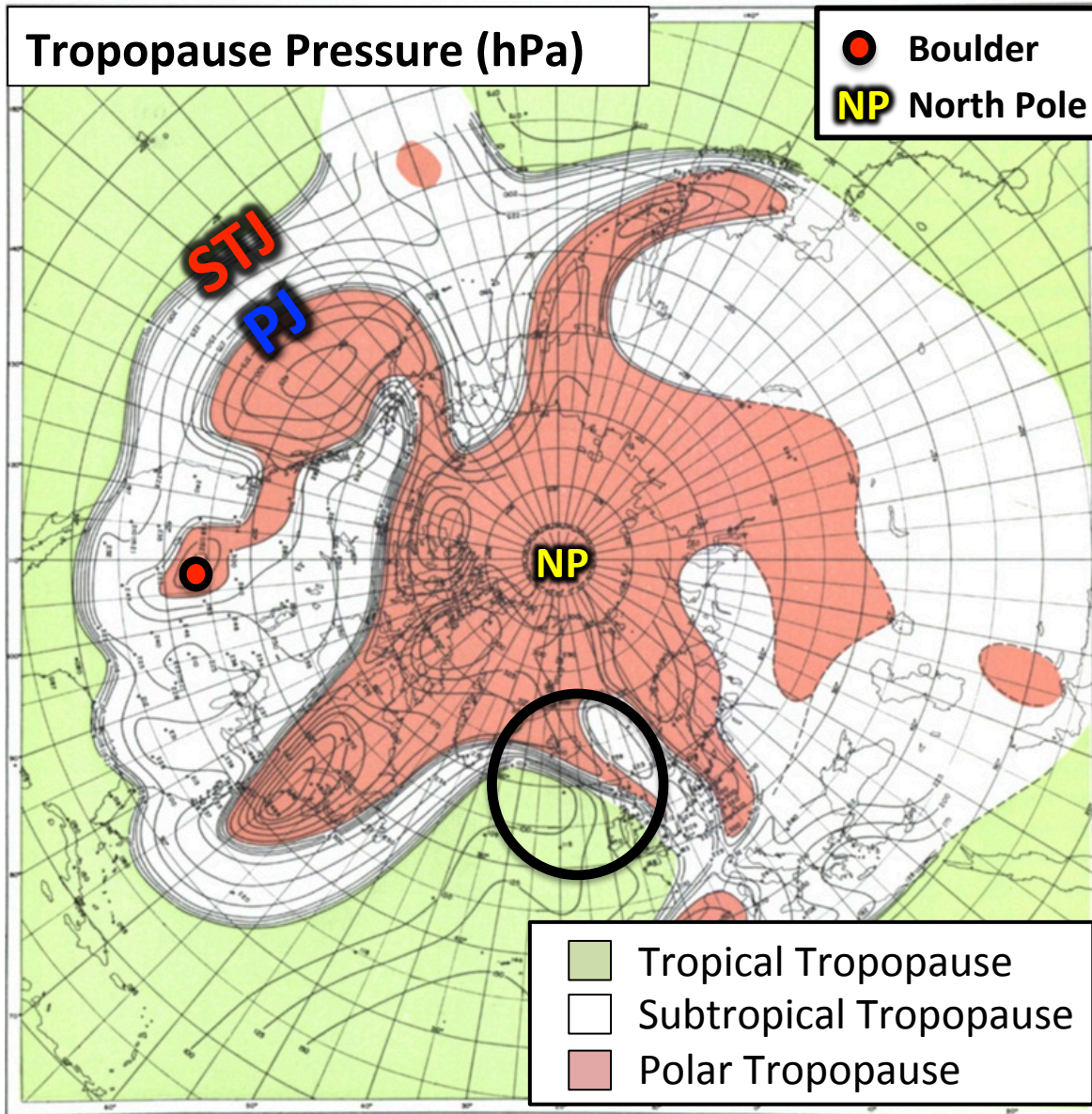


Maps of tropopause pressure help to identify the location of the jets.

While each jet occupies its own climatological latitude band, substantial meanders are common.

**Modified from Defant and Taba
(1957)**

Background



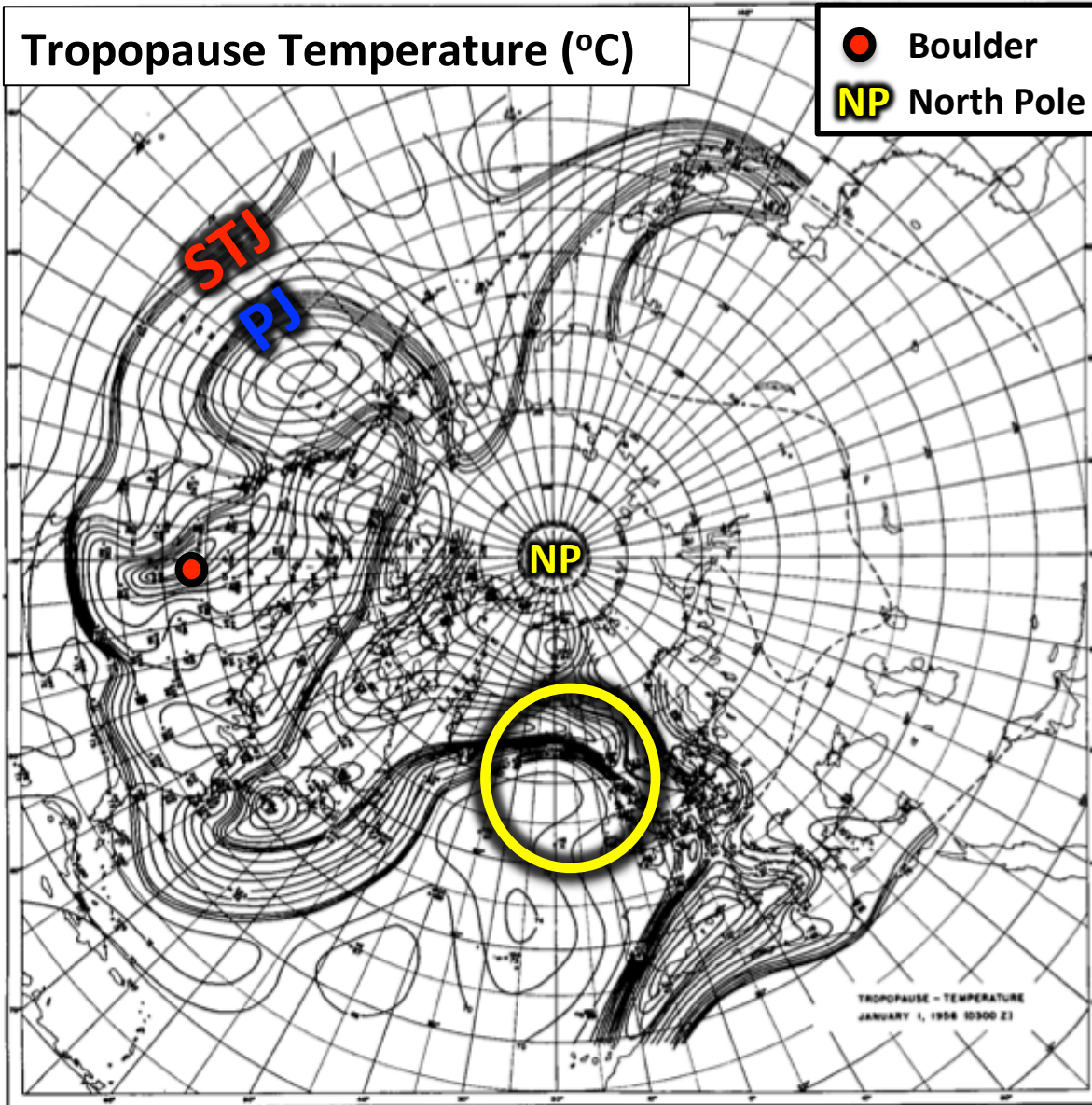
Maps of tropopause pressure help to identify the location of the jets.

While each jet occupies its own climatological latitude band, substantial meanders are common.

Occasionally, the latitudinal separation between the jets can vanish resulting in a **vertical jet superposition**.

Modified from Defant and Taba (1957)

Background



The pole-to-equator baroclinicity is combined into a much narrower zone of contrast in the vicinity of a jet superposition.

Intensified frontal structure is often attended by a strengthening of the superposed jet's transverse circulation.

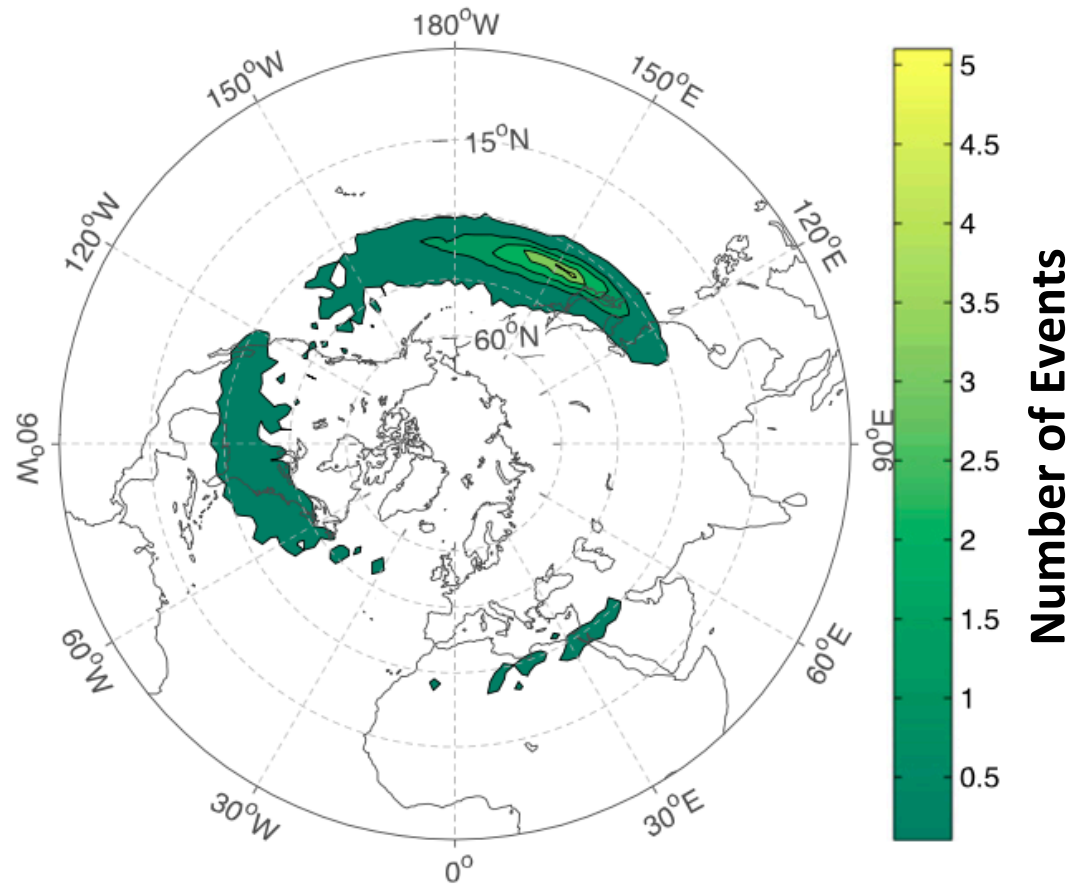
Modified from Defant and Taba
(1957)

Background

Christenson et al. (2017) highlight three locations that experience the greatest frequency of jet superpositions:

- 1) Western Pacific
- 2) North America
- 3) Northern Africa

Climatological frequency of Northern Hemisphere jet superposition events per cold season (Nov–Mar) 1960–2010



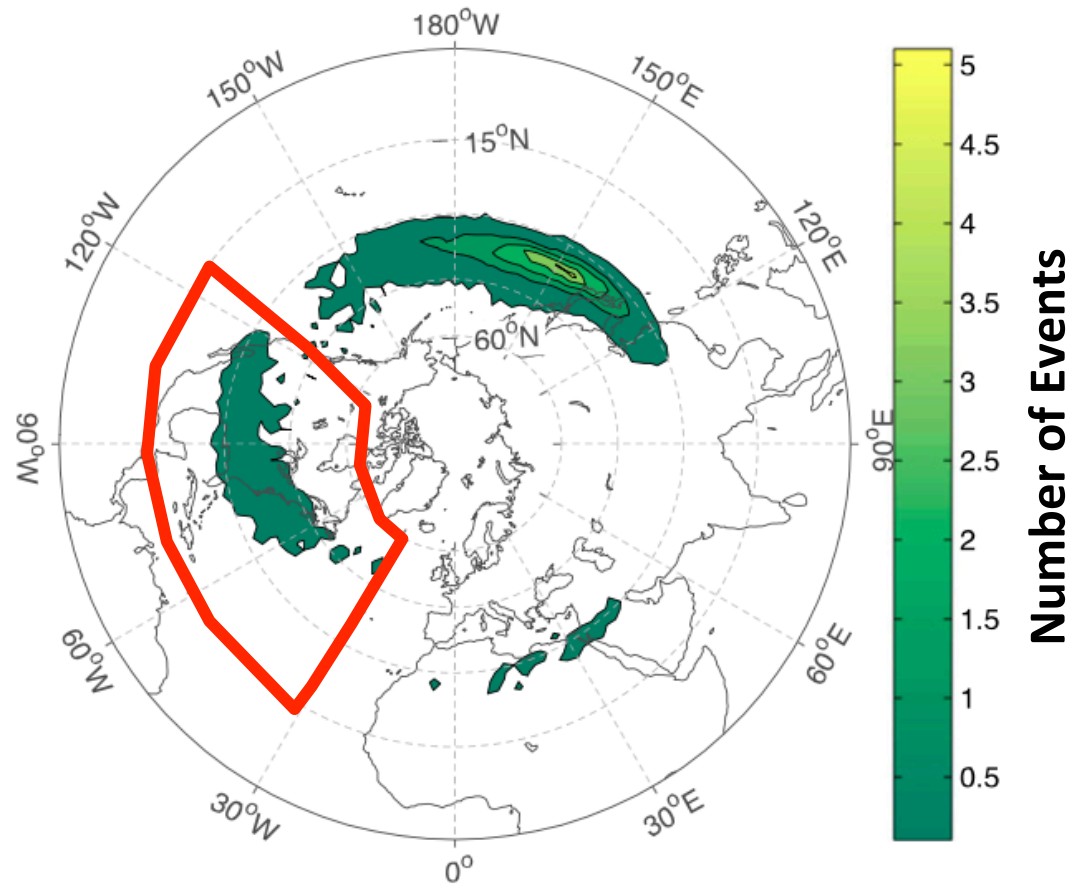
Christenson et al. (2017)

Background

Christenson et al. (2017) highlight three locations that experience the greatest frequency of jet superpositions:

- 1) Western Pacific
- 2) North America
- 3) Northern Africa

Climatological frequency of Northern Hemisphere jet superposition events per cold season (Nov–Mar) 1960–2010



Christenson et al. (2017)

Jet Superpositions and High-Impact Weather

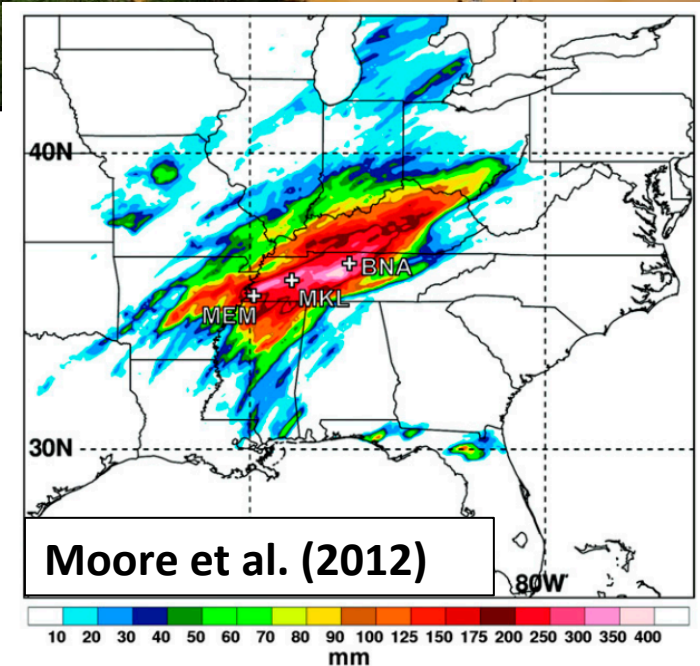
The Tennessean



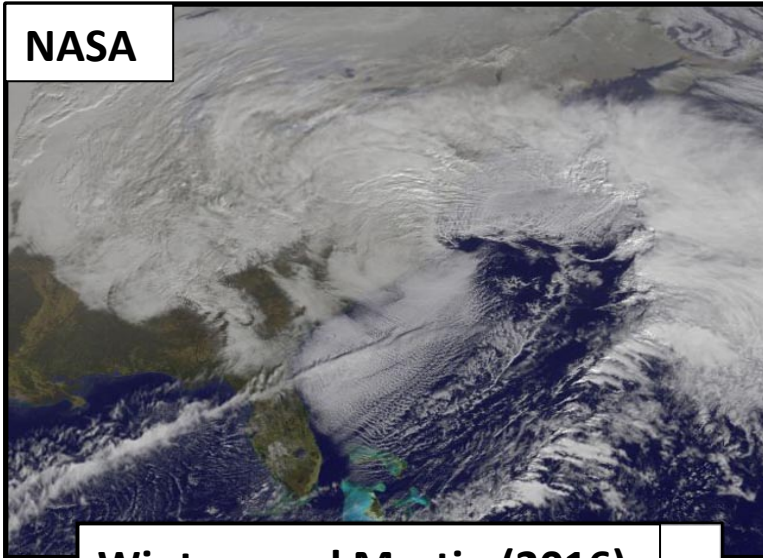
Jet superpositions can be an element of high-impact weather events

1–3 May 2010 Nashville Flood

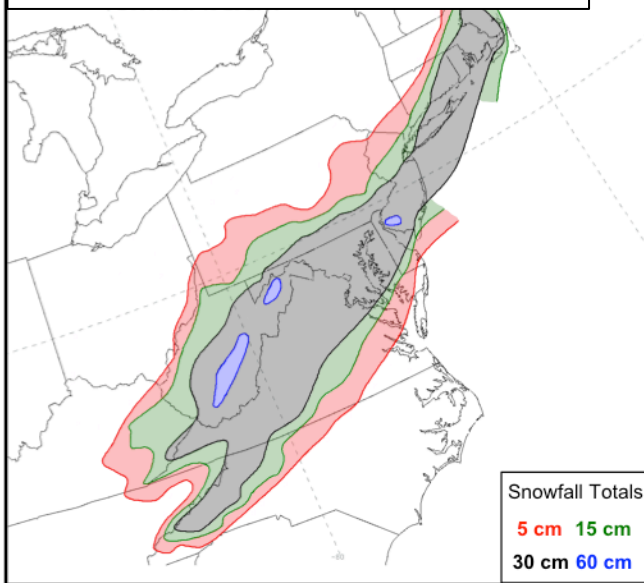
- Jet superposition enhanced the poleward moisture transport via its ageostrophic circulation (Winters and Martin 2014; 2016).



Jet Superpositions and High-Impact Weather



Winters and Martin (2016)



Jet superpositions can be an element of high-impact weather events

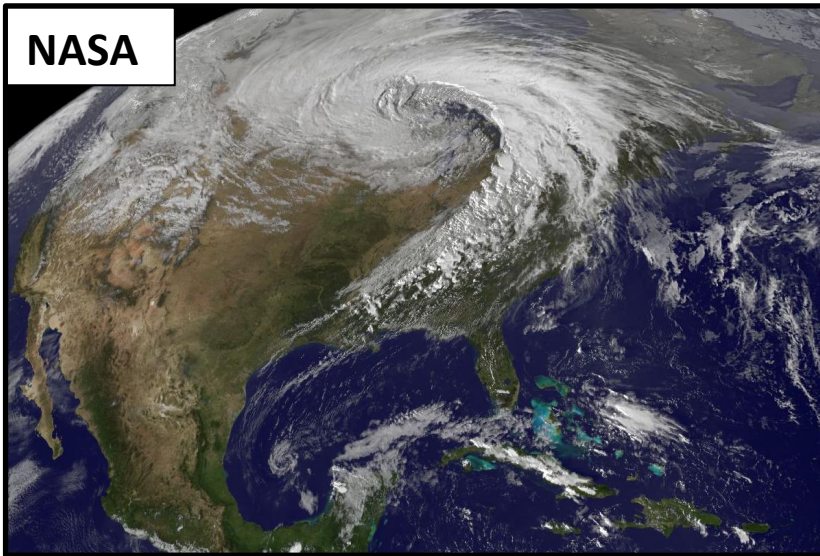
1–3 May 2010 Nashville Flood

- Jet superposition enhanced the poleward moisture transport via its ageostrophic circulation (Winters and Martin 2014; 2016).

18–20 December 2009 Mid-Atlantic Blizzard

- Jet superposition was associated with a rapidly deepening East Coast cyclone (Winters and Martin 2016; 2017).

Jet Superpositions and High-Impact Weather



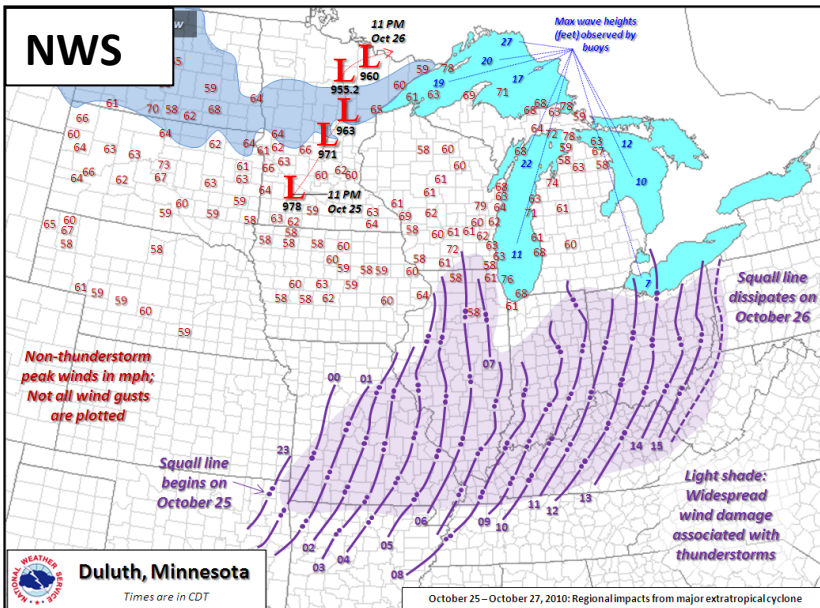
Jet superpositions can be an element of high-impact weather events

1–3 May 2010 Nashville Flood

- Jet superposition enhanced the poleward moisture transport via its ageostrophic circulation (Winters and Martin 2014; 2016).

18–20 December 2009 Mid-Atlantic Blizzard

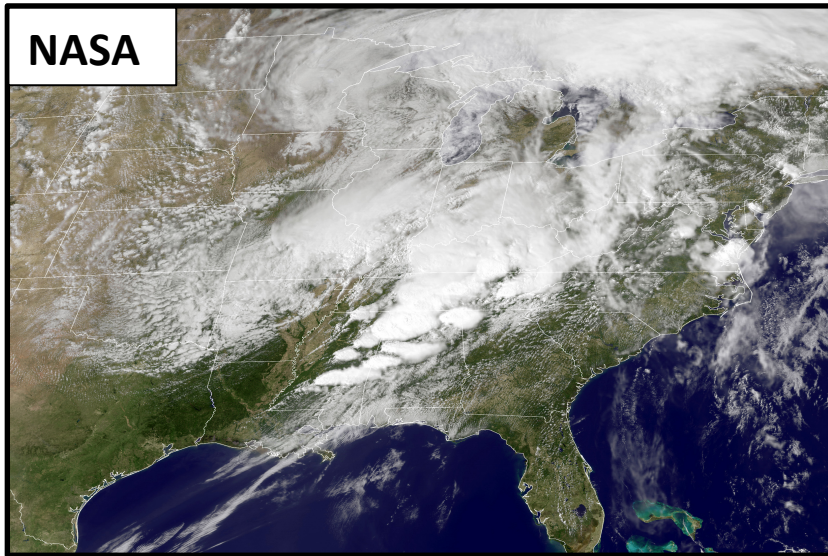
- Jet superposition was associated with a rapidly deepening East Coast cyclone (Winters and Martin 2016; 2017).



26 October 2010: Explosive Cyclogenesis Event

- Jet superposition over the West Pacific preceded the development of an intense Midwest U.S. cyclone.

Jet Superpositions and High-Impact Weather



Jet superpositions can be an element of high-impact weather events

1–3 May 2010 Nashville Flood

- Jet superposition enhanced the poleward moisture transport via its ageostrophic circulation (Winters and Martin 2014; 2016).

18–20 December 2009 Mid-Atlantic Blizzard

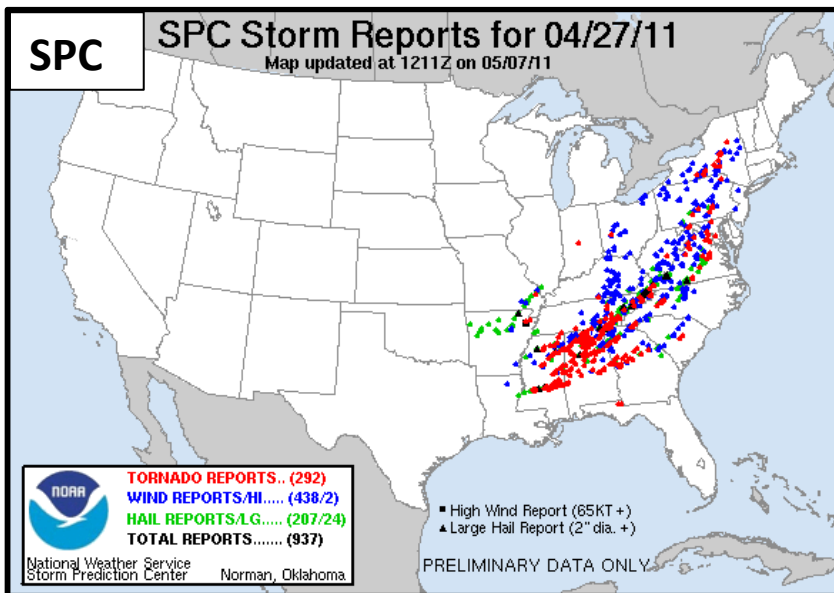
- Jet superposition was associated with a rapidly deepening East Coast cyclone (Winters and Martin 2016; 2017).

26 October 2010: Explosive Cyclogenesis Event

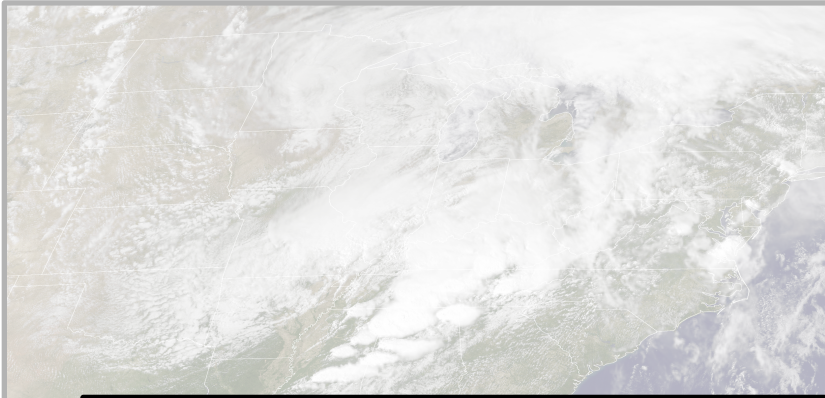
- Jet superposition over the West Pacific preceded the development of an intense Midwest U.S. cyclone.

25–28 April 2011 Tornado Outbreak

- Jet superposition occurred over the West Pacific prior to the outbreak (Knupp et al. 2014; Christenson and Martin 2012).



Jet Superpositions and High-Impact Weather

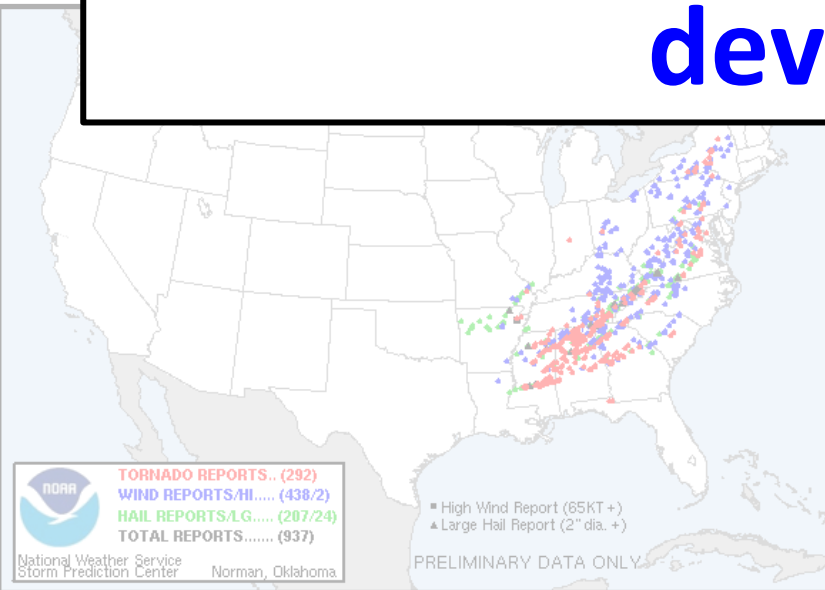


Jet superpositions can be an element of high-impact weather events

1–3 May 2010 Nashville Flood

- Jet superposition enhanced the poleward moisture transport via its ageostrophic circulation (Winters and Martin 2014; 2016).

How do these structures develop?



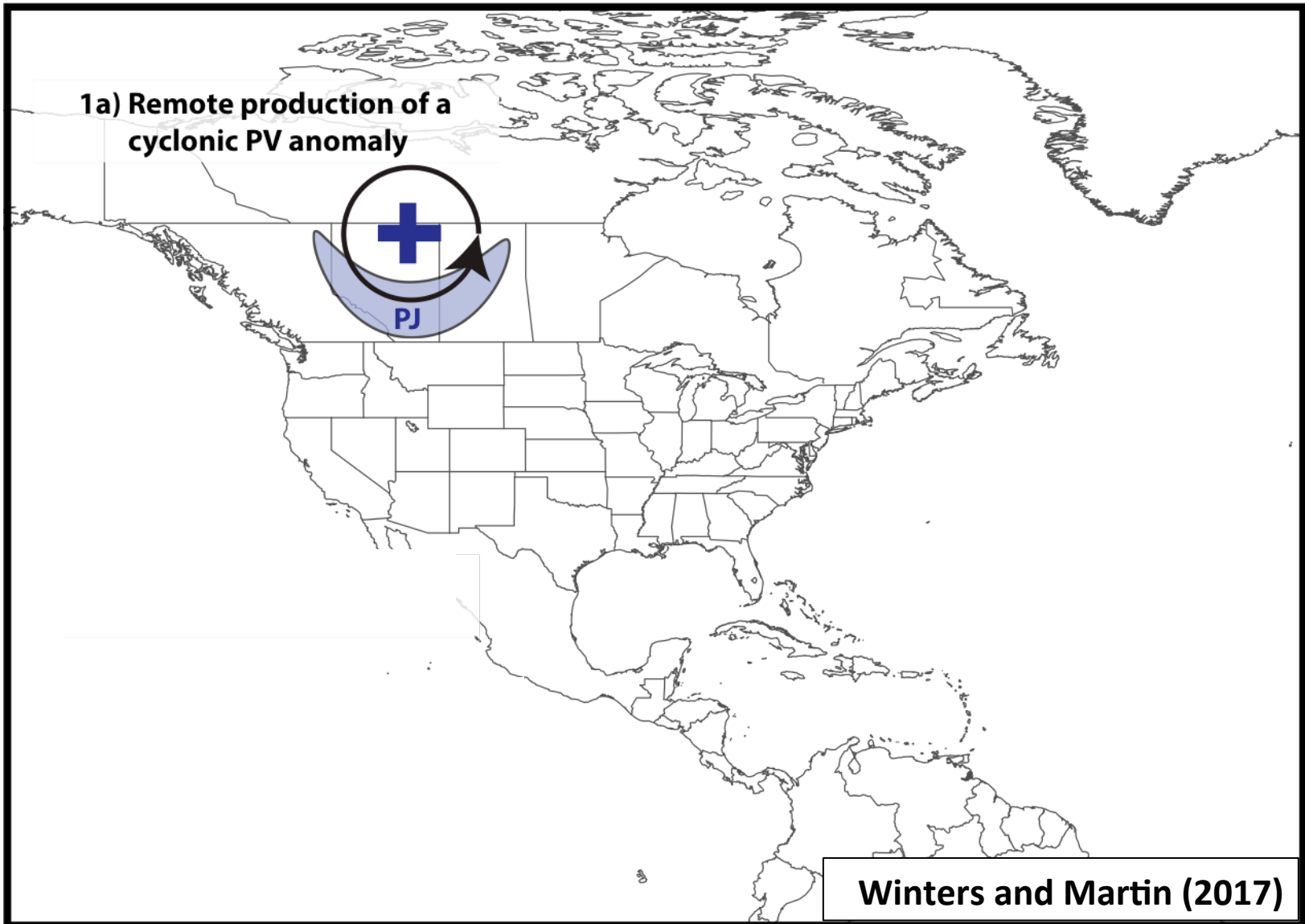
20 October 2010: Explosive Cyclogenesis Event

- Jet superposition over the West Pacific preceded the development of an intense Midwest U.S. cyclone.

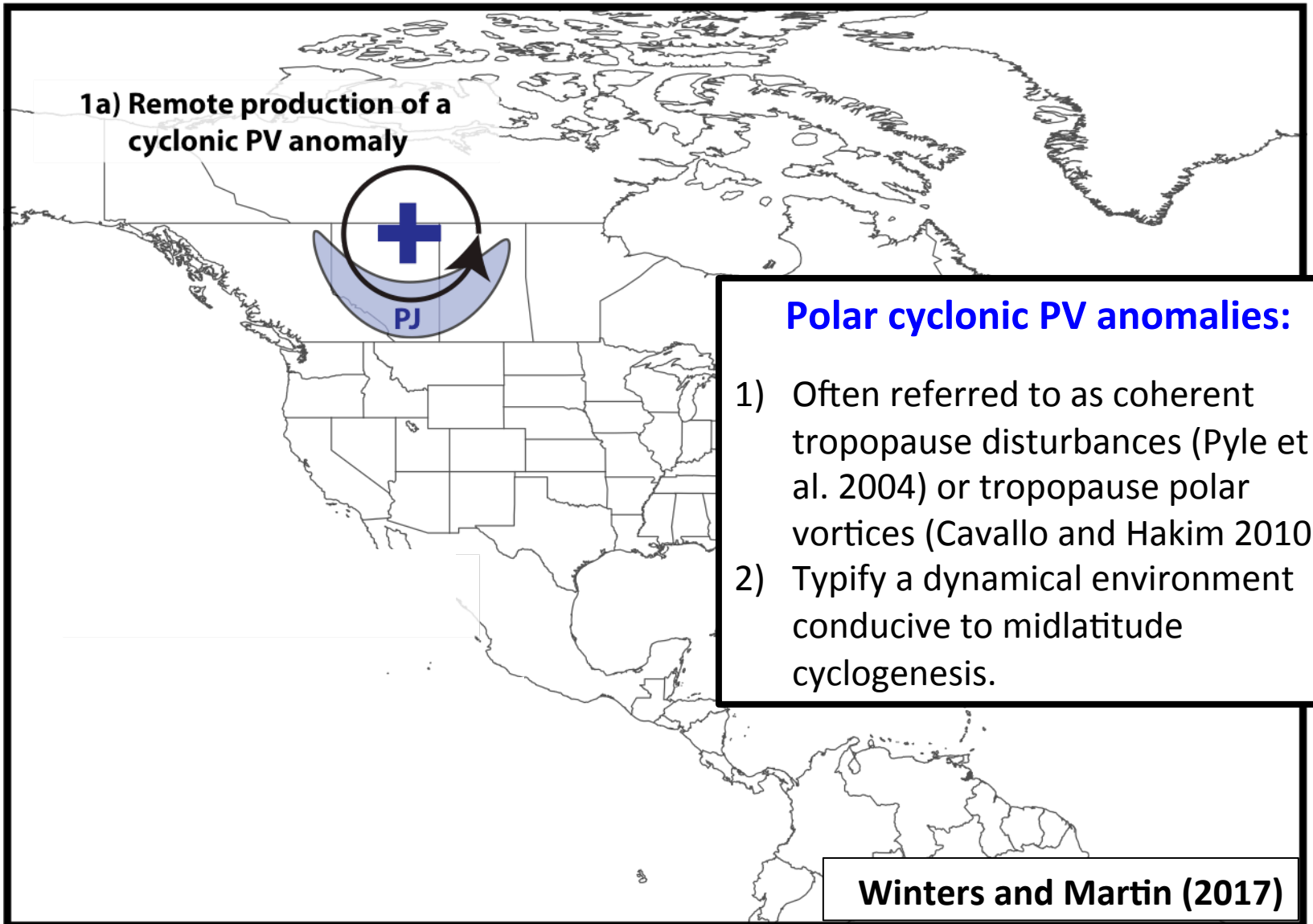
25–28 April 2011 Tornado Outbreak

- Jet superposition occurred over the West Pacific prior to the outbreak (Knupp et al. 2014; Christenson and Martin 2012).

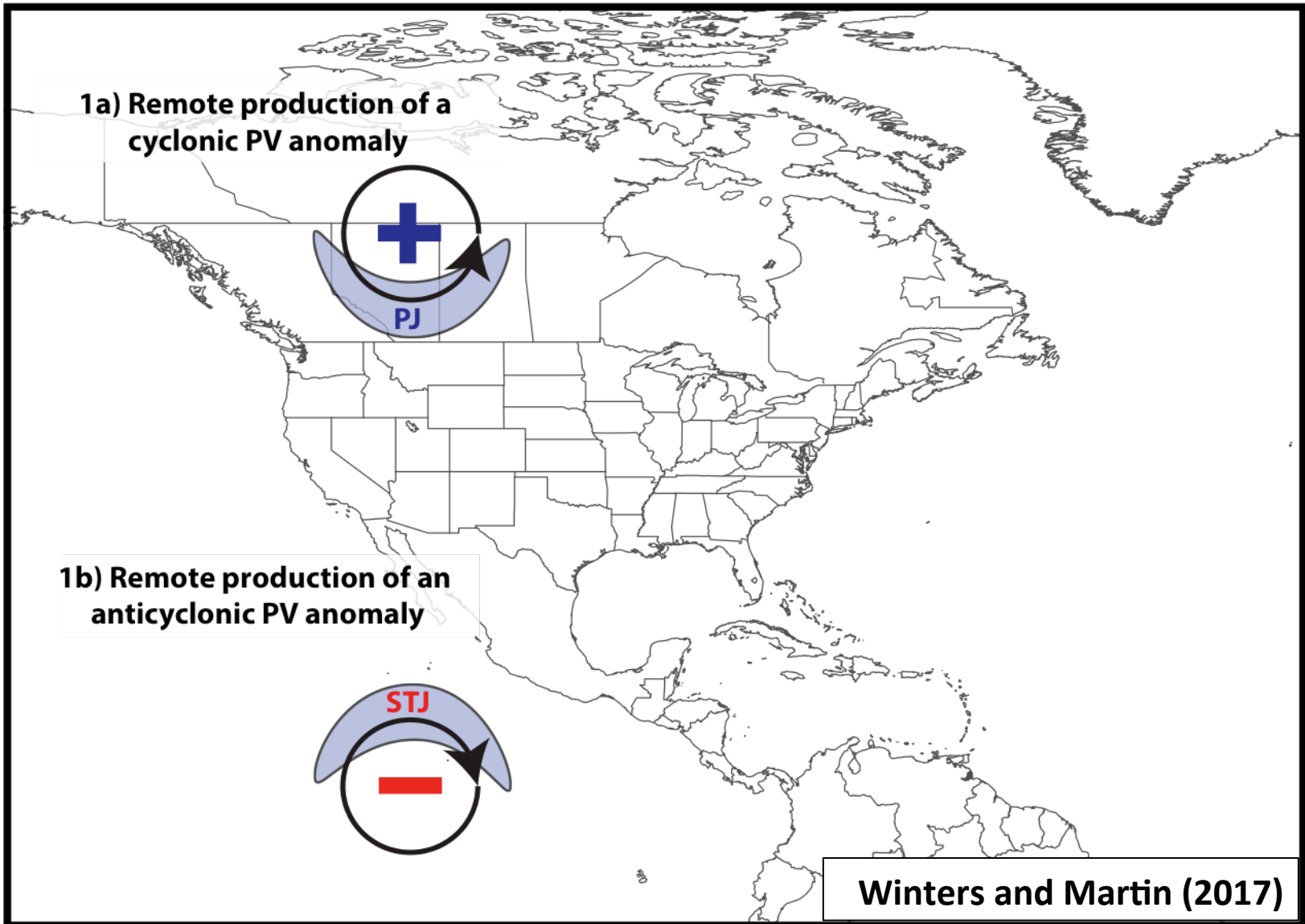
Jet Superposition Conceptual Model



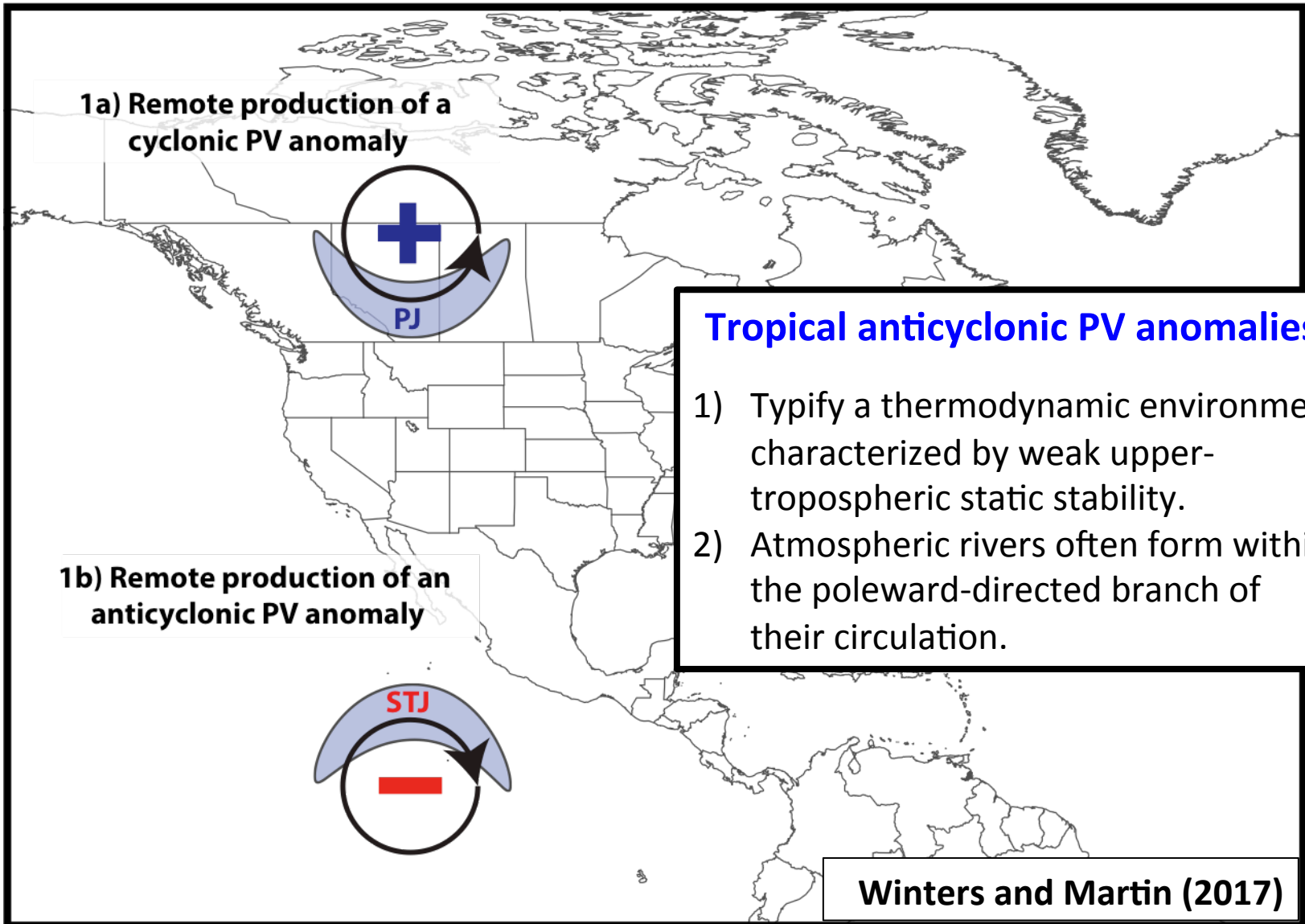
Jet Superposition Conceptual Model



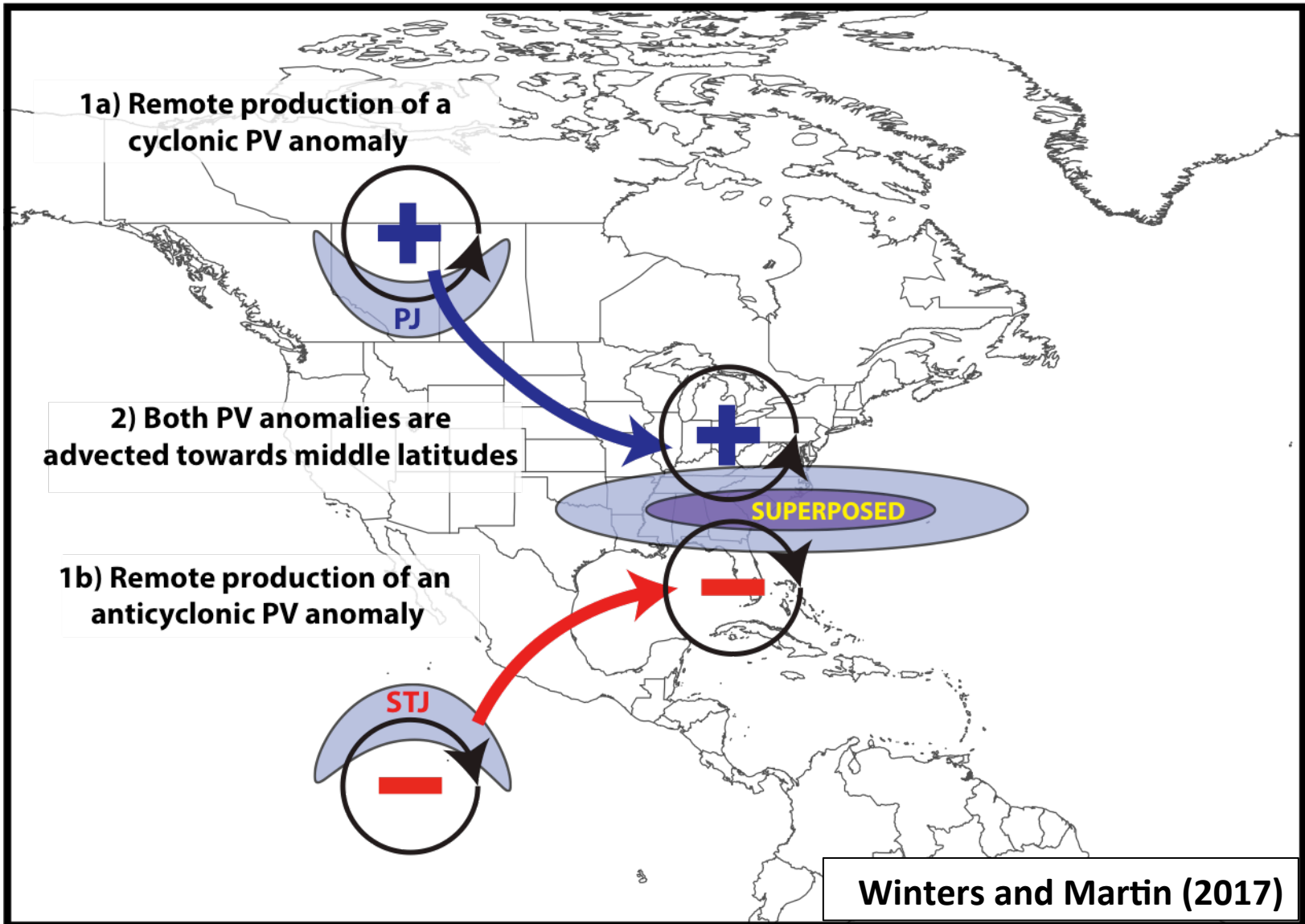
Jet Superposition Conceptual Model



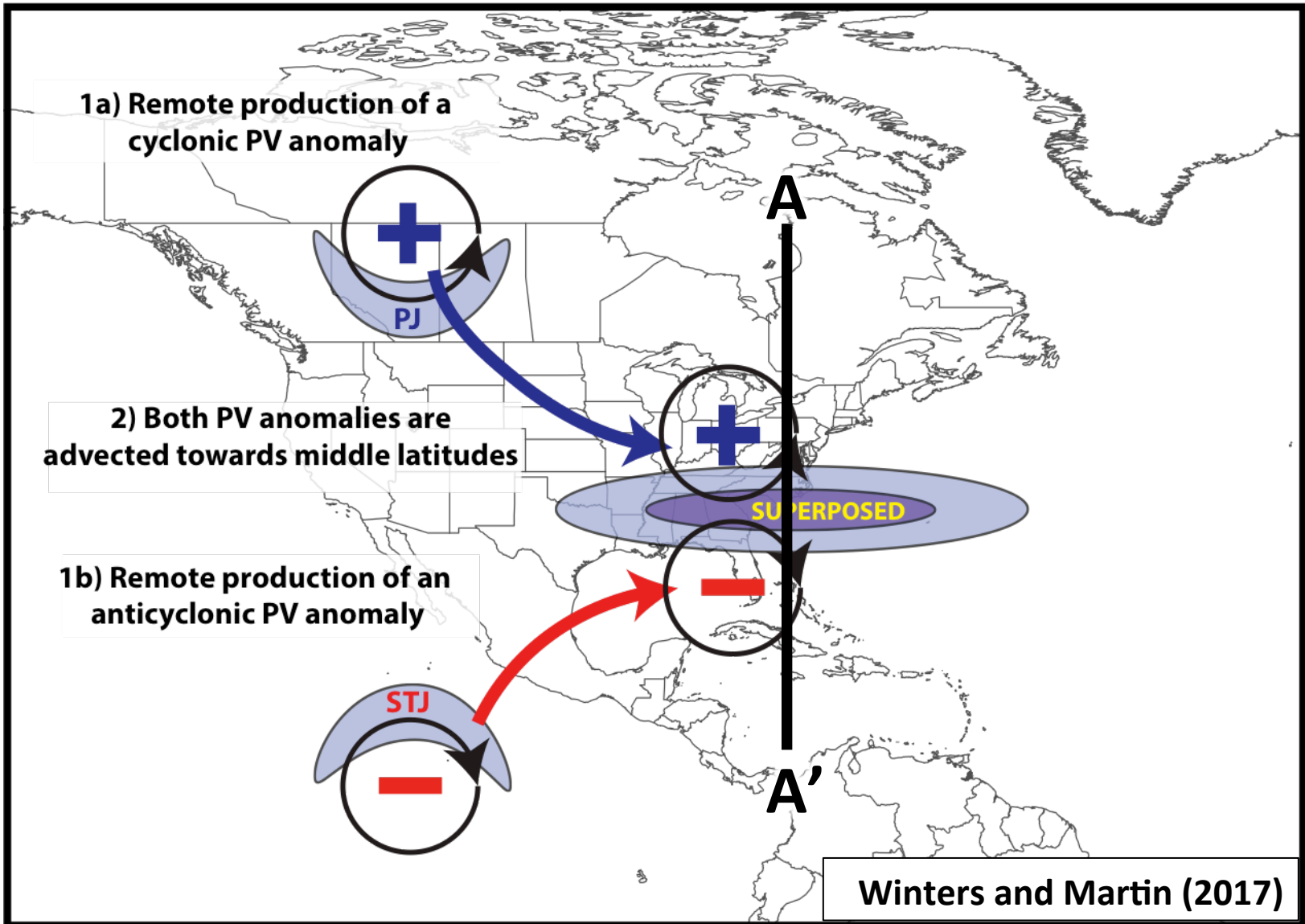
Jet Superposition Conceptual Model



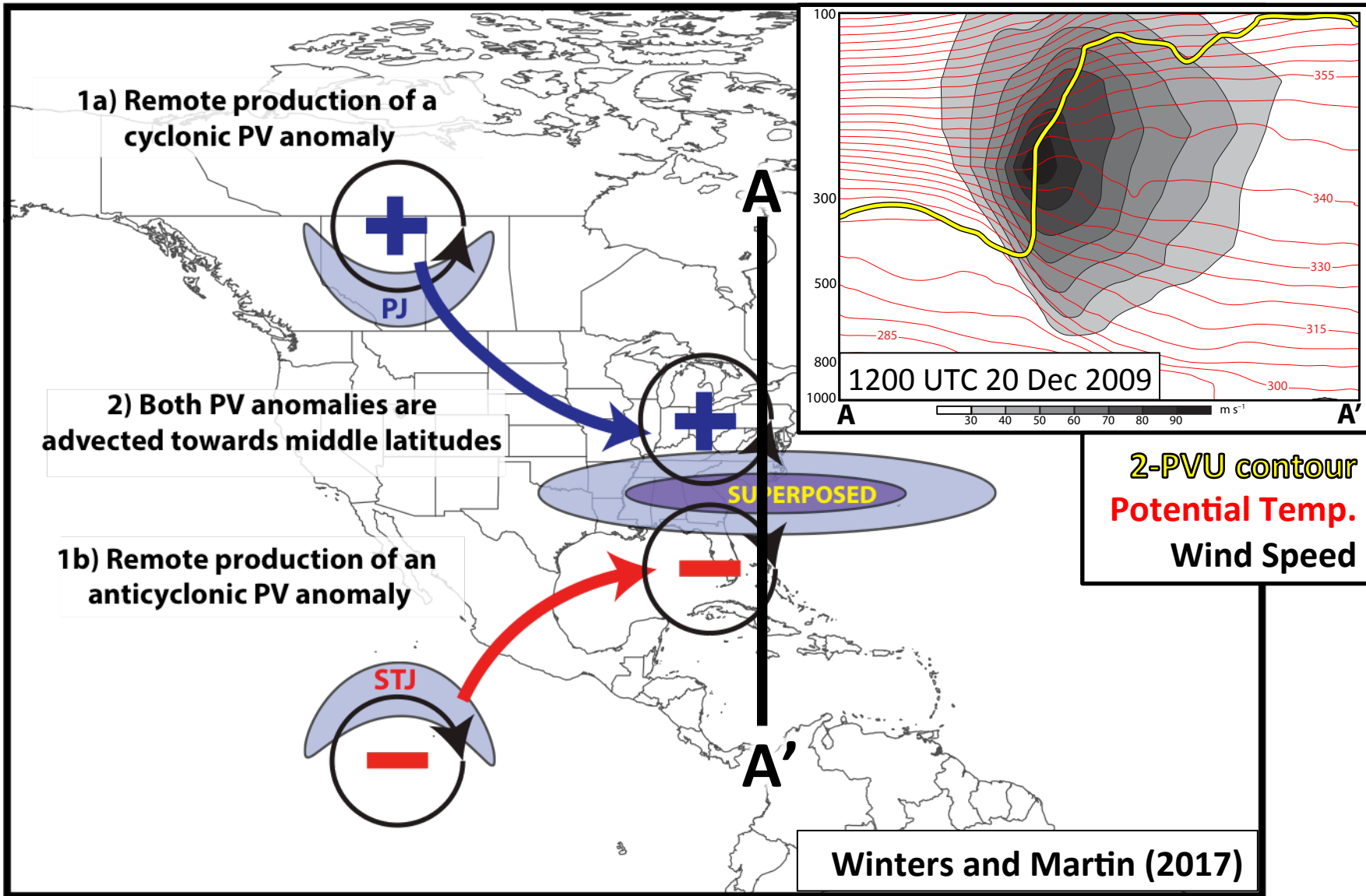
Jet Superposition Conceptual Model



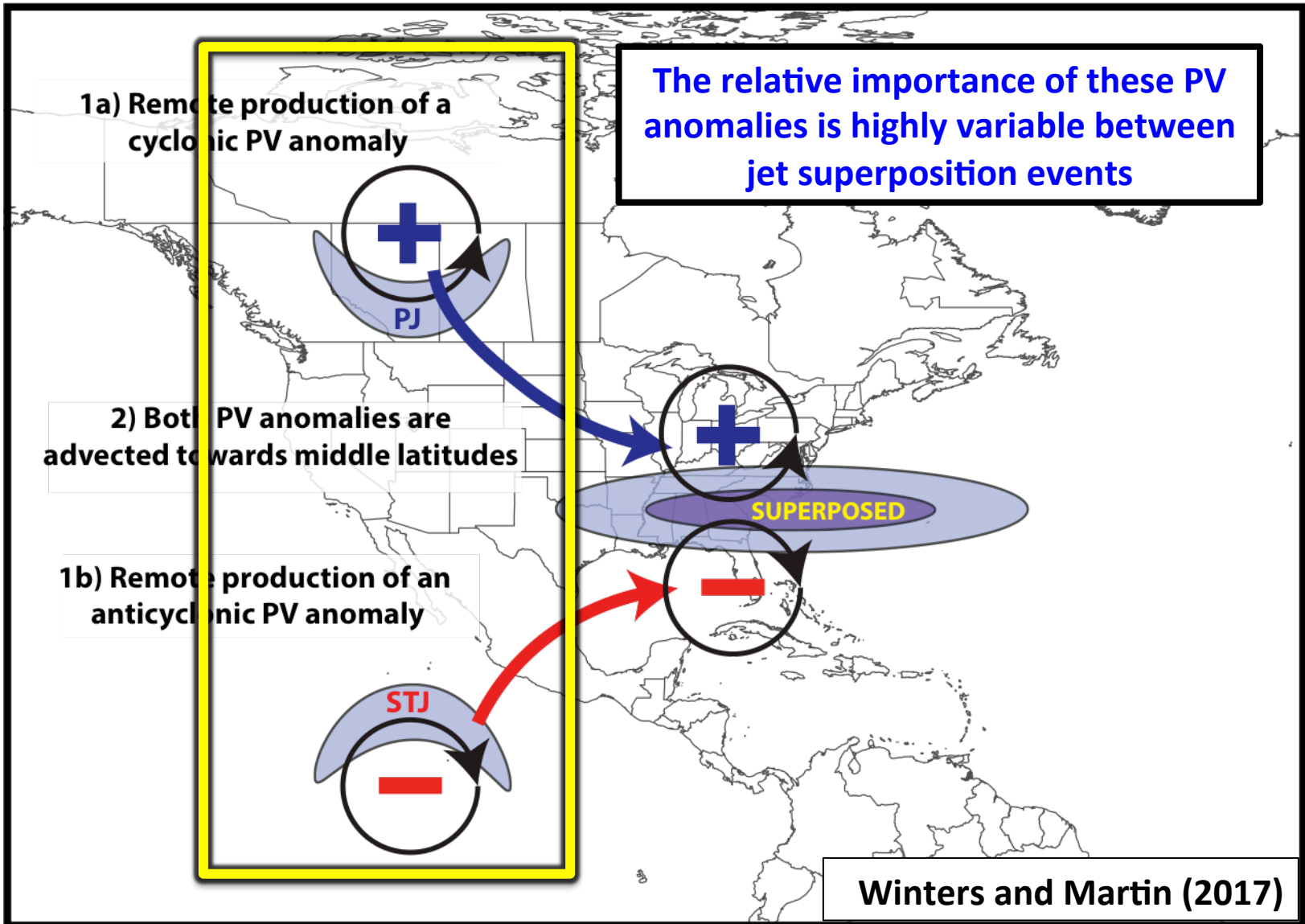
Jet Superposition Conceptual Model



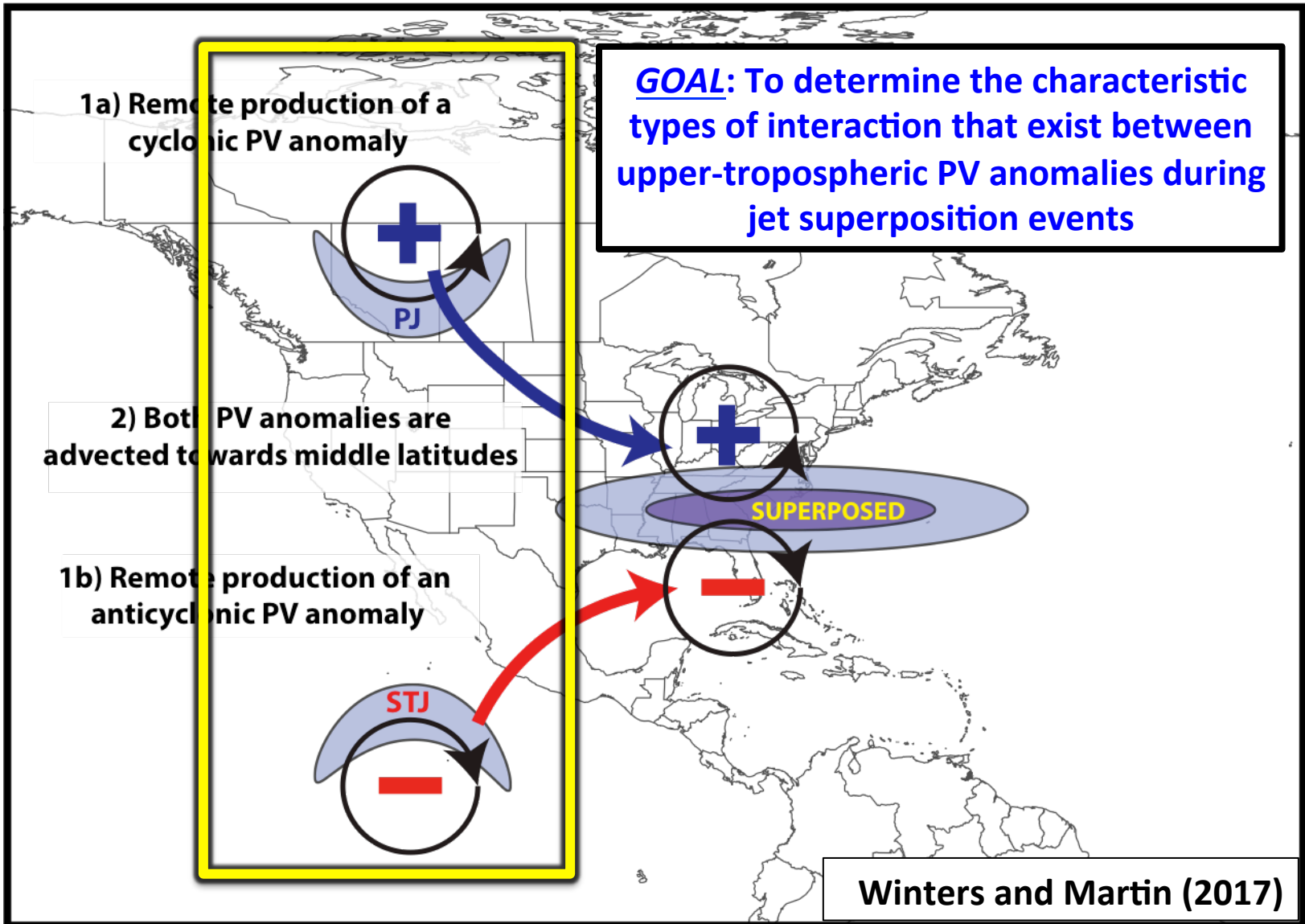
Jet Superposition Conceptual Model



Jet Superposition Conceptual Model



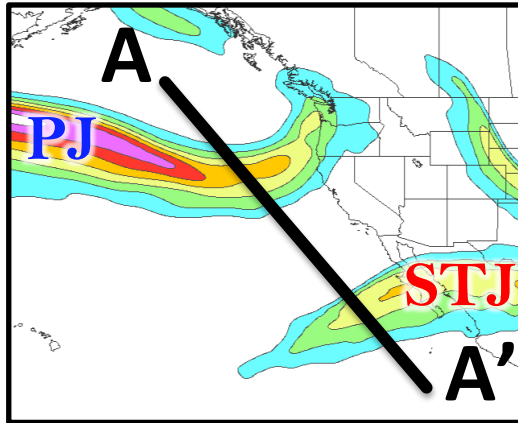
Jet Superposition Conceptual Model



Jet Superposition Event Identification and Classification

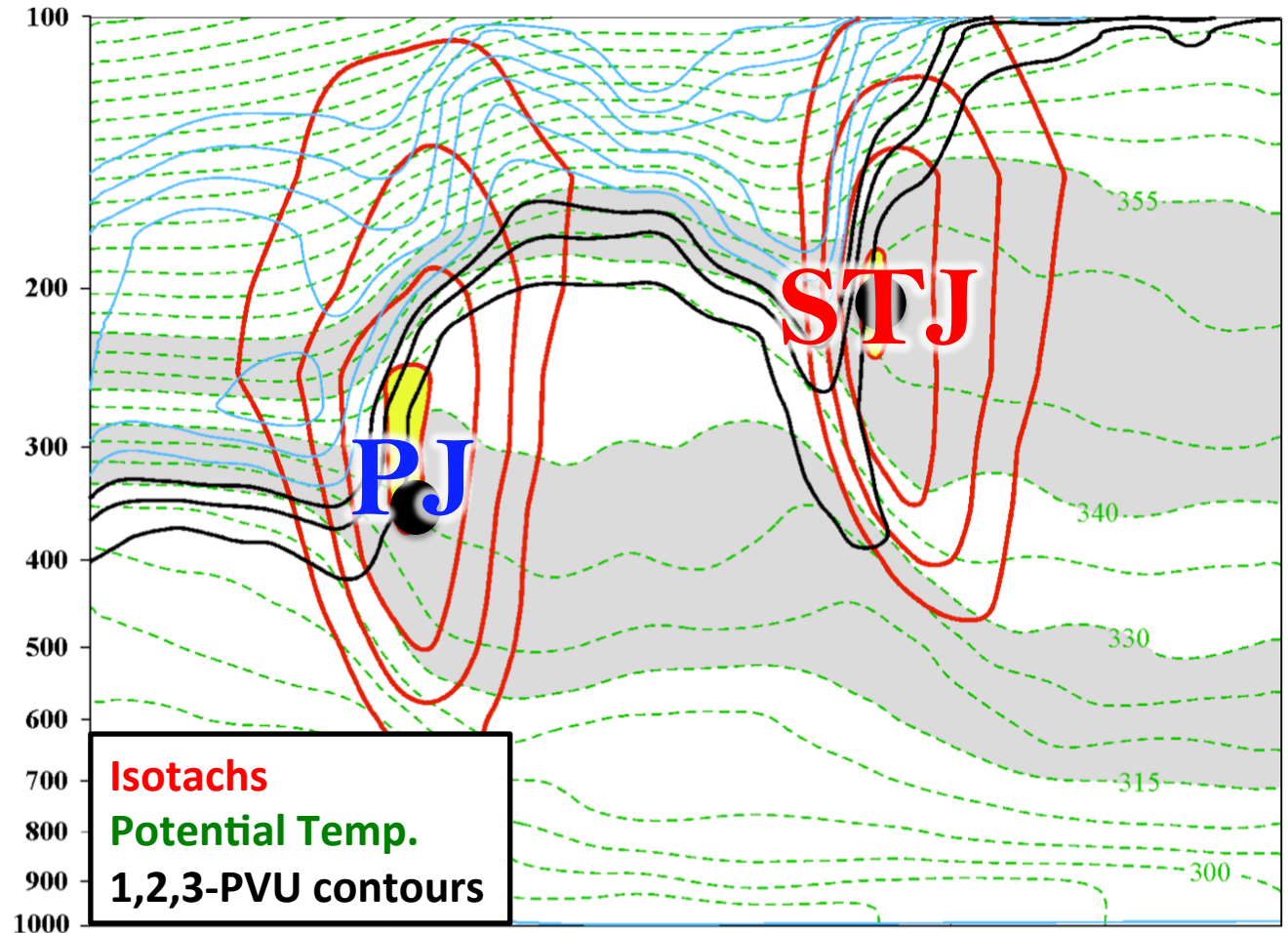
Jet Superposition Event Identification

0000 UTC 27 April 2010



250-hPa wind speed

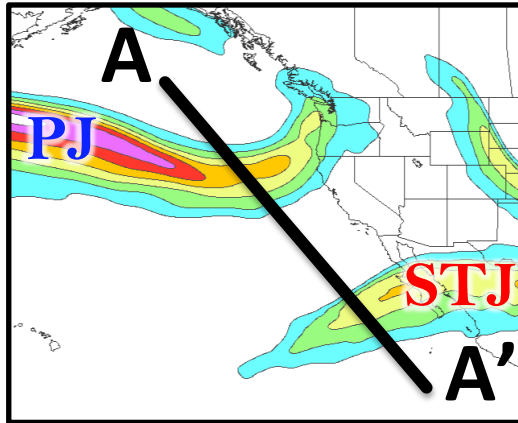
Isolated grid points over North America in the CFSR (Saha et al. 2014) characterized by polar and subtropical jets during Nov–Mar 1979–2010.



A Winters and Martin (2014, 2016, 2017); Christenson et al. (2017); Handlos and Martin (2016) **A'**

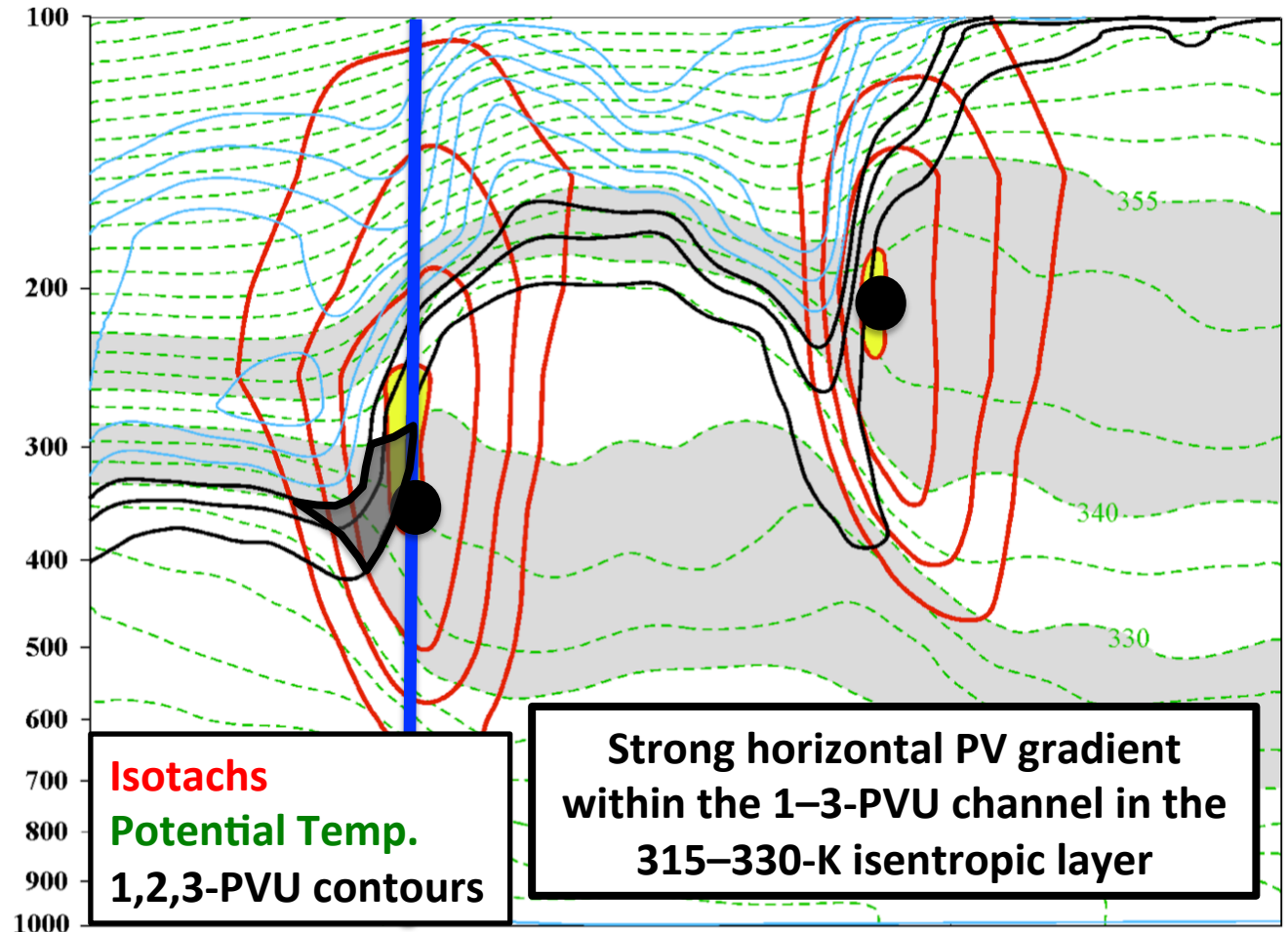
Jet Superposition Event Identification

0000 UTC 27 April 2010



250-hPa wind speed

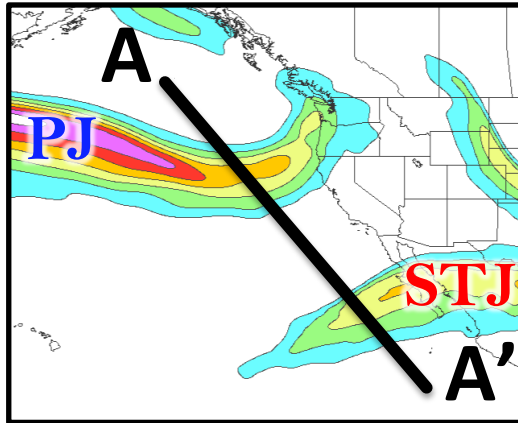
Isolated grid points over North America in the CFSR (Saha et al. 2014) characterized by polar and subtropical jets during Nov–Mar 1979–2010.



A Winters and Martin (2014, 2016, 2017); Christenson et al. (2017); Handlos and Martin (2016) **A'**

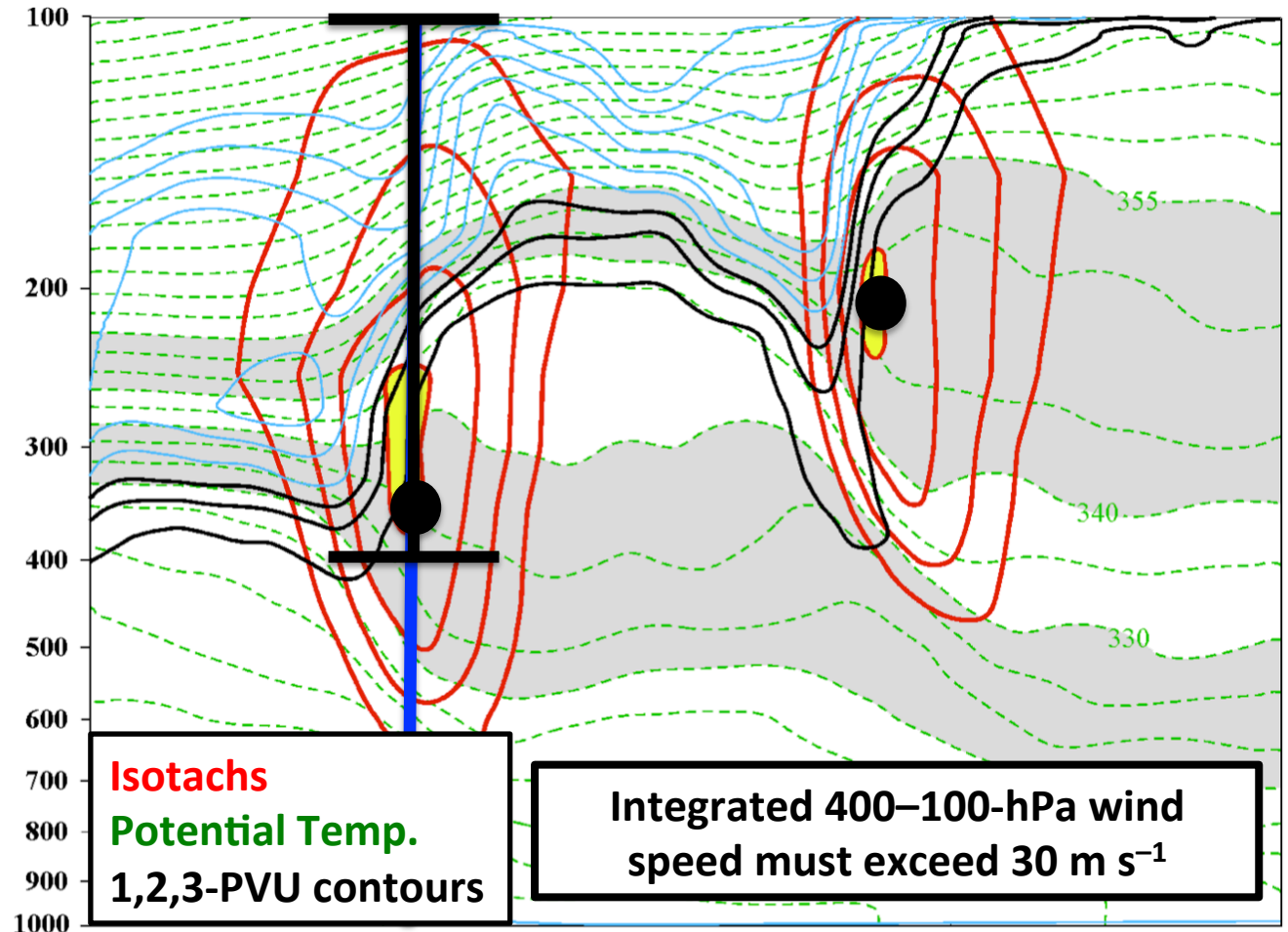
Jet Superposition Event Identification

0000 UTC 27 April 2010



250-hPa wind speed

Isolated grid points over North America in the CFSR (Saha et al. 2014) characterized by polar and subtropical jets during Nov–Mar 1979–2010.



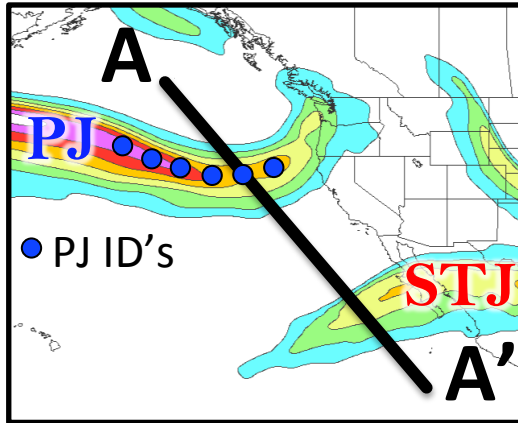
Isotachs
Potential Temp.
1,2,3-PVU contours

Integrated 400–100-hPa wind speed must exceed 30 m s^{-1}

A Winters and Martin (2014, 2016, 2017); Christenson et al. (2017); Handlos and Martin (2016) **A'**

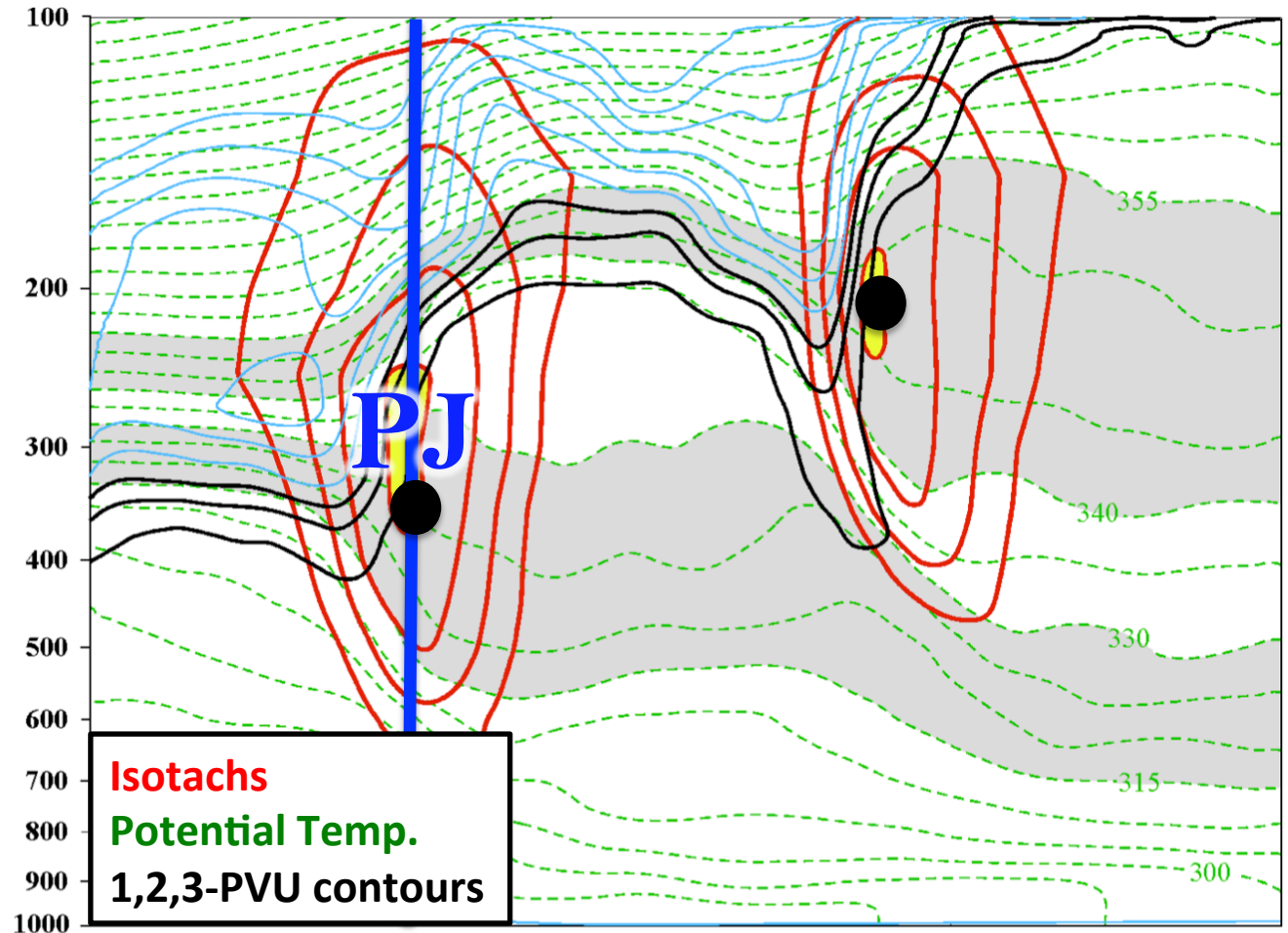
Jet Superposition Event Identification

0000 UTC 27 April 2010



250-hPa wind speed

Isolated grid points over North America in the CFSR (Saha et al. 2014) characterized by polar and subtropical jets during Nov–Mar 1979–2010.

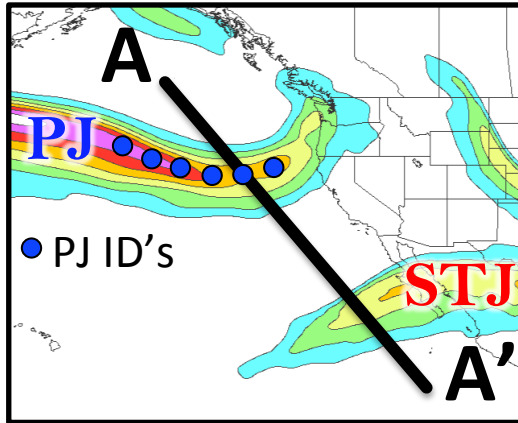


Isotachs
Potential Temp.
1,2,3-PVU contours

A Winters and Martin (2014, 2016, 2017); Christenson et al. (2017); Handlos and Martin (2016) **A'**

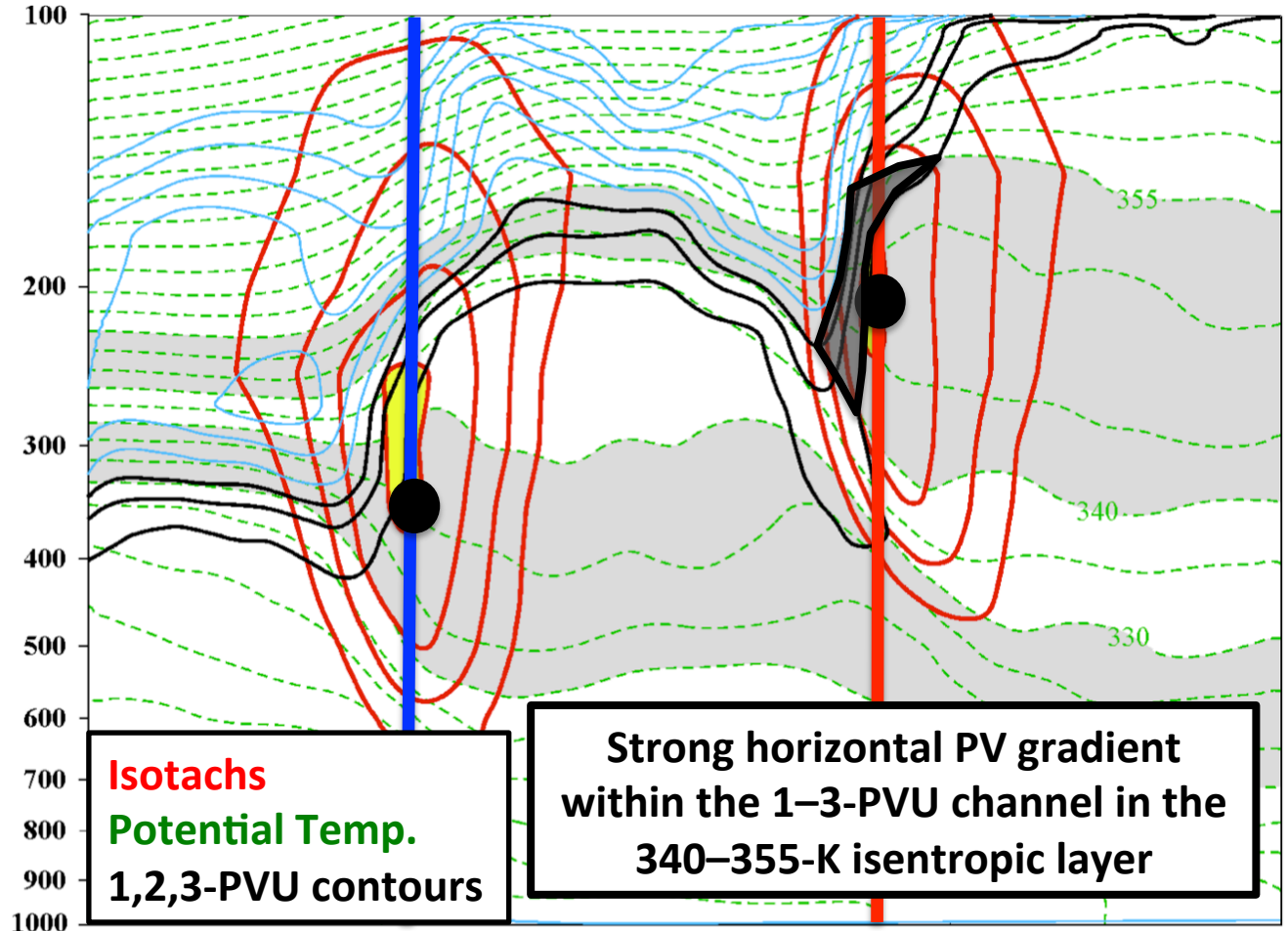
Jet Superposition Event Identification

0000 UTC 27 April 2010



250-hPa wind speed

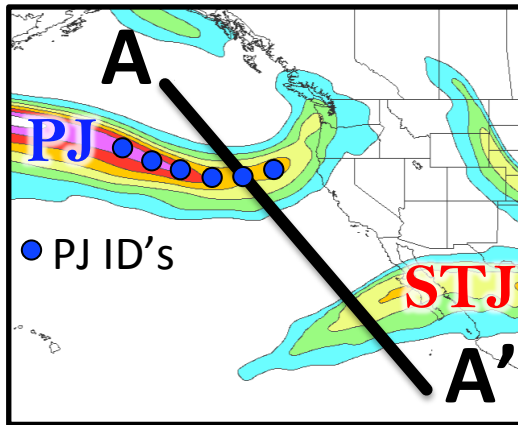
Isolated grid points over North America in the CFSR (Saha et al. 2014) characterized by polar and subtropical jets during Nov–Mar 1979–2010.



A Winters and Martin (2014, 2016, 2017); Christenson et al. (2017); Handlos and Martin (2016) **A'**

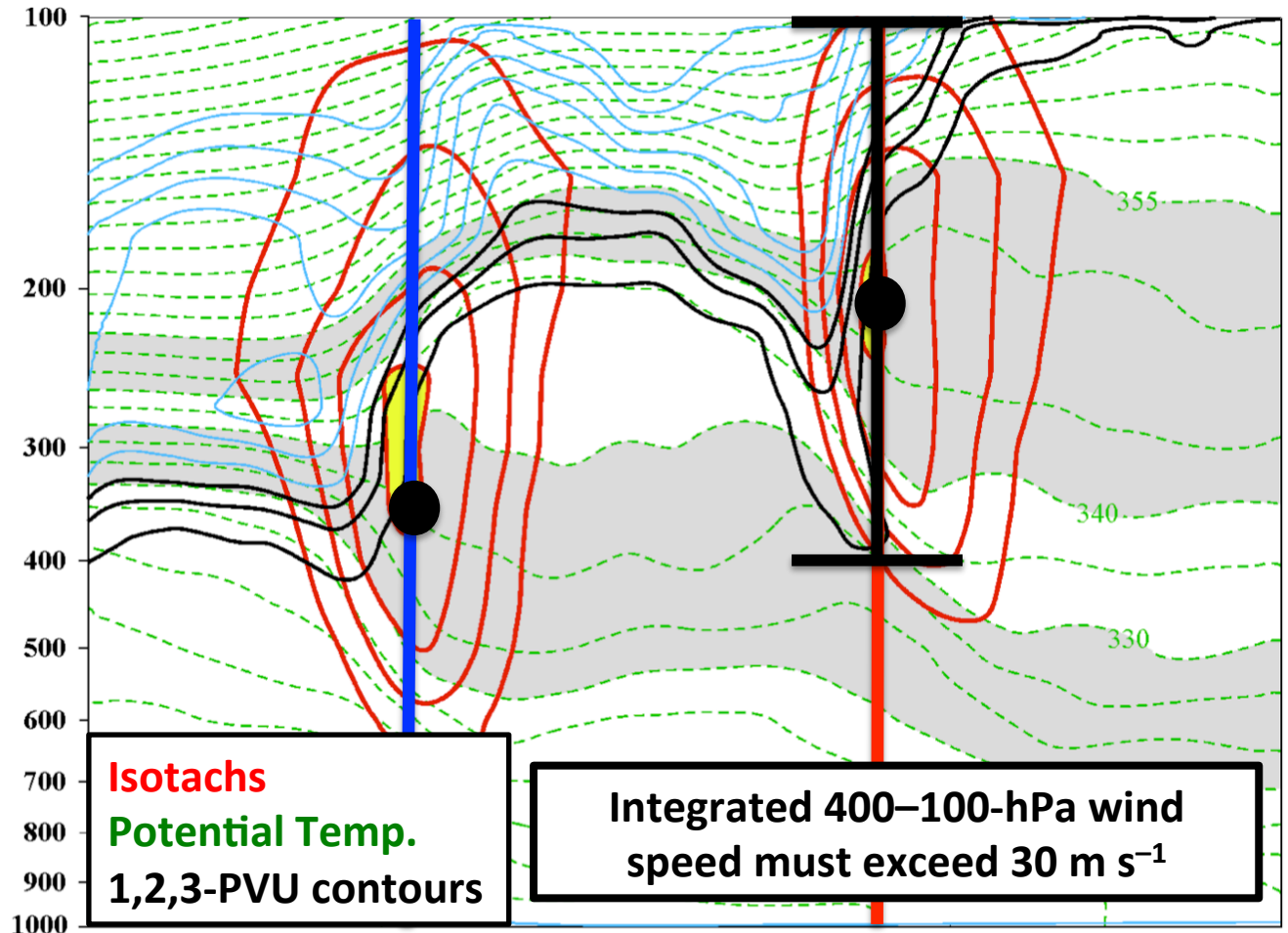
Jet Superposition Event Identification

0000 UTC 27 April 2010



250-hPa wind speed

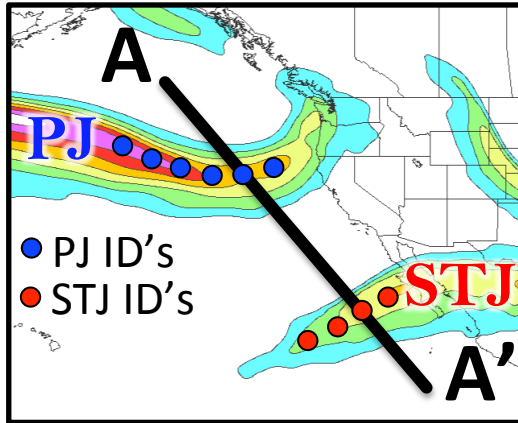
Isolated grid points over North America in the CFSR (Saha et al. 2014) characterized by polar and subtropical jets during Nov–Mar 1979–2010.



A Winters and Martin (2014, 2016, 2017); Christenson et al. (2017); Handlos and Martin (2016) **A'**

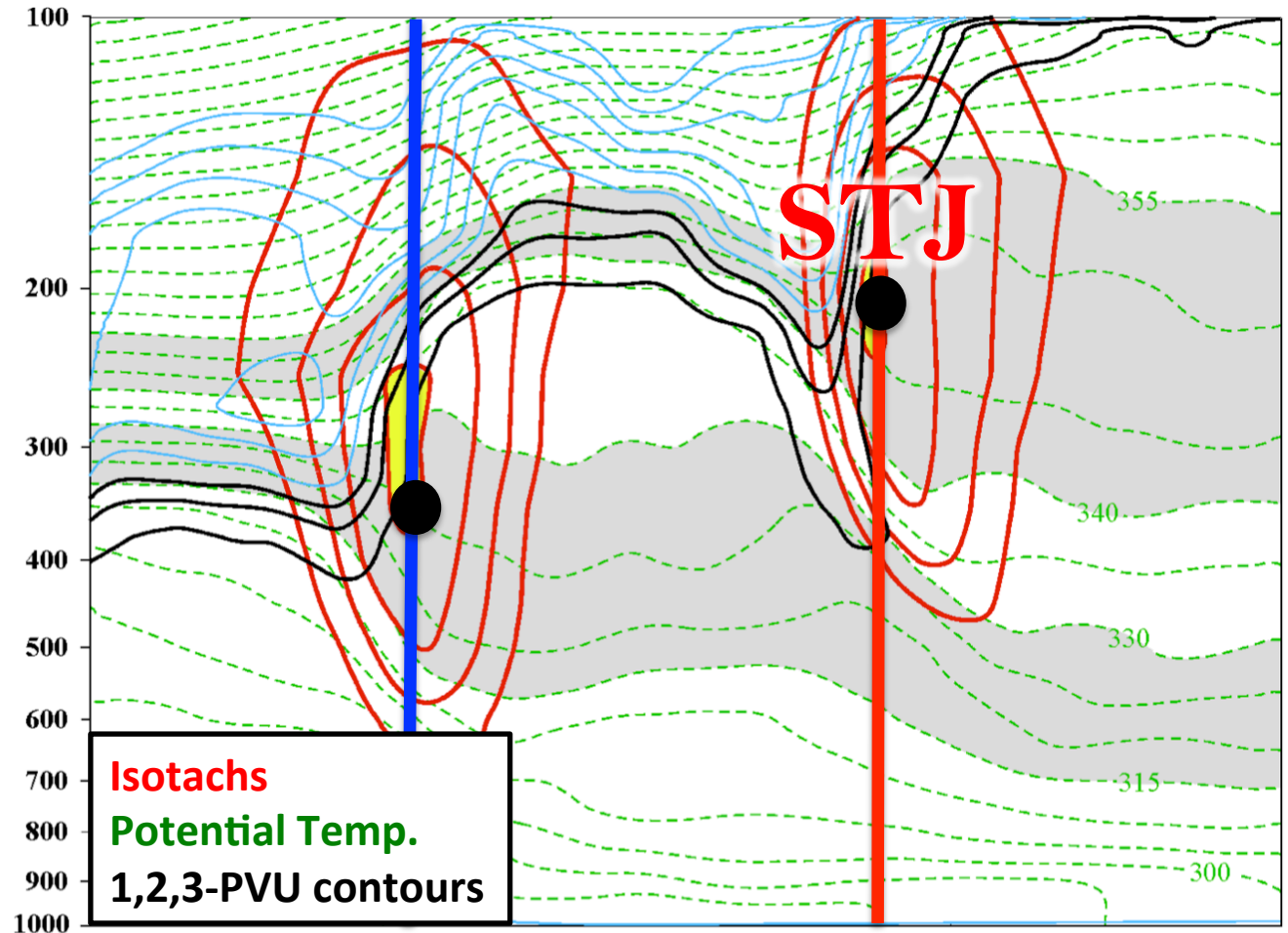
Jet Superposition Event Identification

0000 UTC 27 April 2010



250-hPa wind speed

Isolated grid points over North America in the CFSR (Saha et al. 2014) characterized by polar and subtropical jets during Nov–Mar 1979–2010.

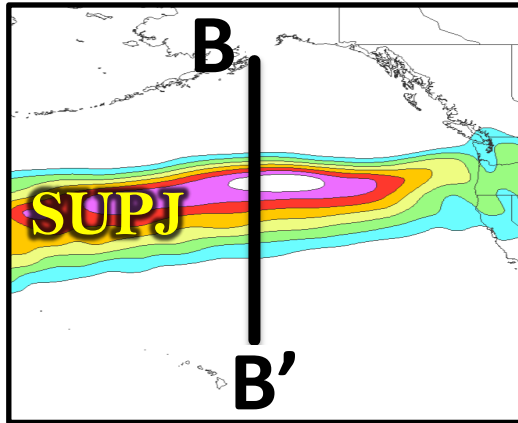


Isotachs
Potential Temp.
1,2,3-PVU contours

A Winters and Martin (2014, 2016, 2017); Christenson et al. (2017); Handlos and Martin (2016) A'

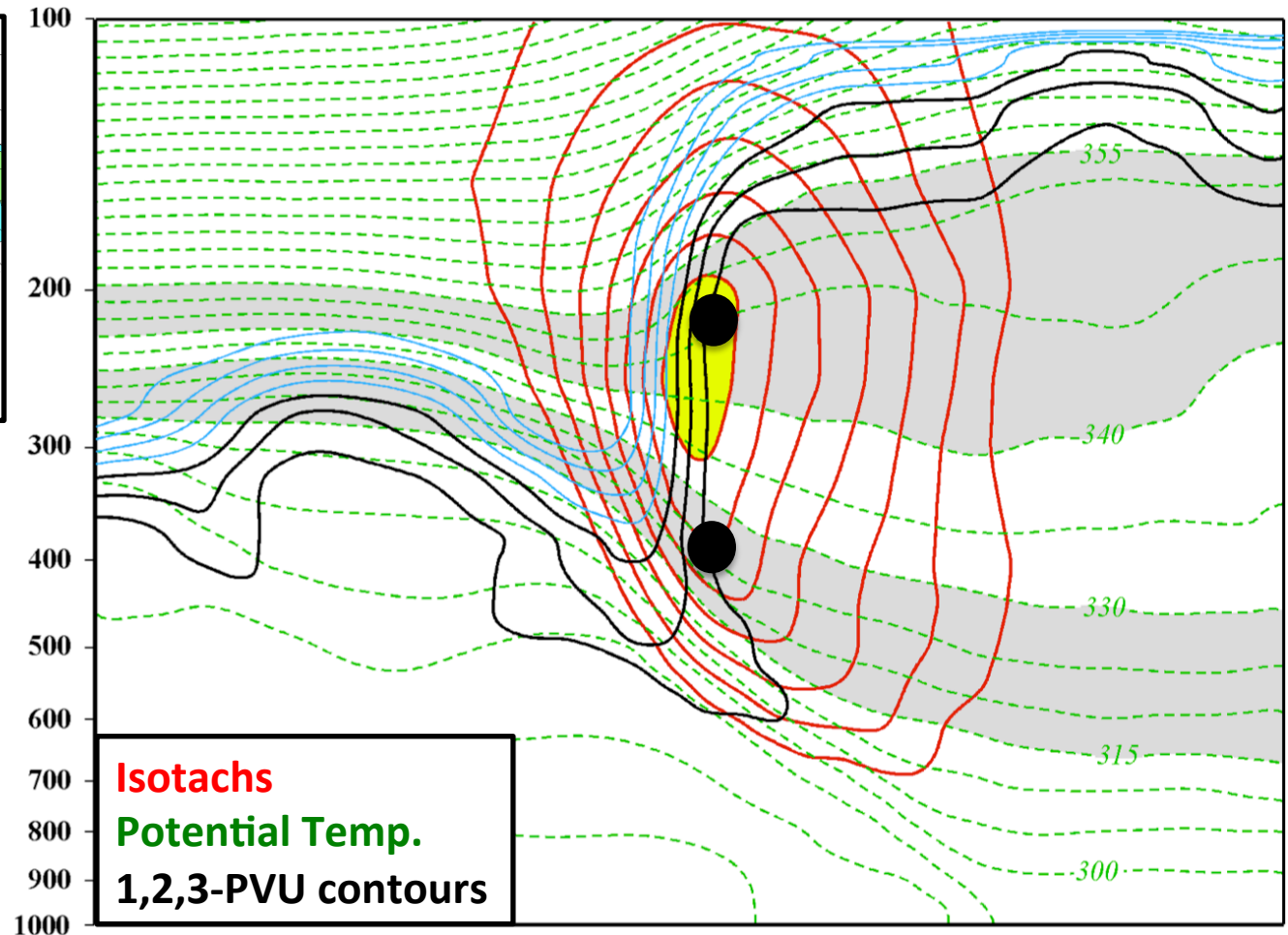
Jet Superposition Event Identification

0000 UTC 24 October 2010



250-hPa wind speed

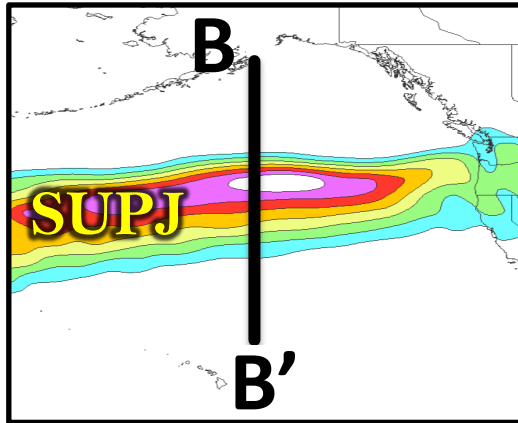
Isolated grid points over North America in the CFSR (Saha et al. 2014) characterized by a jet superposition during Nov–Mar 1979–2010.



B Winters and Martin (2014, 2016, 2017); Christenson et al. (2017); Handlos and Martin (2016) **B'**

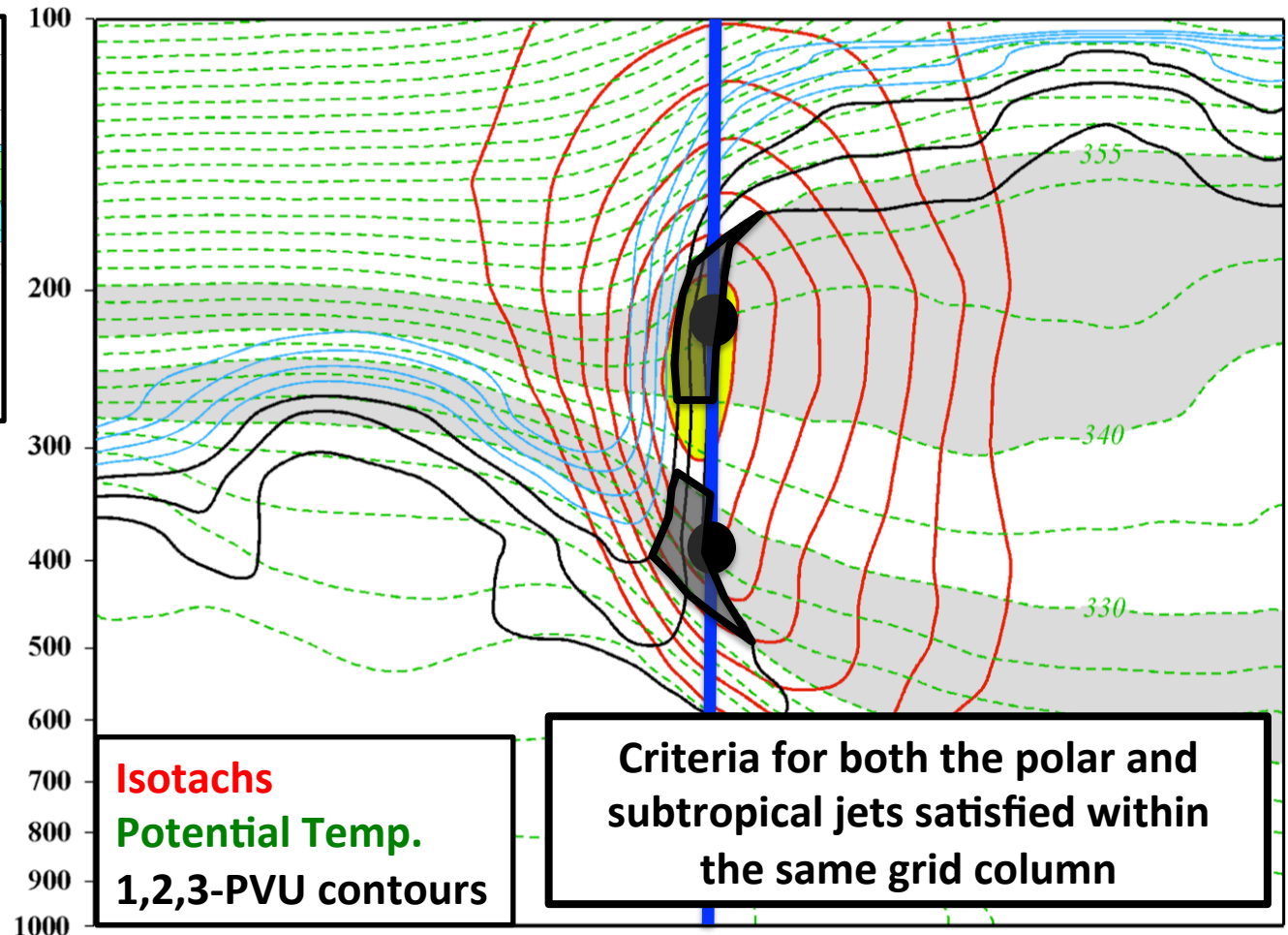
Jet Superposition Event Identification

0000 UTC 24 October 2010



250-hPa wind speed

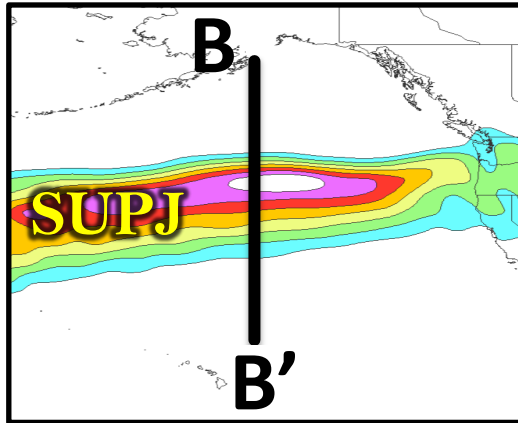
Isolated grid points over North America in the CFSR (Saha et al. 2014) characterized by a jet superposition during Nov–Mar 1979–2010.



B Winters and Martin (2014, 2016, 2017); Christenson et al. (2017); Handlos and Martin (2016) **B'**

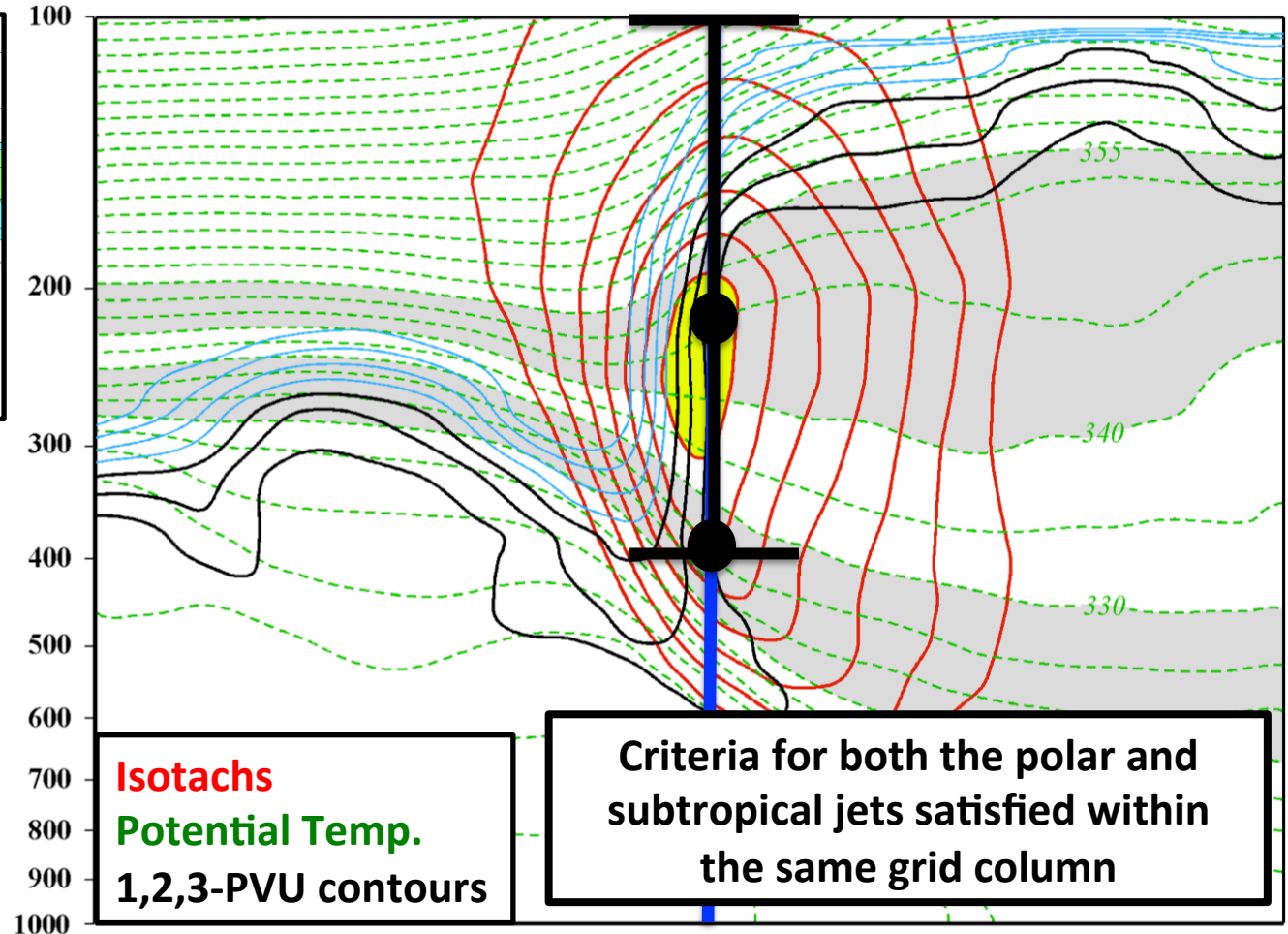
Jet Superposition Event Identification

0000 UTC 24 October 2010



250-hPa wind speed

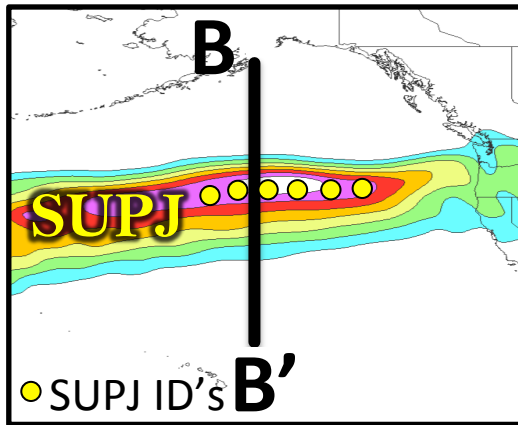
Isolated grid points over North America in the CFSR (Saha et al. 2014) characterized by a jet superposition during Nov–Mar 1979–2010.



B Winters and Martin (2014, 2016, 2017); Christenson et al. (2017); Handlos and Martin (2016) **B'**

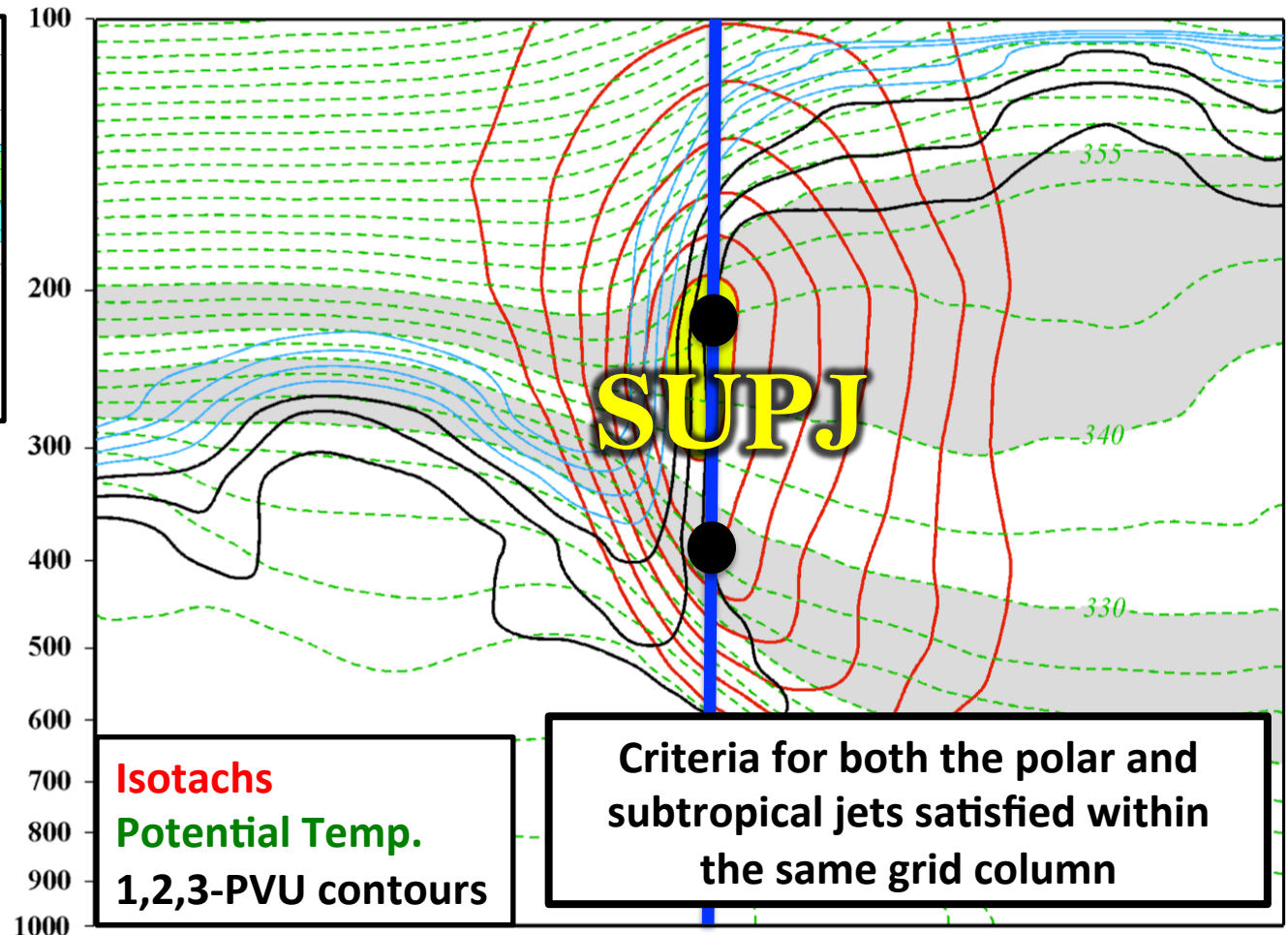
Jet Superposition Event Identification

0000 UTC 24 October 2010



250-hPa wind speed

Isolated grid points over North America in the CFSR (Saha et al. 2014) characterized by a jet superposition during Nov–Mar 1979–2010.

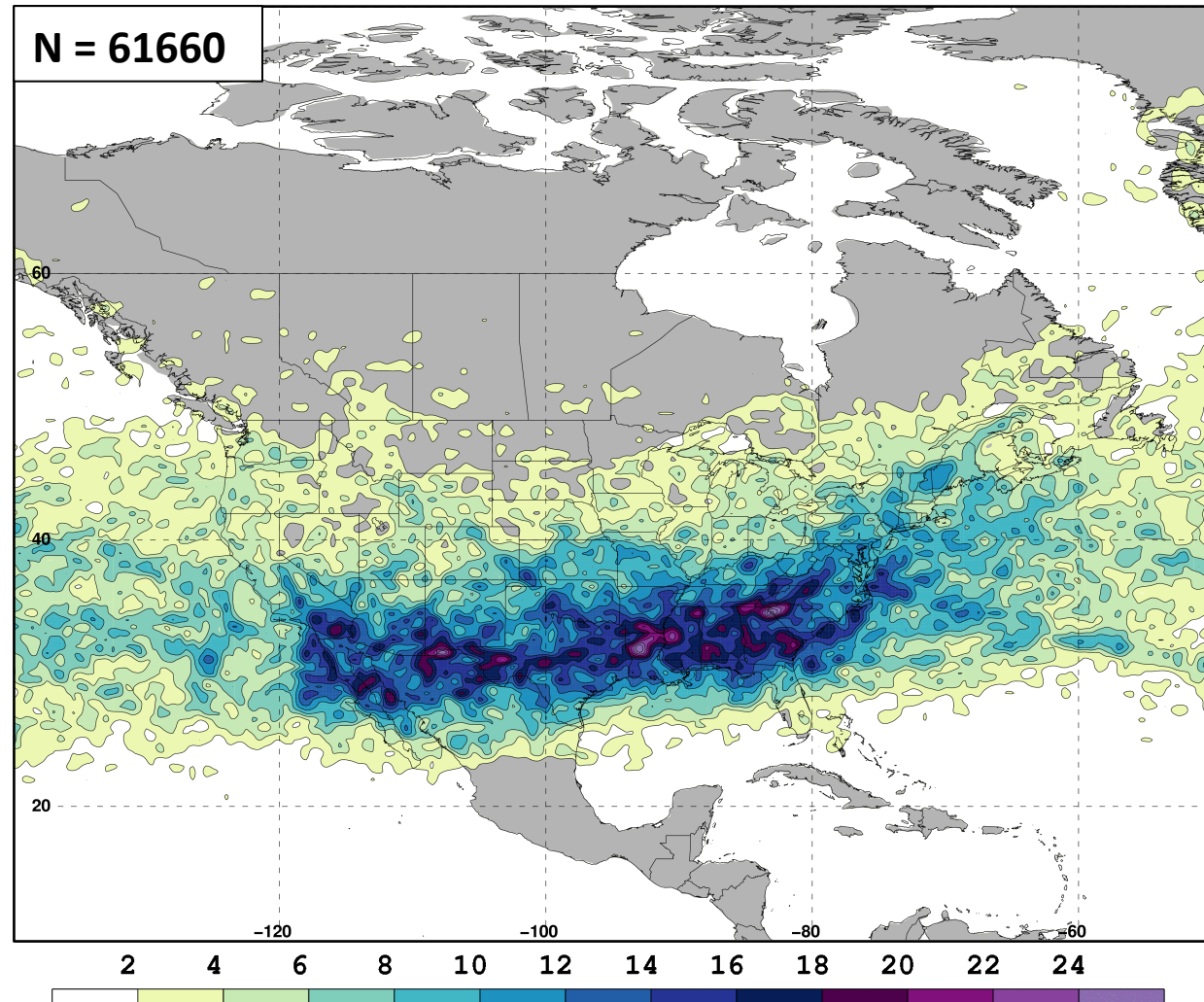


B Winters and Martin (2014, 2016, 2017); Christenson et al. (2017); Handlos and Martin (2016) **B'**

Jet Superposition Event Identification

1. Isolated grid points over North America in the CFSR (Saha et al. 2014) characterized by a jet superposition during Nov–Mar 1979–2010.

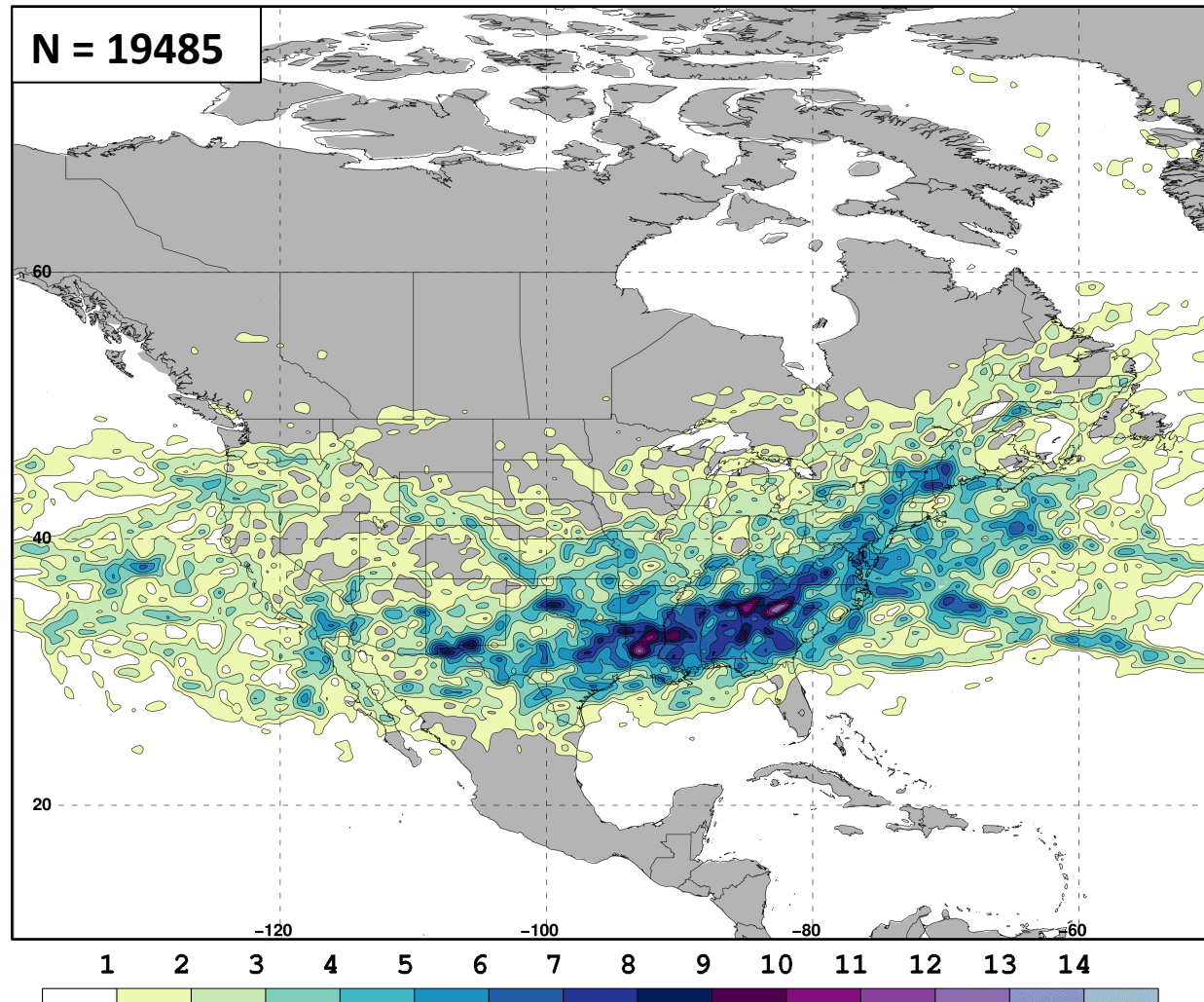
Jet Superposition Frequency – All Times



Jet Superposition Event Identification

1. Isolated grid points over North America in the CFSR (Saha et al. 2014) characterized by a jet superposition during Nov–Mar 1979–2010.
2. Retained analysis times that rank in the top 10% in terms the number of grid points characterized by a jet superposition.

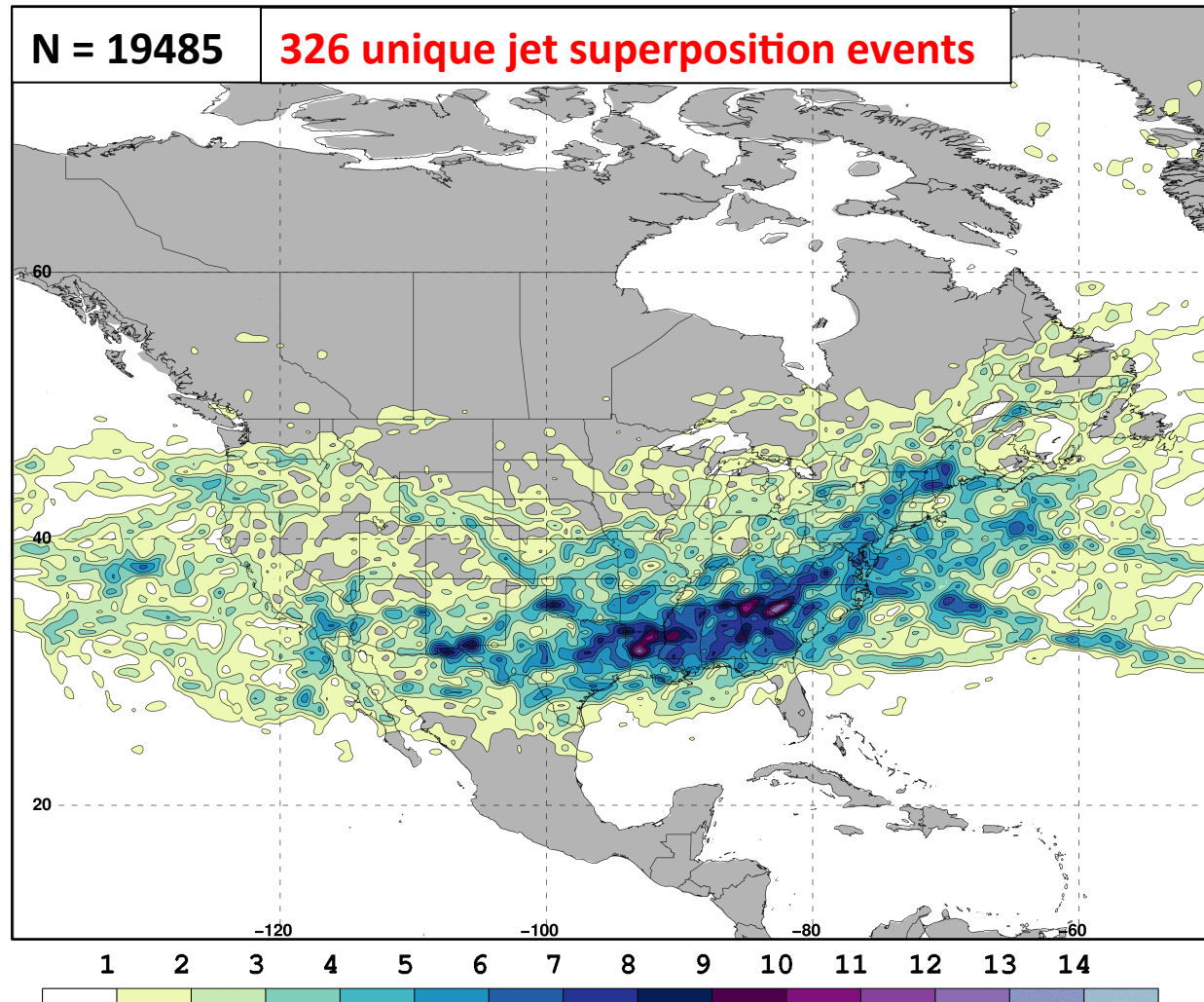
Jet Superposition Frequency – Top 10% Times



Jet Superposition Event Identification

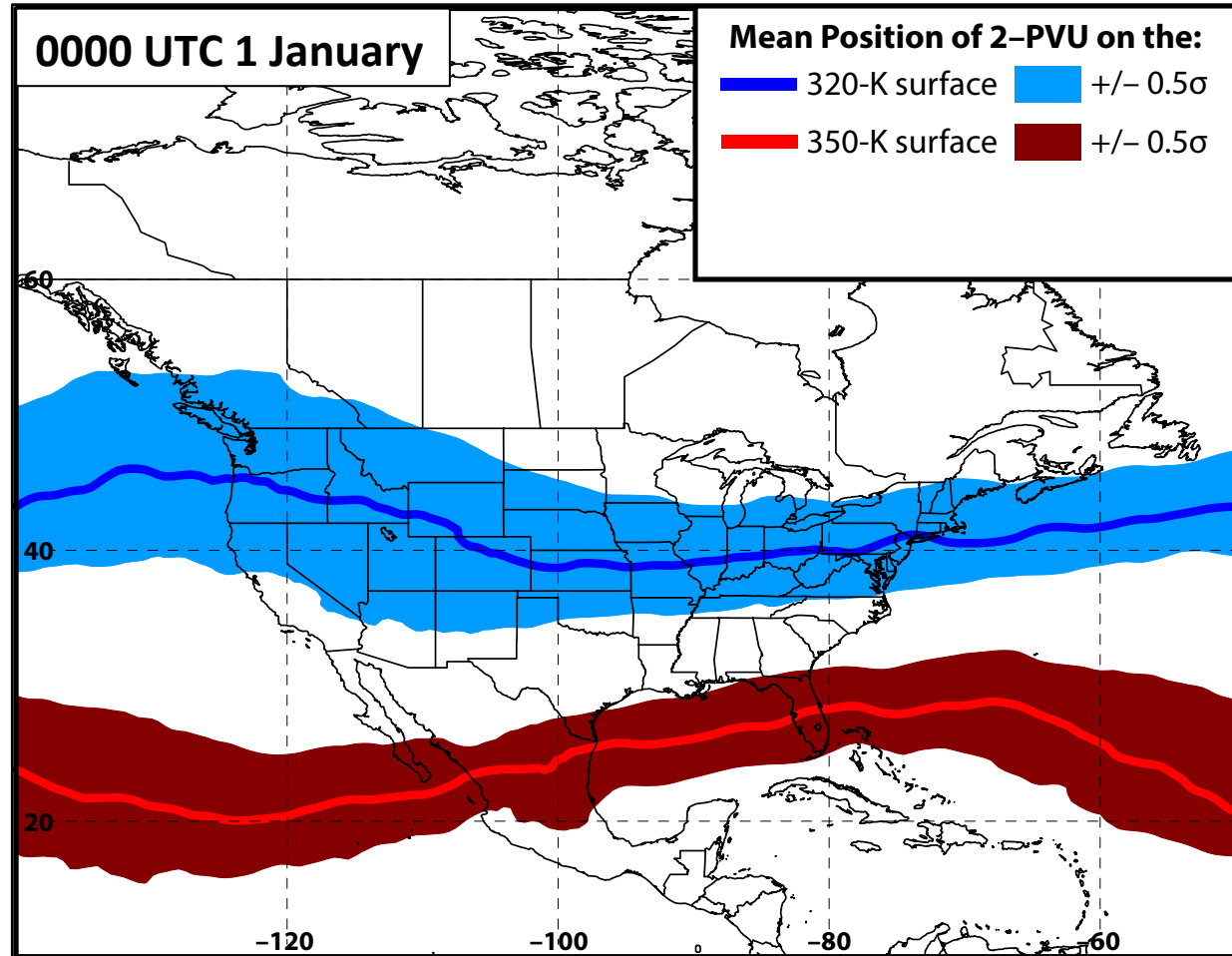
1. Isolated grid points over North America in the CFSR (Saha et al. 2014) characterized by a jet superposition during Nov–Mar 1979–2010.
2. Retained analysis times that rank in the top 10% in terms the number of grid points characterized by a jet superposition.
3. Filtered retained analysis times to group together jet superpositions that are < 30 h and < 1500 km apart.

Jet Superposition Frequency – Top 10% Times



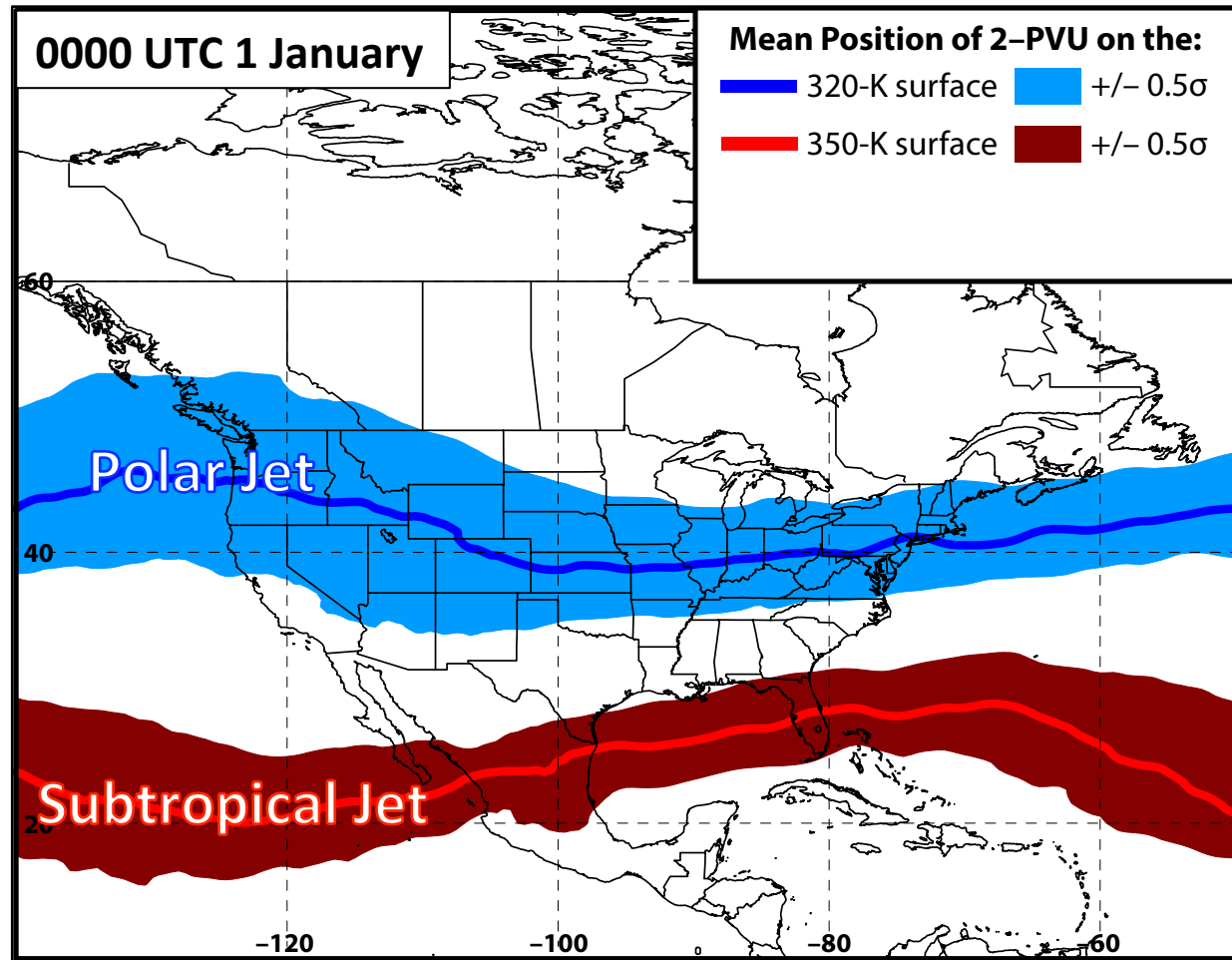
Jet Superposition Event Classification

1. Determined the mean position of the 2-PVU contour on the 320-K and 350-K surfaces at each analysis time in the CFSR.



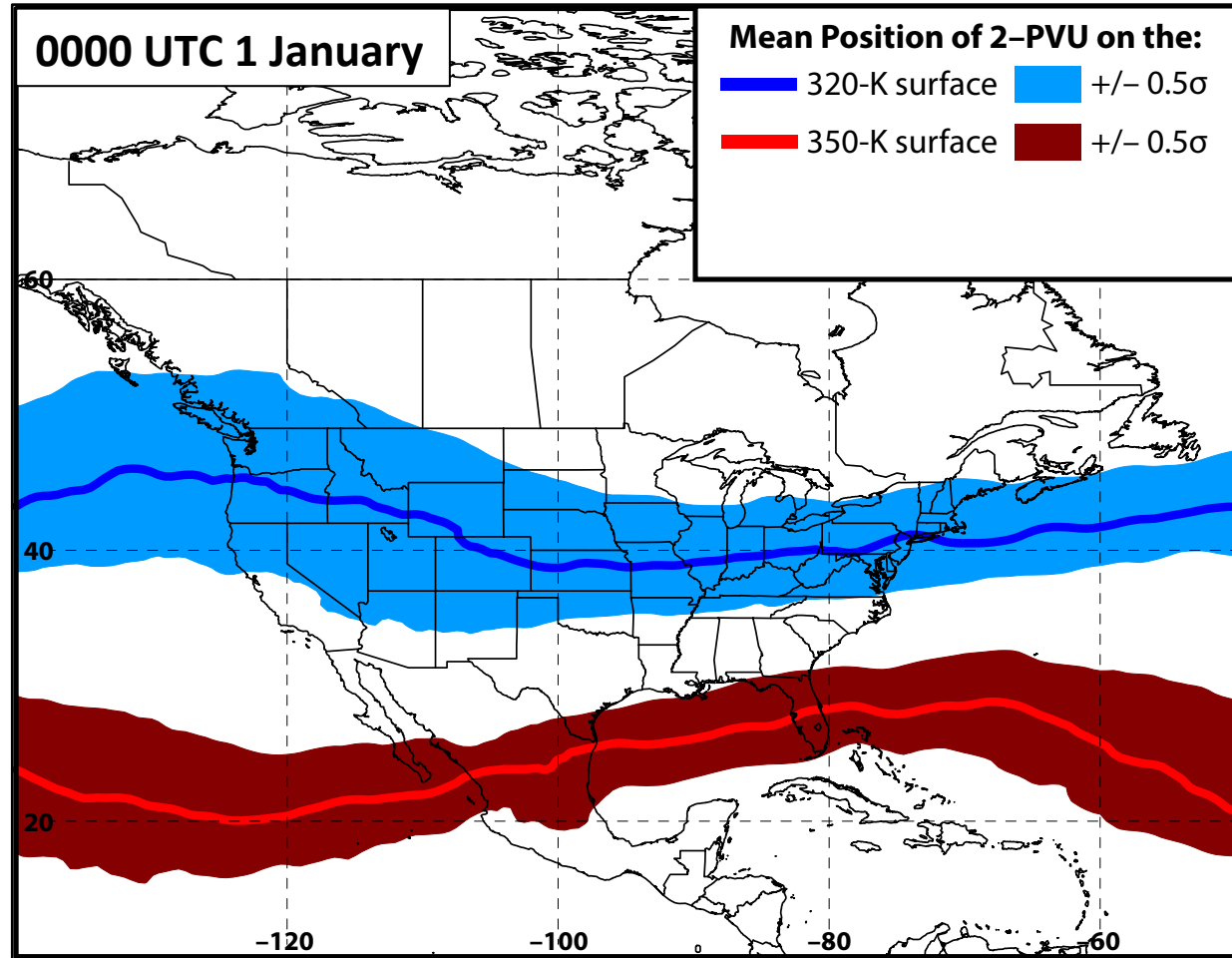
Jet Superposition Event Classification

1. Determined the mean position of the 2-PVU contour on the 320-K and 350-K surfaces at each analysis time in the CFSR.



Jet Superposition Event Classification

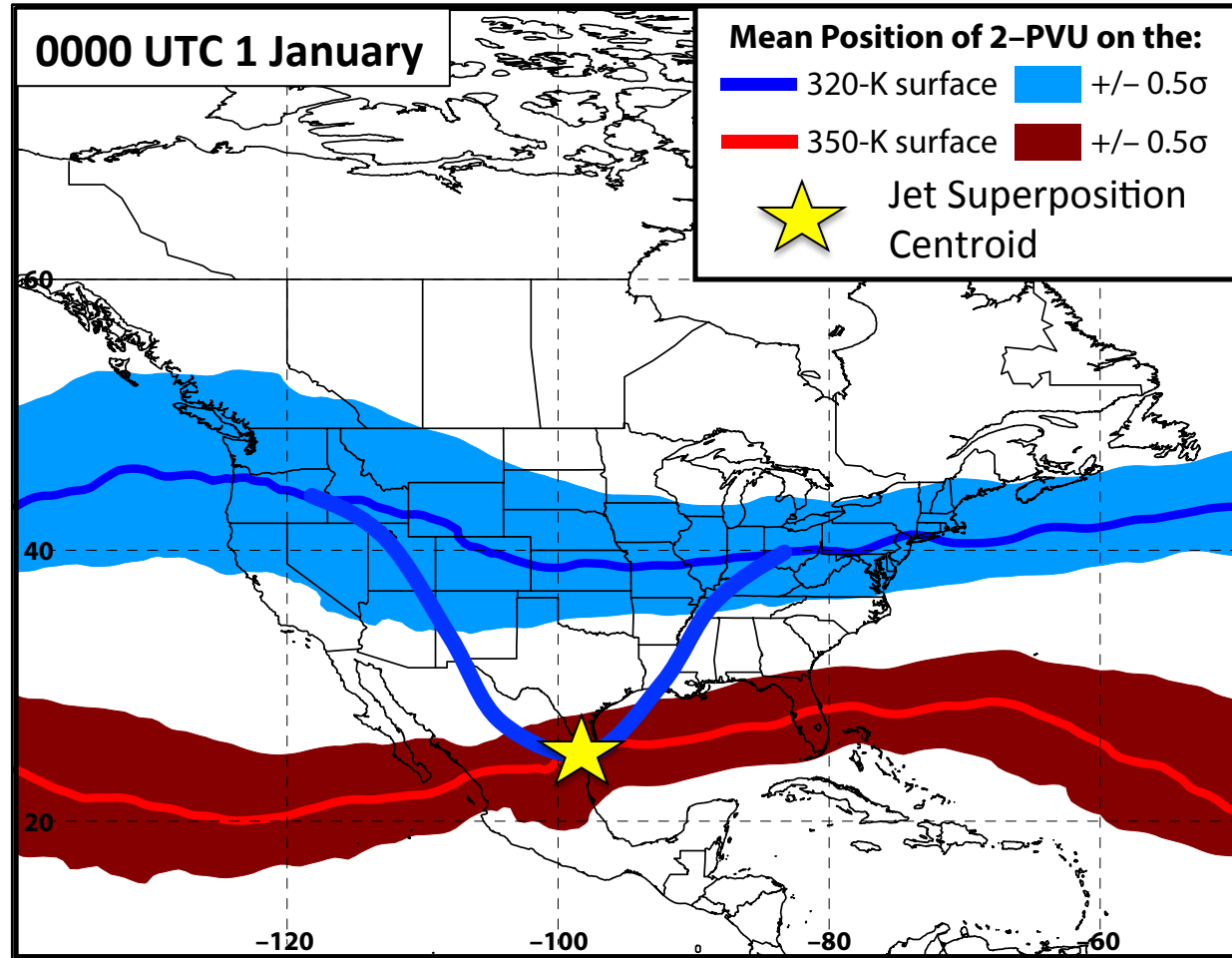
1. Determined the mean position of the 2-PVU contour on the 320-K and 350-K surfaces at each analysis time in the CFSR.
2. Compared the position of the jet superposition centroid at the start of each event against the climatological position of the 2-PVU contour.



Jet Superposition Event Classification

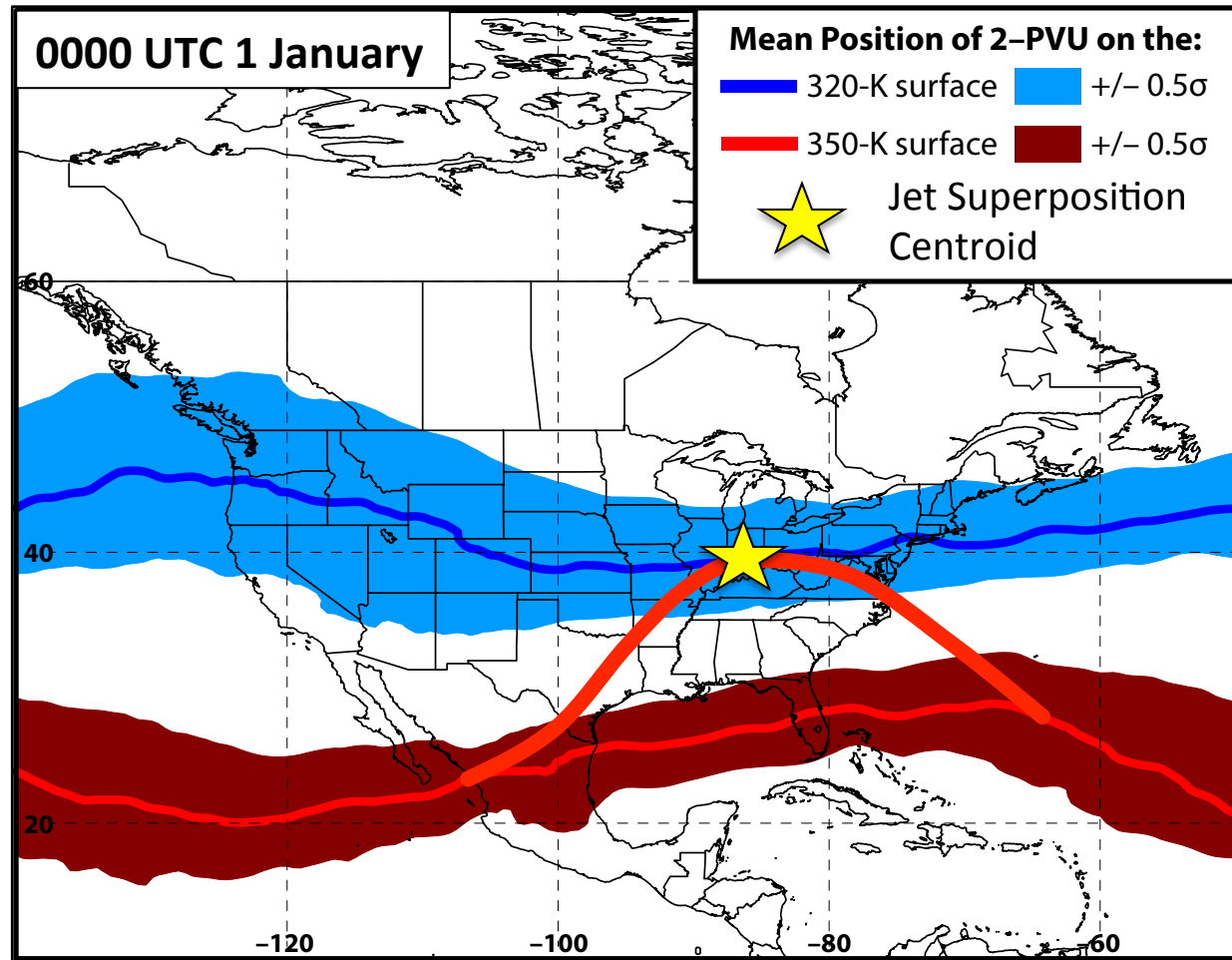
1. Determined the mean position of the 2-PVU contour on the 320-K and 350-K surfaces at each analysis time in the CFSR.
2. Compared the position of the jet superposition centroid at the start of each event against the climatological position of the 2-PVU contour.

- **Polar Dominant**



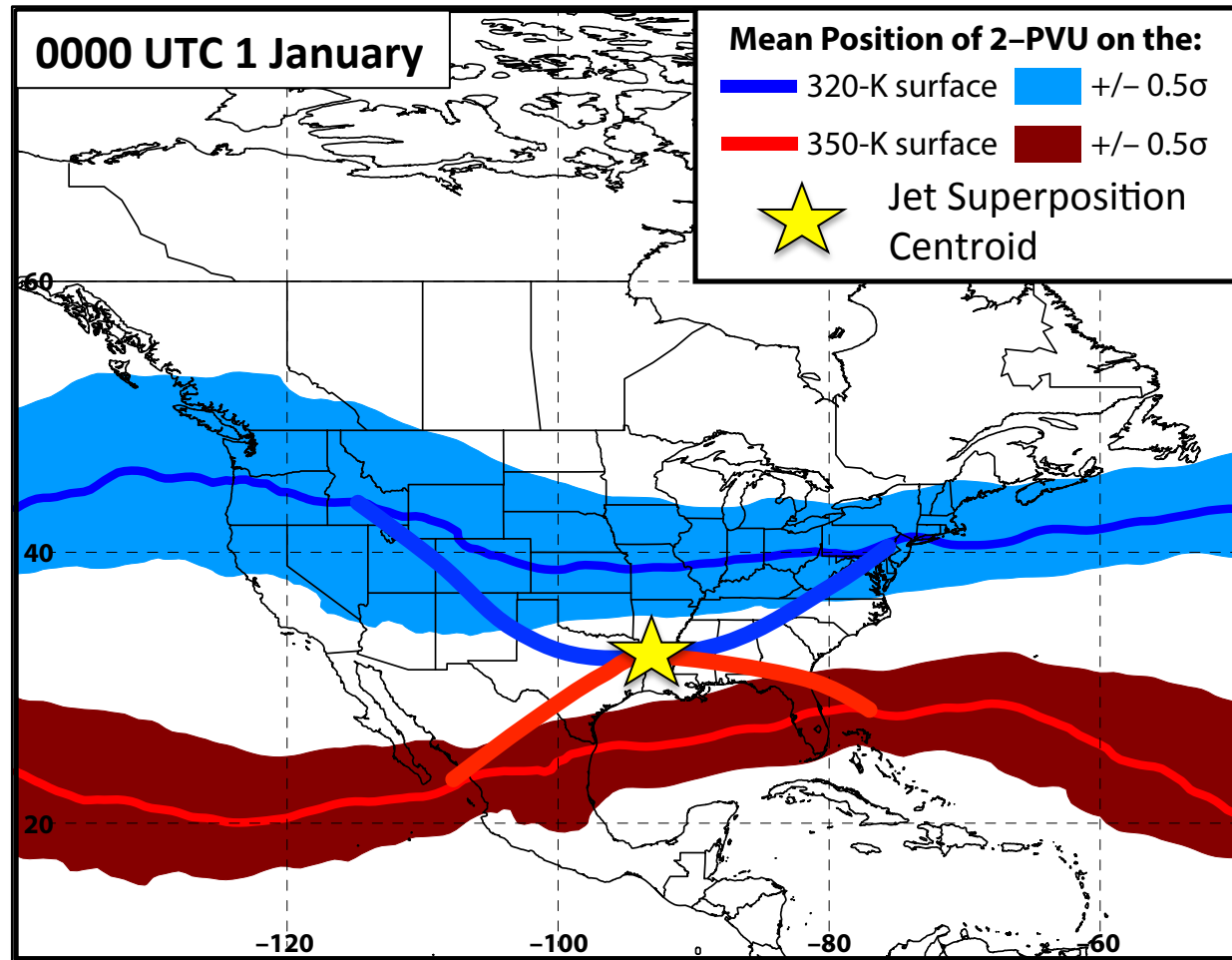
Jet Superposition Event Classification

1. Determined the mean position of the 2-PVU contour on the 320-K and 350-K surfaces at each analysis time in the CFSR.
 2. Compared the position of the jet superposition centroid at the start of each event against the climatological position of the 2-PVU contour.
- Polar Dominant
 - **Subtropical Dominant**



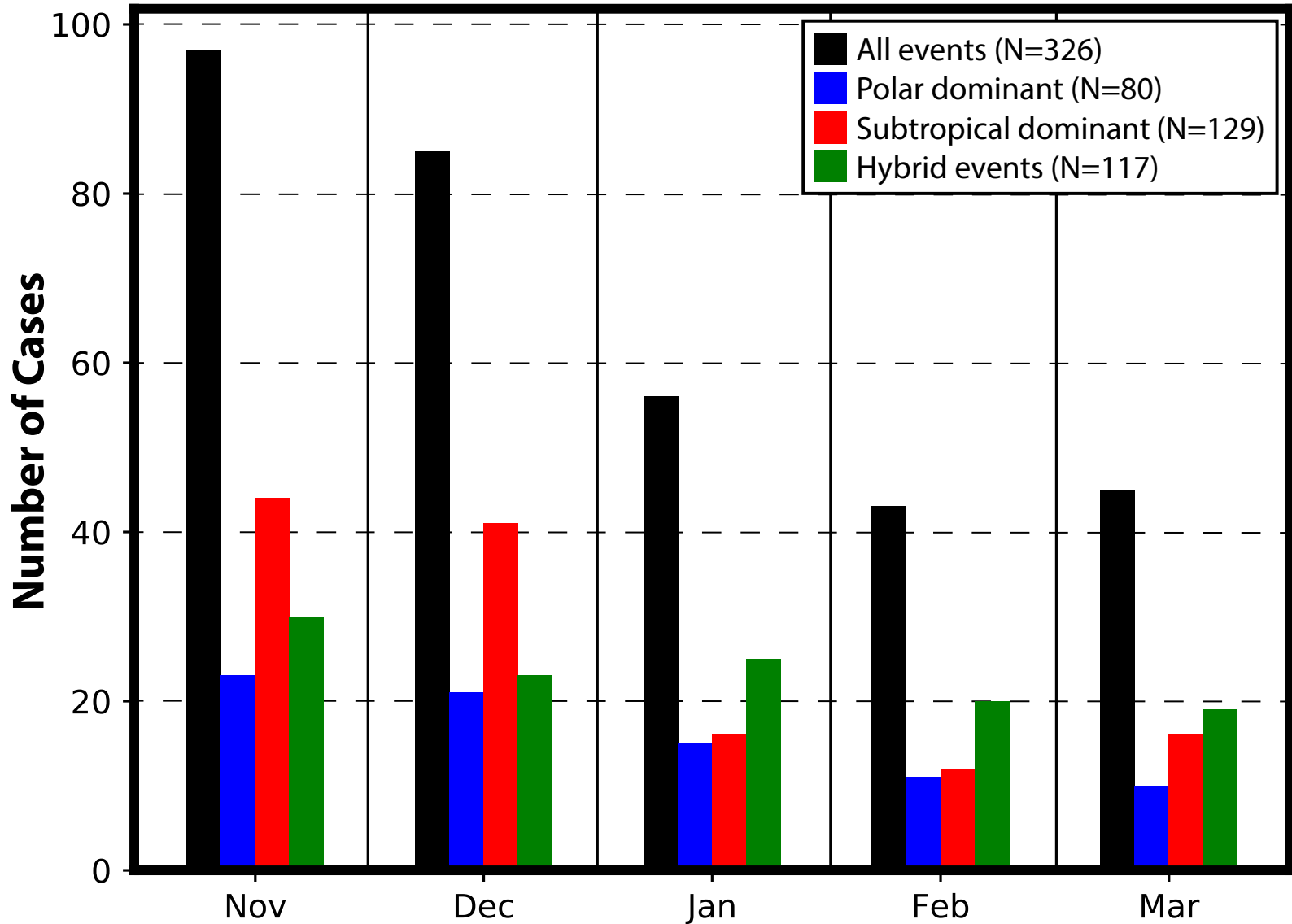
Jet Superposition Event Classification

1. Determined the mean position of the 2-PVU contour on the 320-K and 350-K surfaces at each analysis time in the CFSR.
 2. Compared the position of the jet superposition centroid at the start of each event against the climatological position of the 2-PVU contour.
- Polar Dominant
 - Subtropical Dominant
 - **Hybrid**

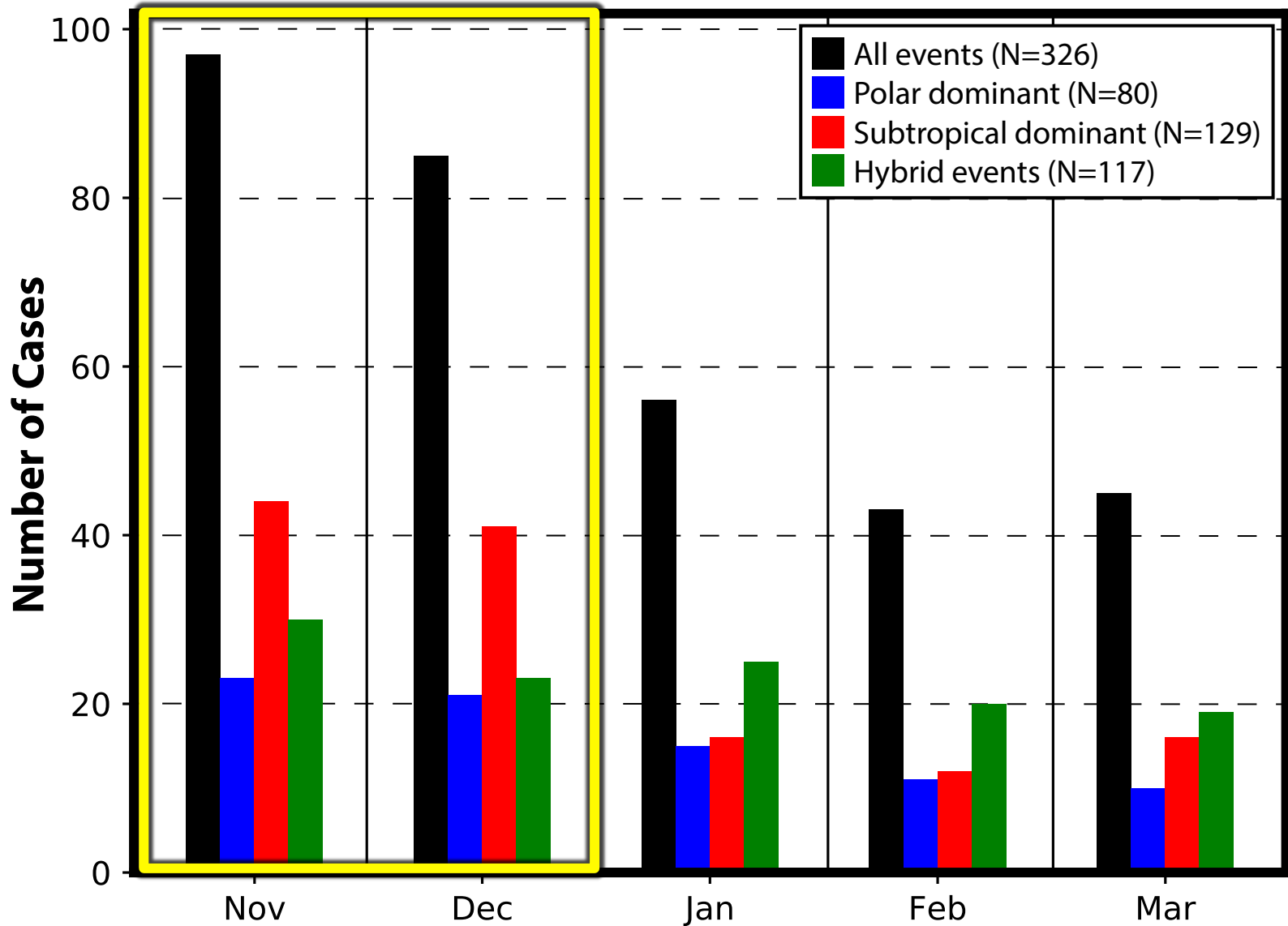


Climatological Characteristics of Jet Superposition Events

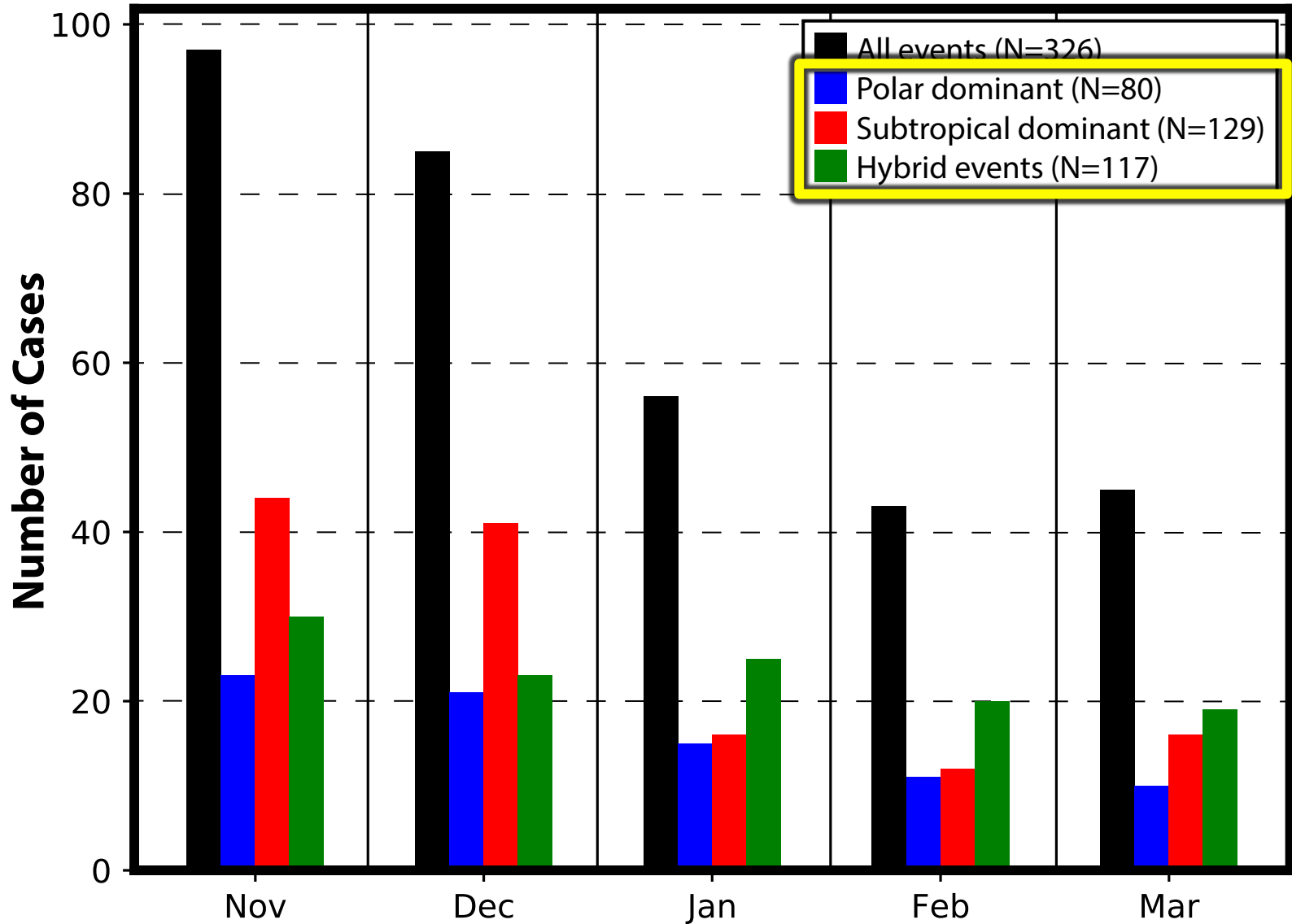
Jet Superposition Event Characteristics



Jet Superposition Event Characteristics

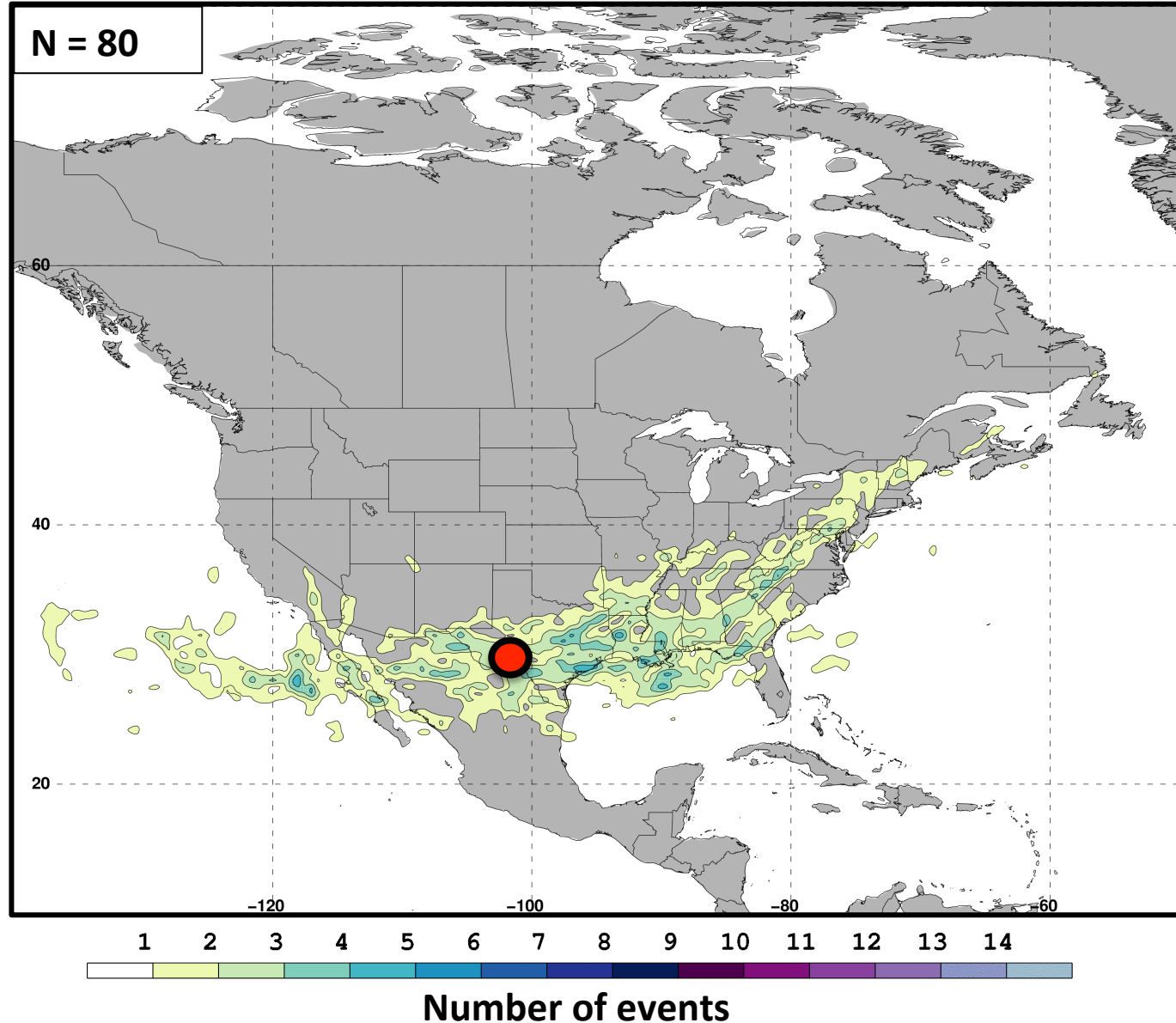


Jet Superposition Event Characteristics



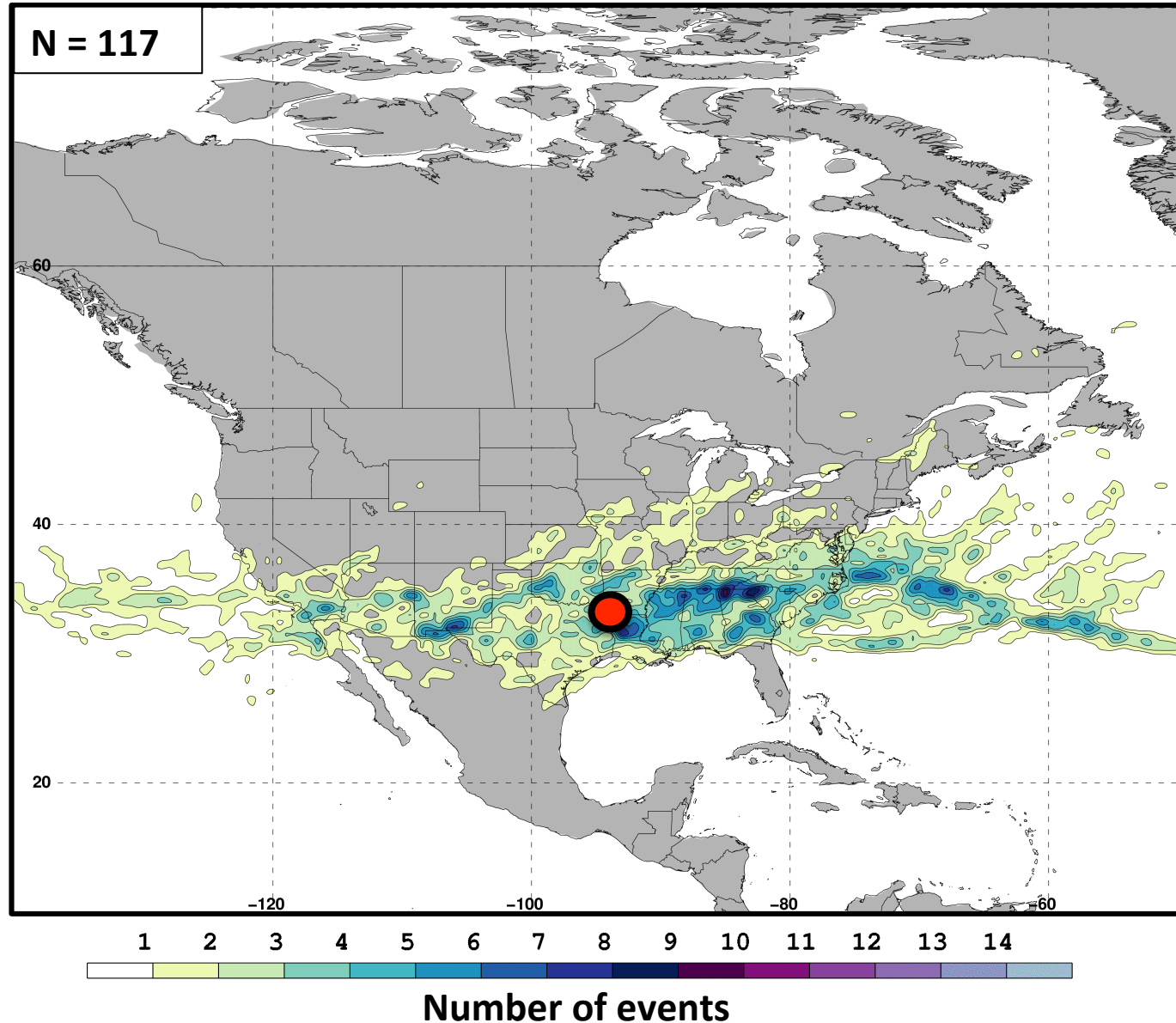
Jet Superposition Event Characteristics

Frequency of
Polar Dominant
Jet
Superposition
Events



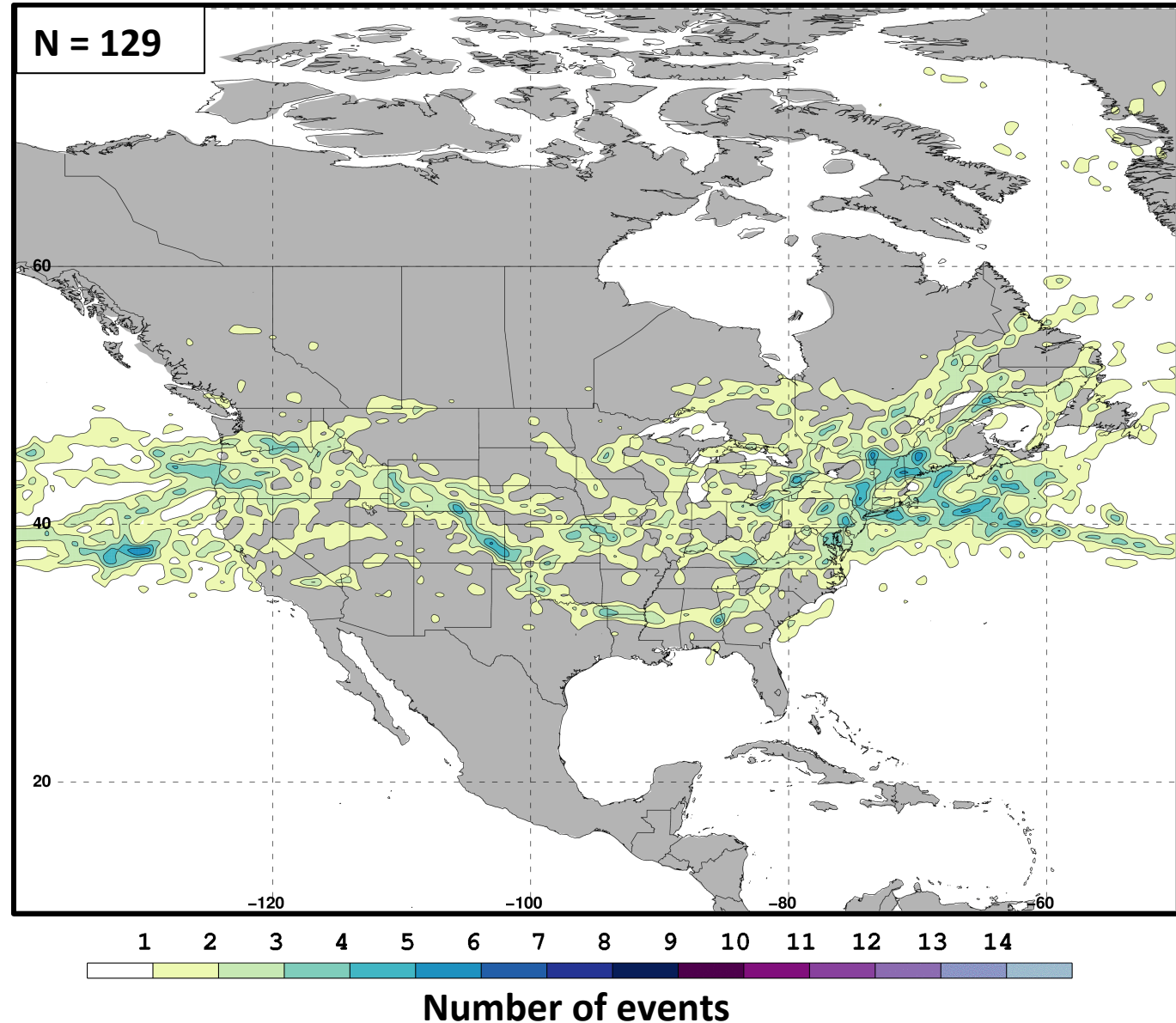
Jet Superposition Event Characteristics

Frequency of
Hybrid
Jet
Superposition
Events



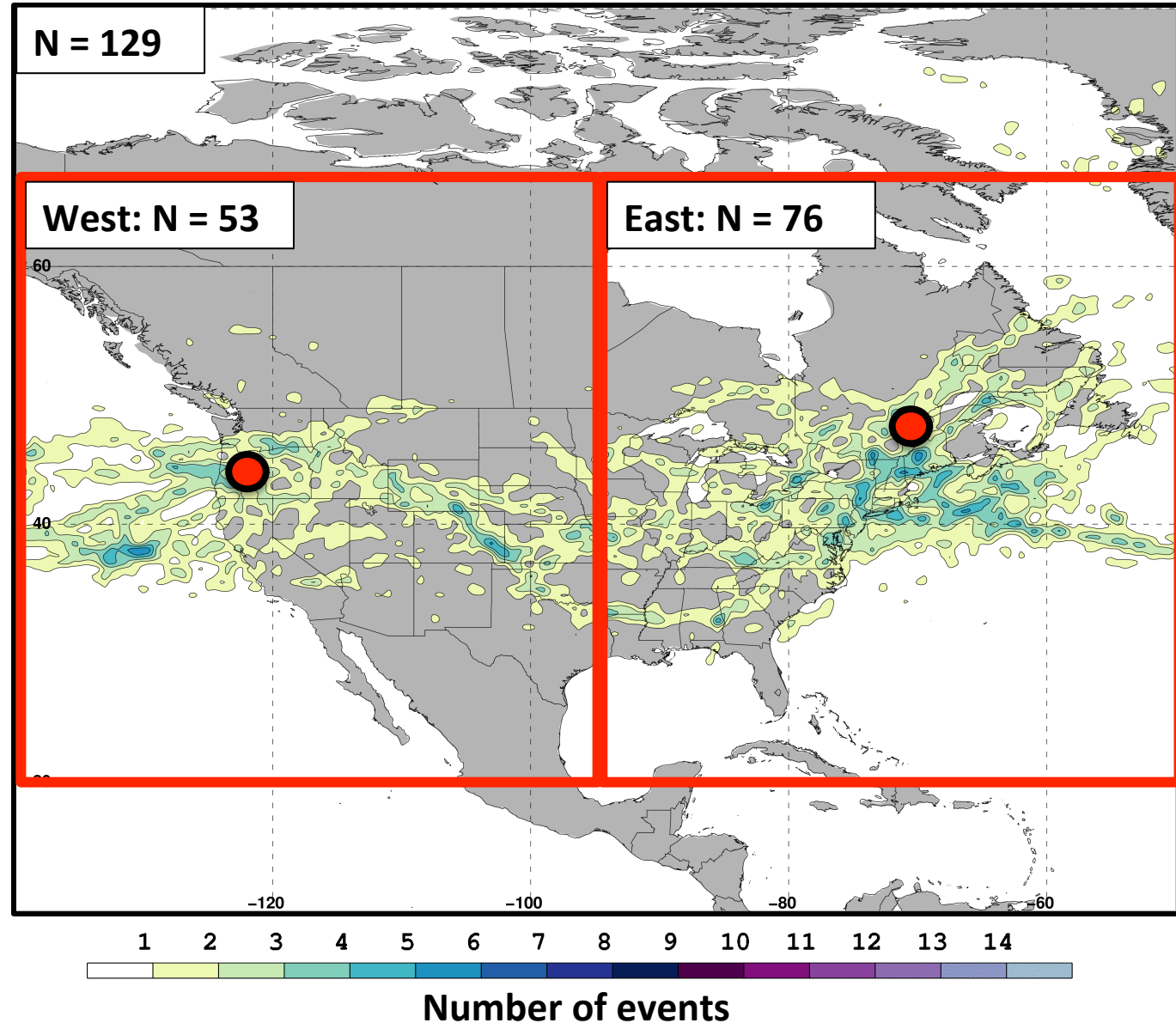
Jet Superposition Event Characteristics

Frequency of
**Subtropical
Dominant** Jet
Superposition
Events



Jet Superposition Event Characteristics

Frequency of
Subtropical
Dominant Jet
Superposition
Events



**Jet Superposition Event
Composites:**

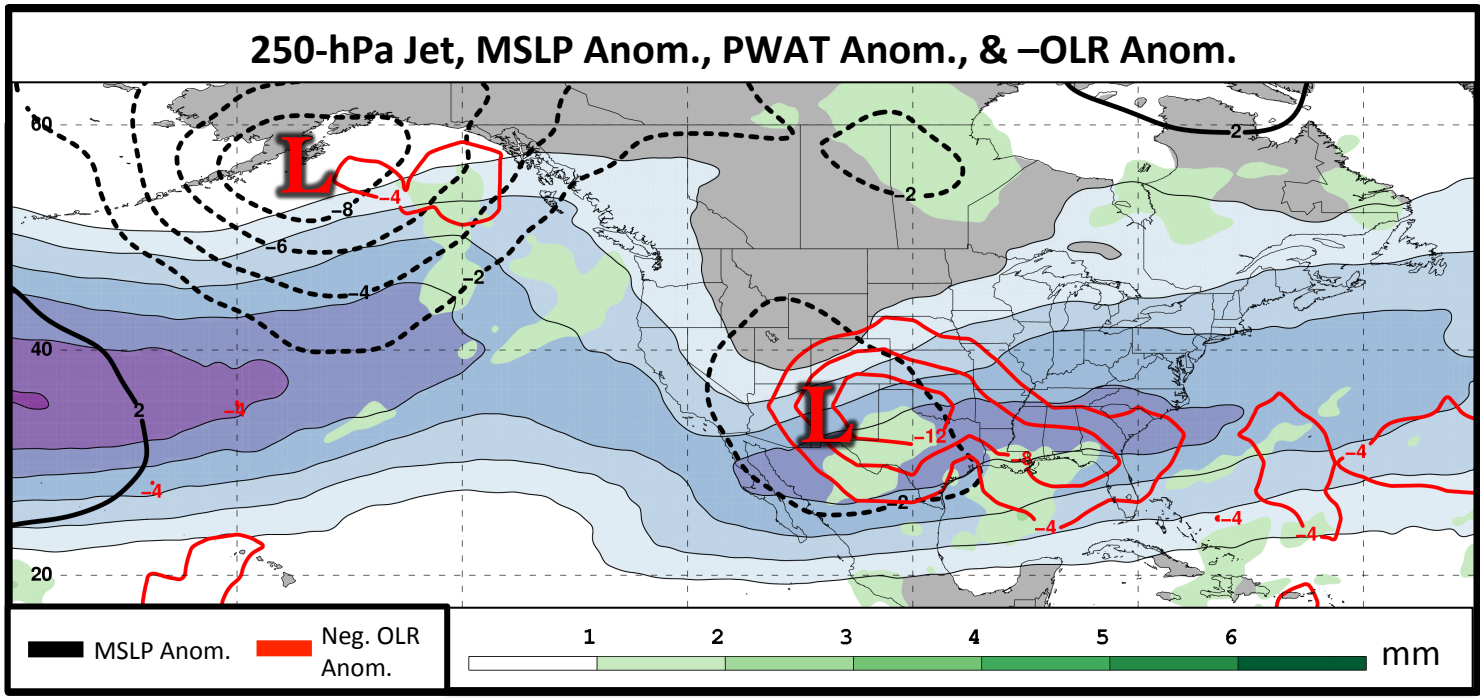
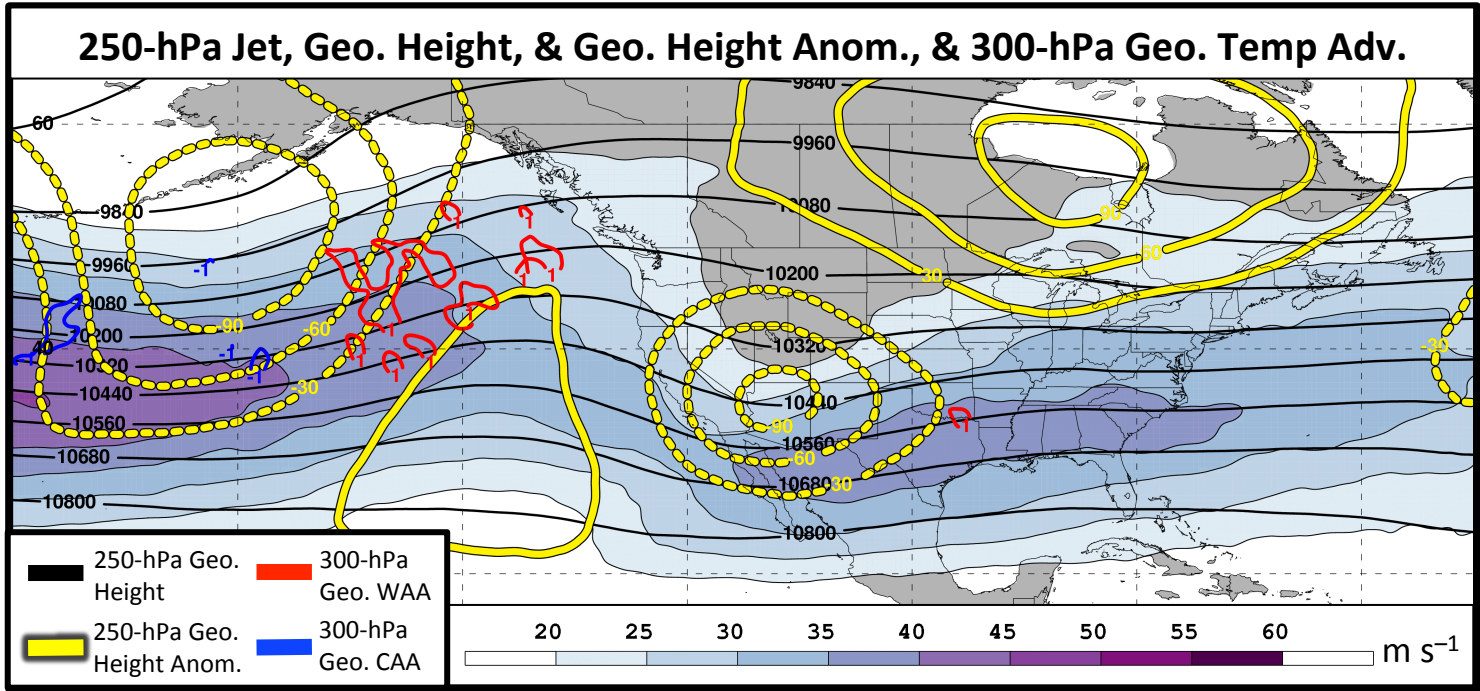
Polar Dominant

vs.

East Subtropical Dominant

Polar Dominant Jet Superposition Events

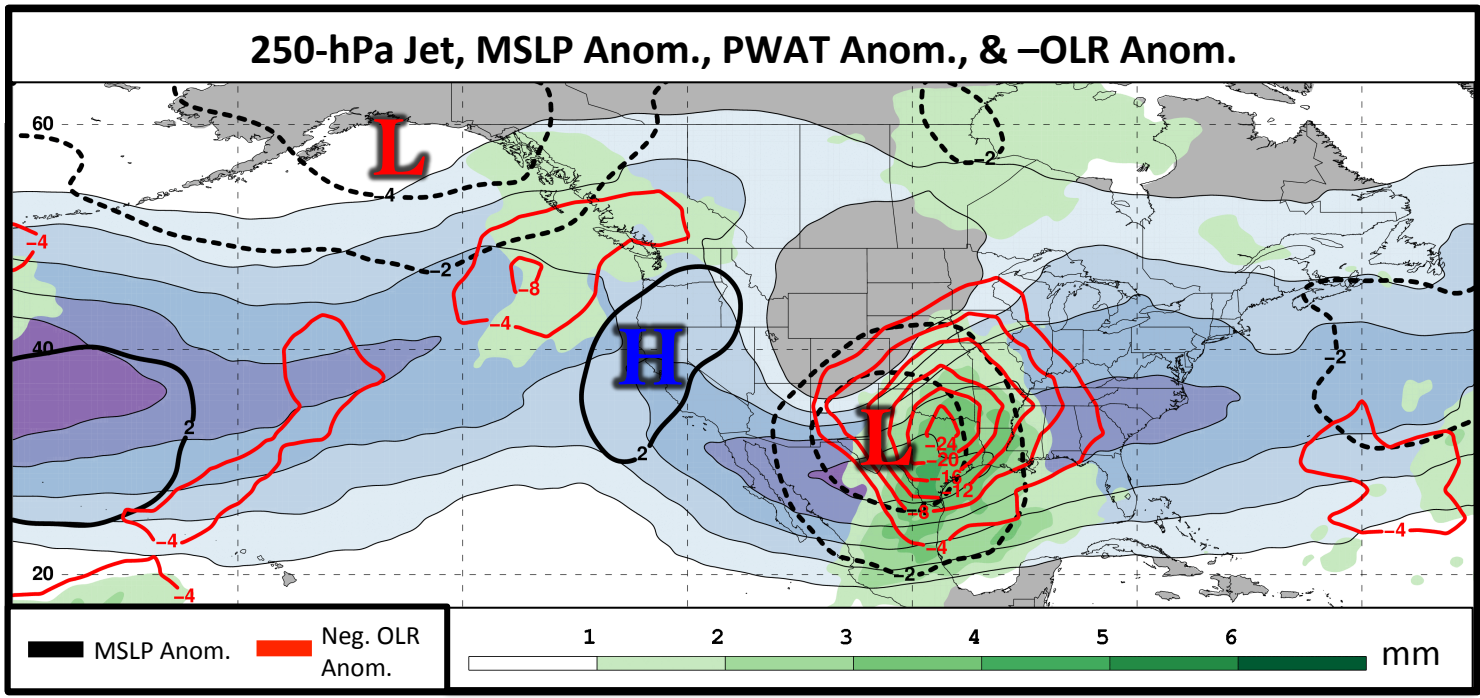
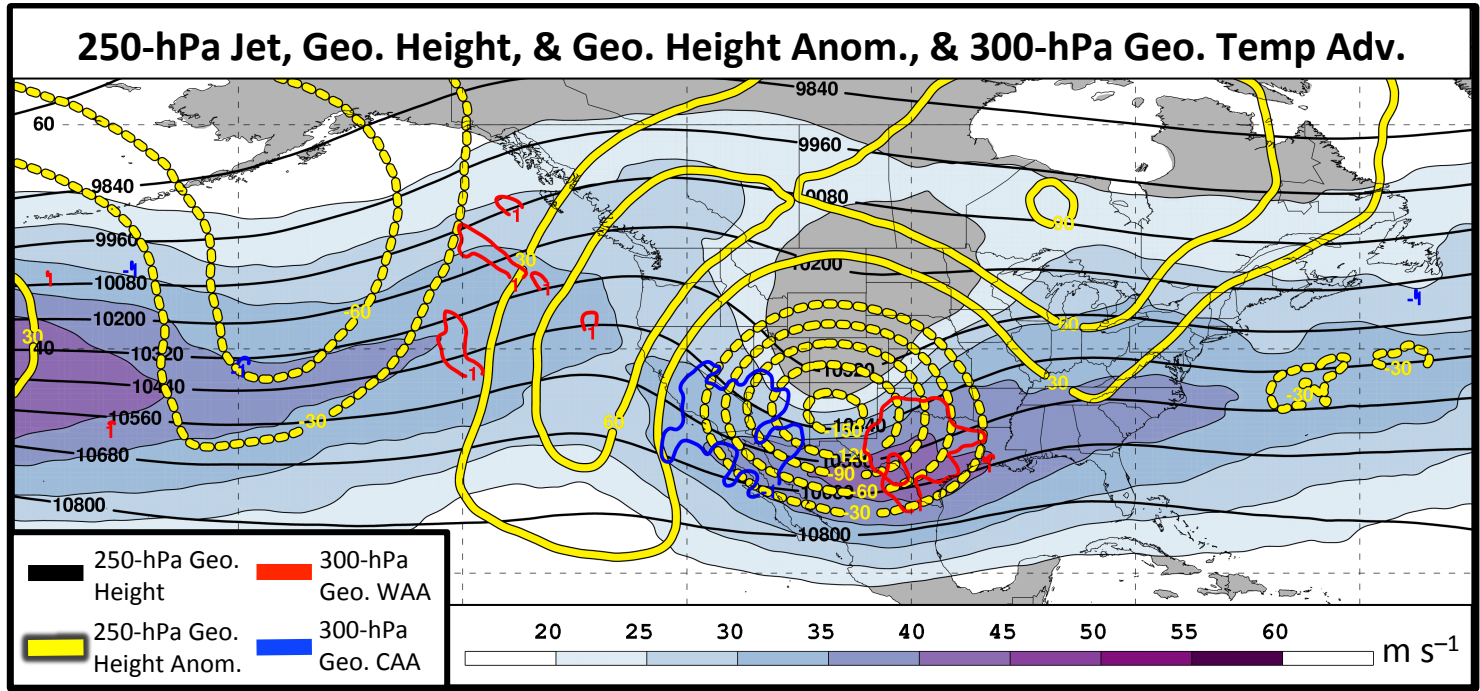
2 Days
Prior to Jet
Superposition



N=80

Polar Dominant Jet Superposition Events

1 Day
Prior to Jet
Superposition



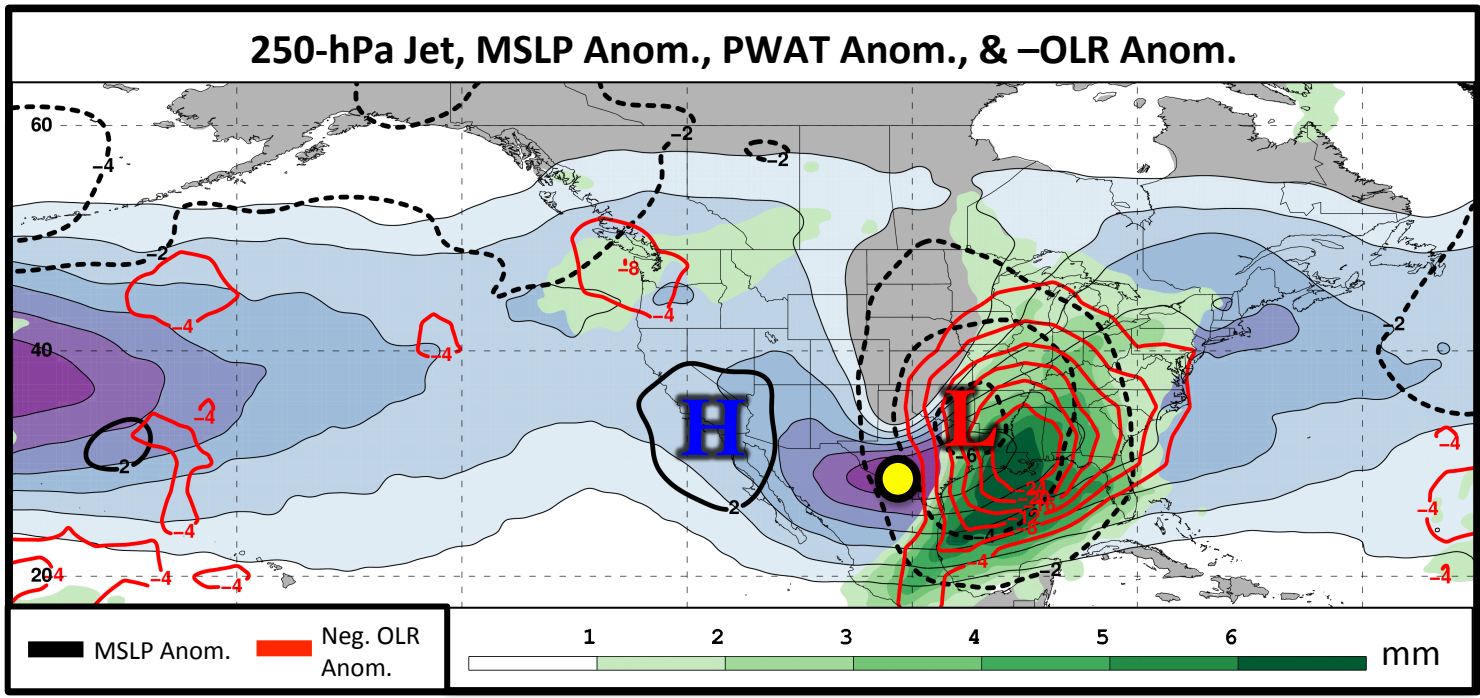
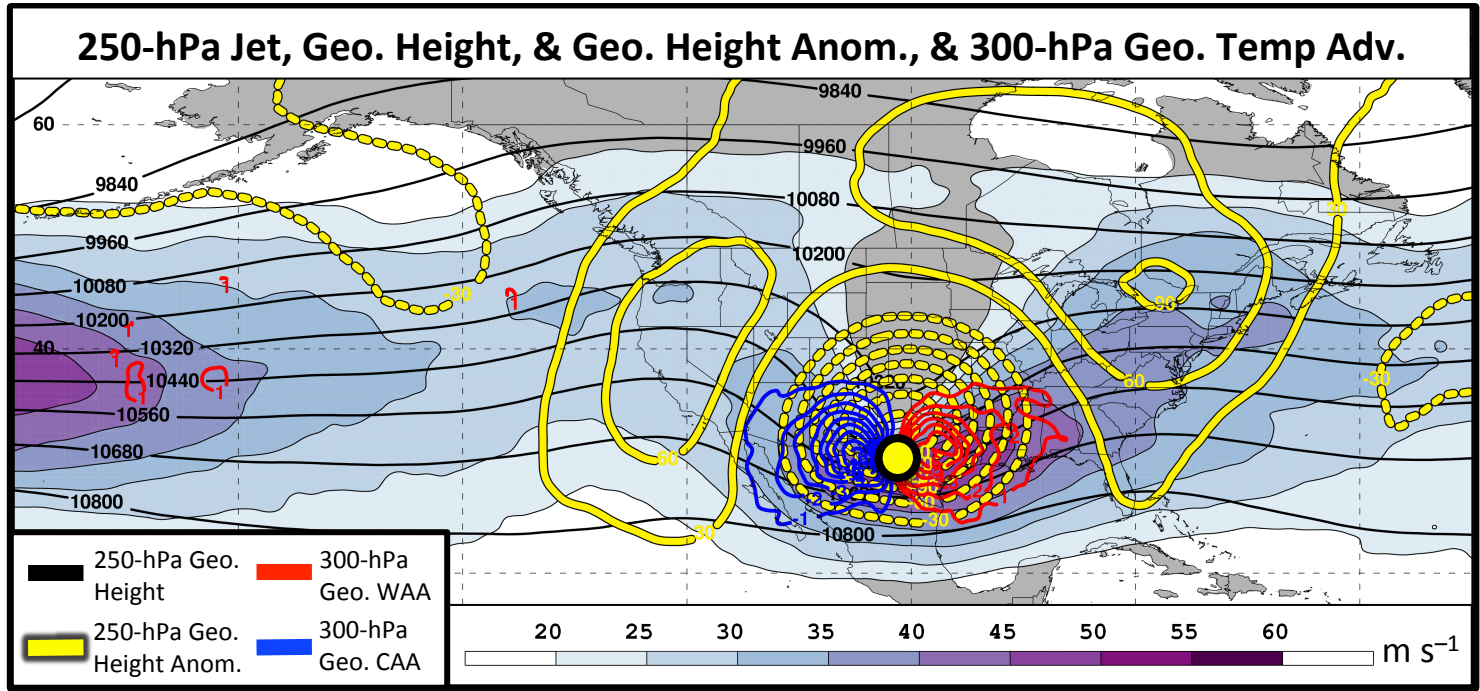
N=80

Polar Dominant Jet Superposition Events

0 Days
Prior to Jet
Superposition

Average
Location of
Superposition

N=80

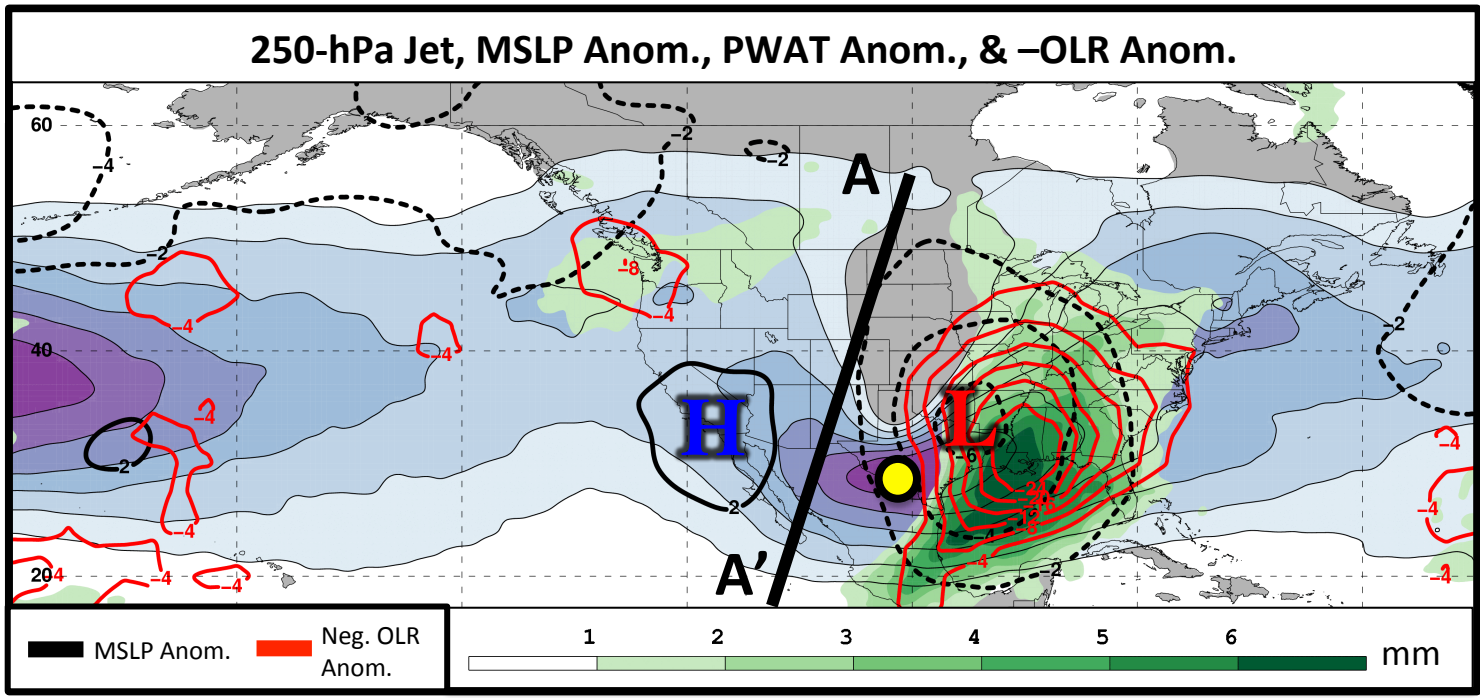
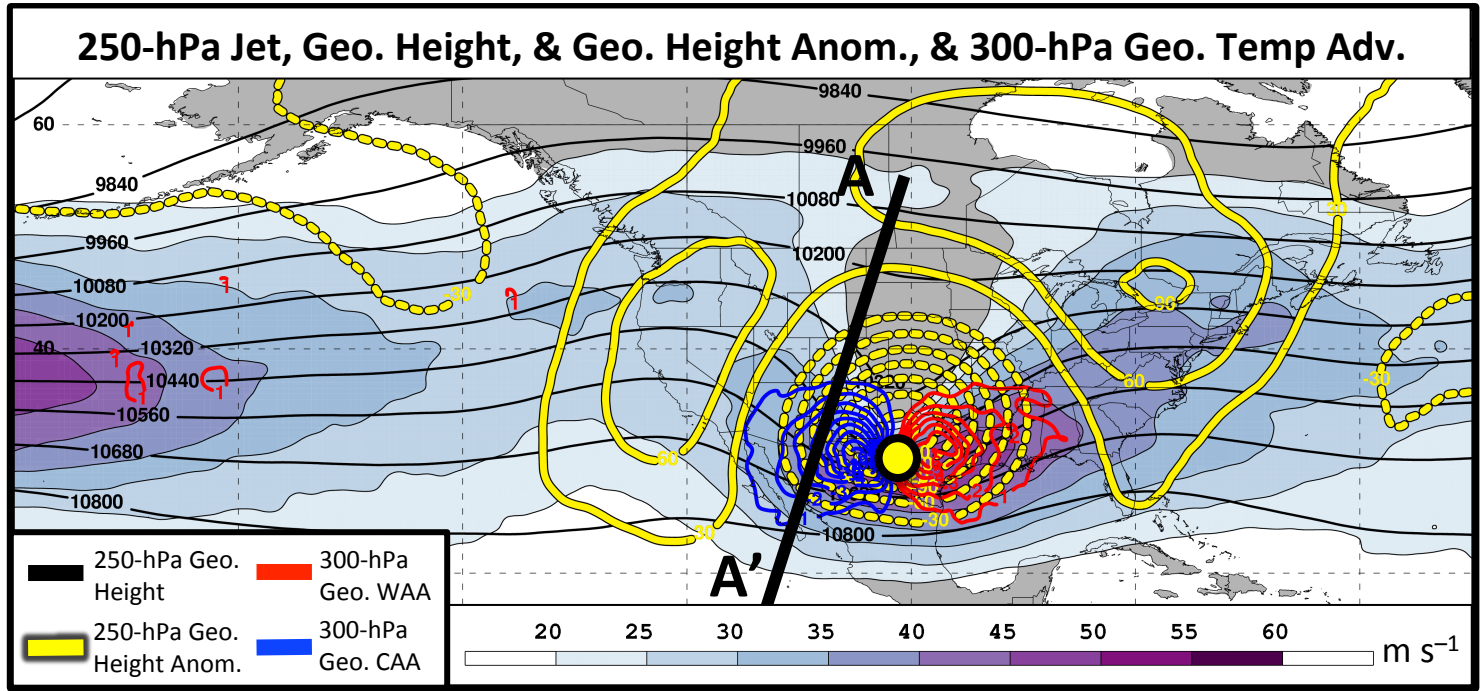


Polar Dominant Jet Superposition Events

0 Days
Prior to Jet
Superposition

Average
Location of
Superposition

N=80

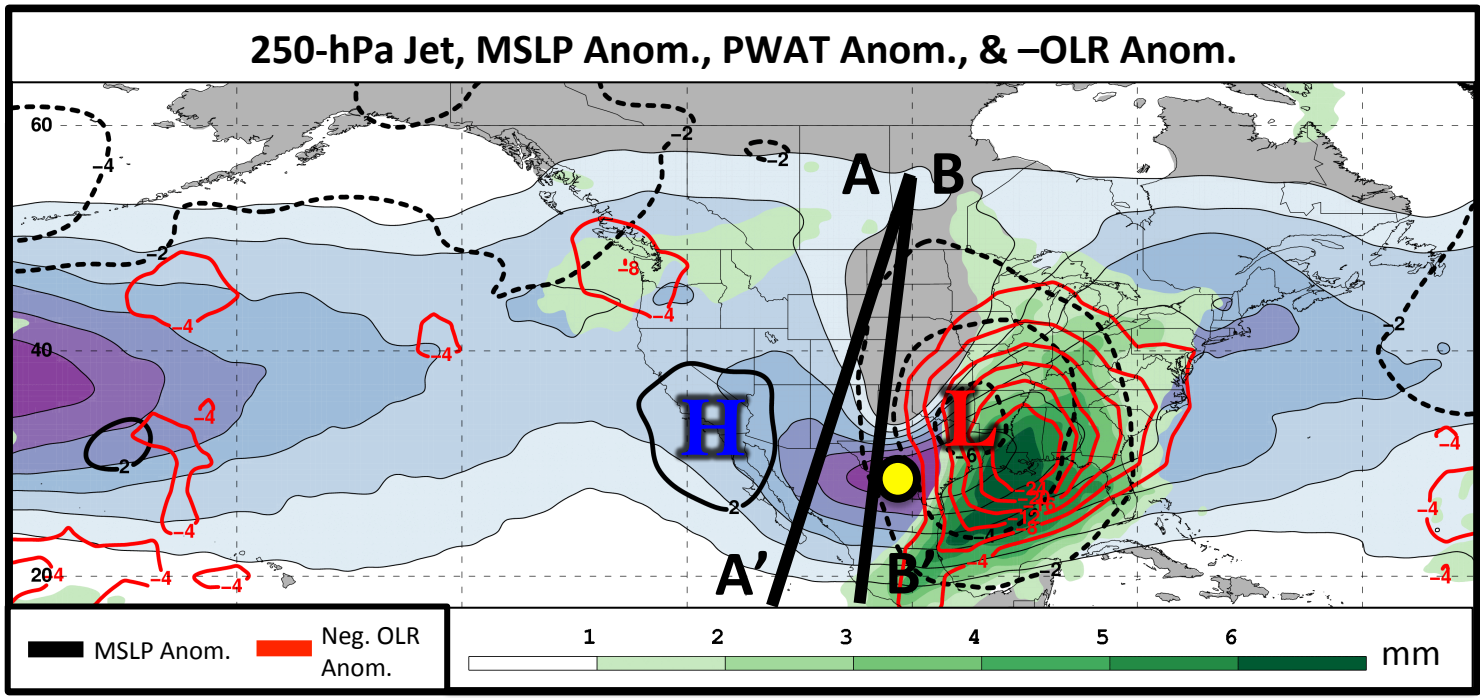
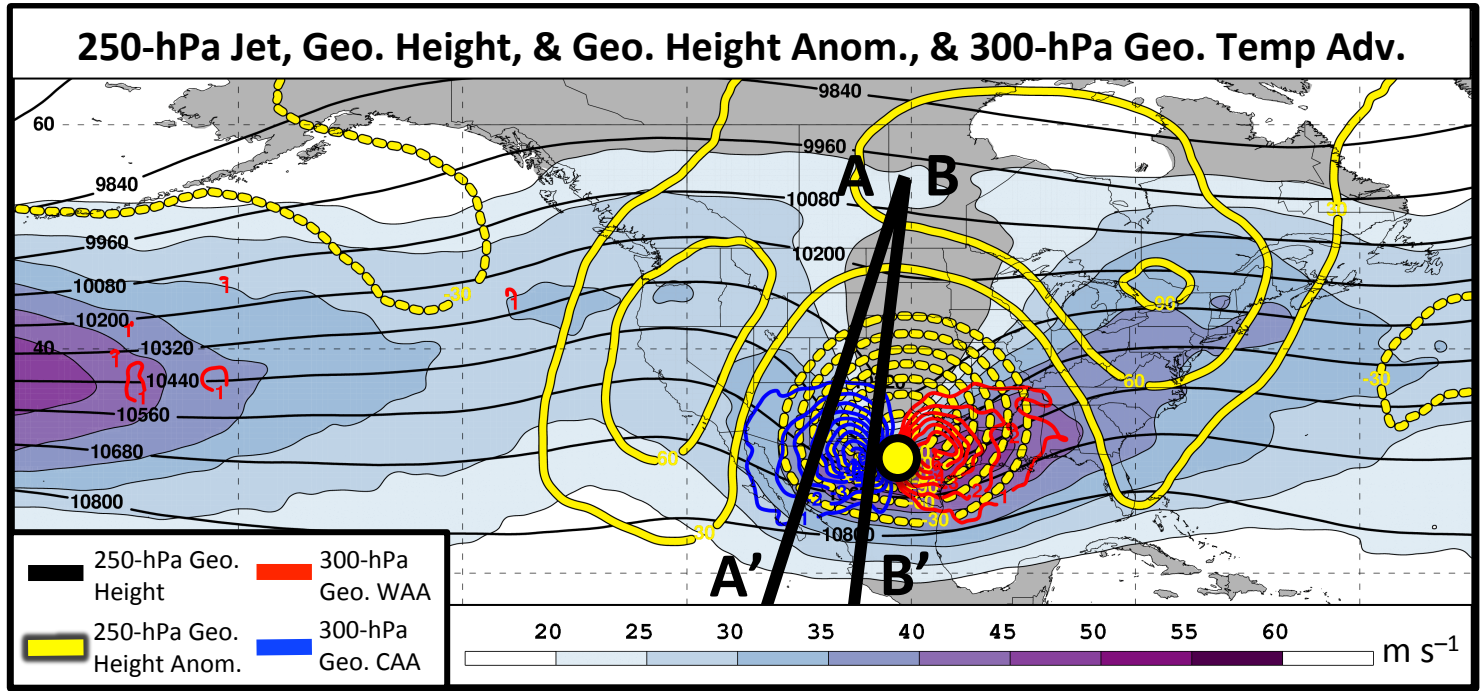


Polar Dominant Jet Superposition Events

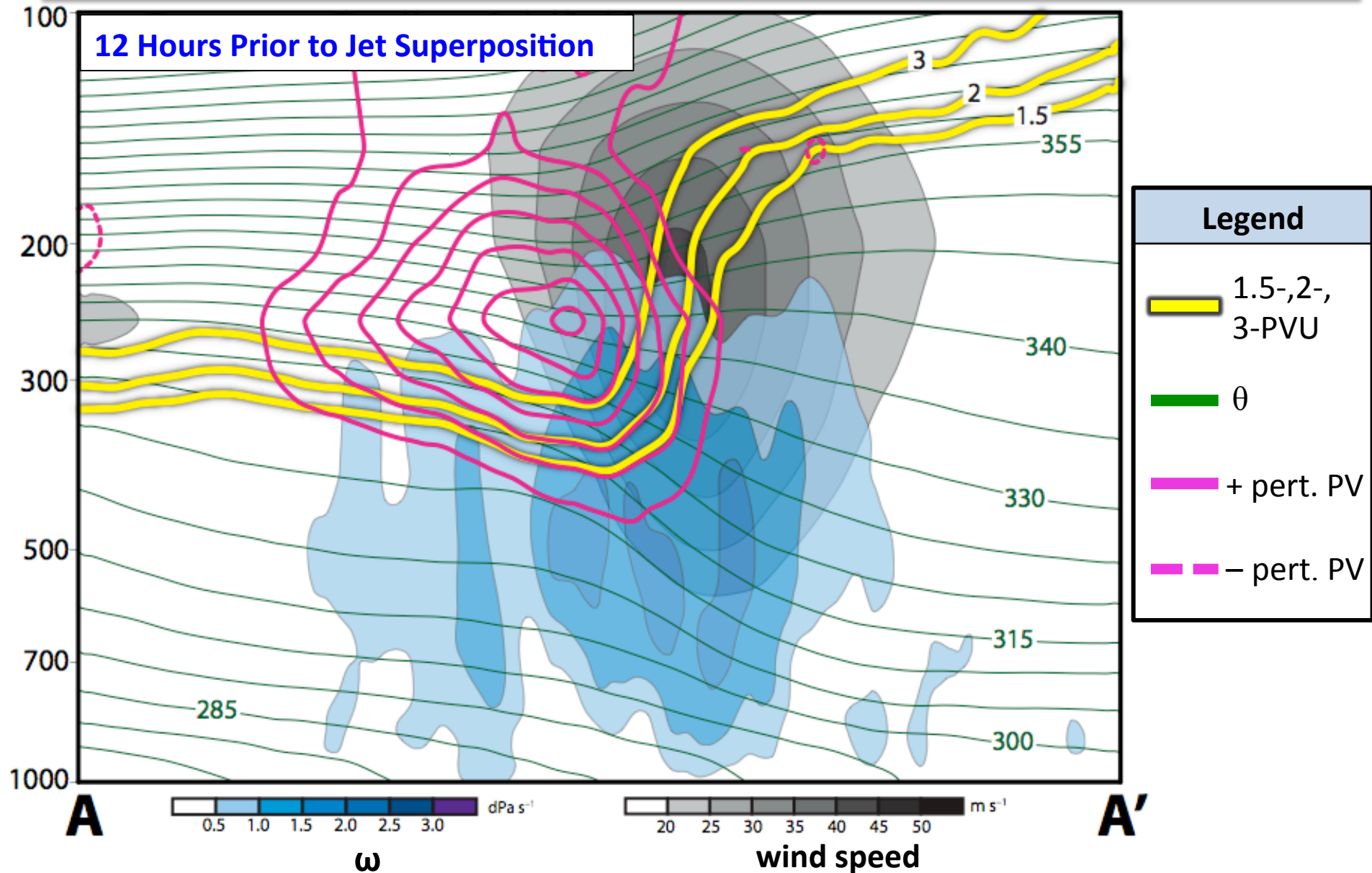
0 Days
Prior to Jet
Superposition

Average
Location of
Superposition

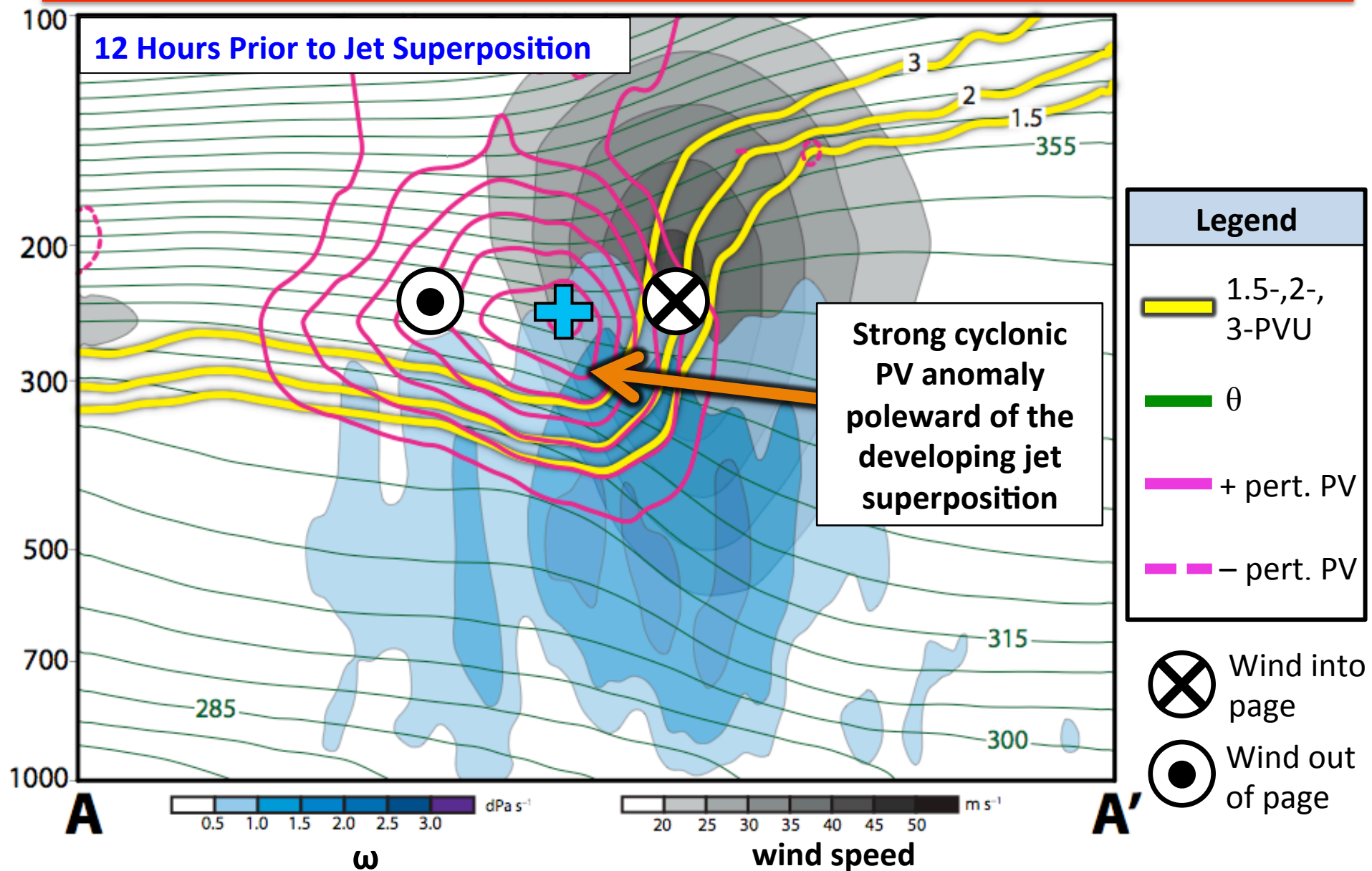
N=80



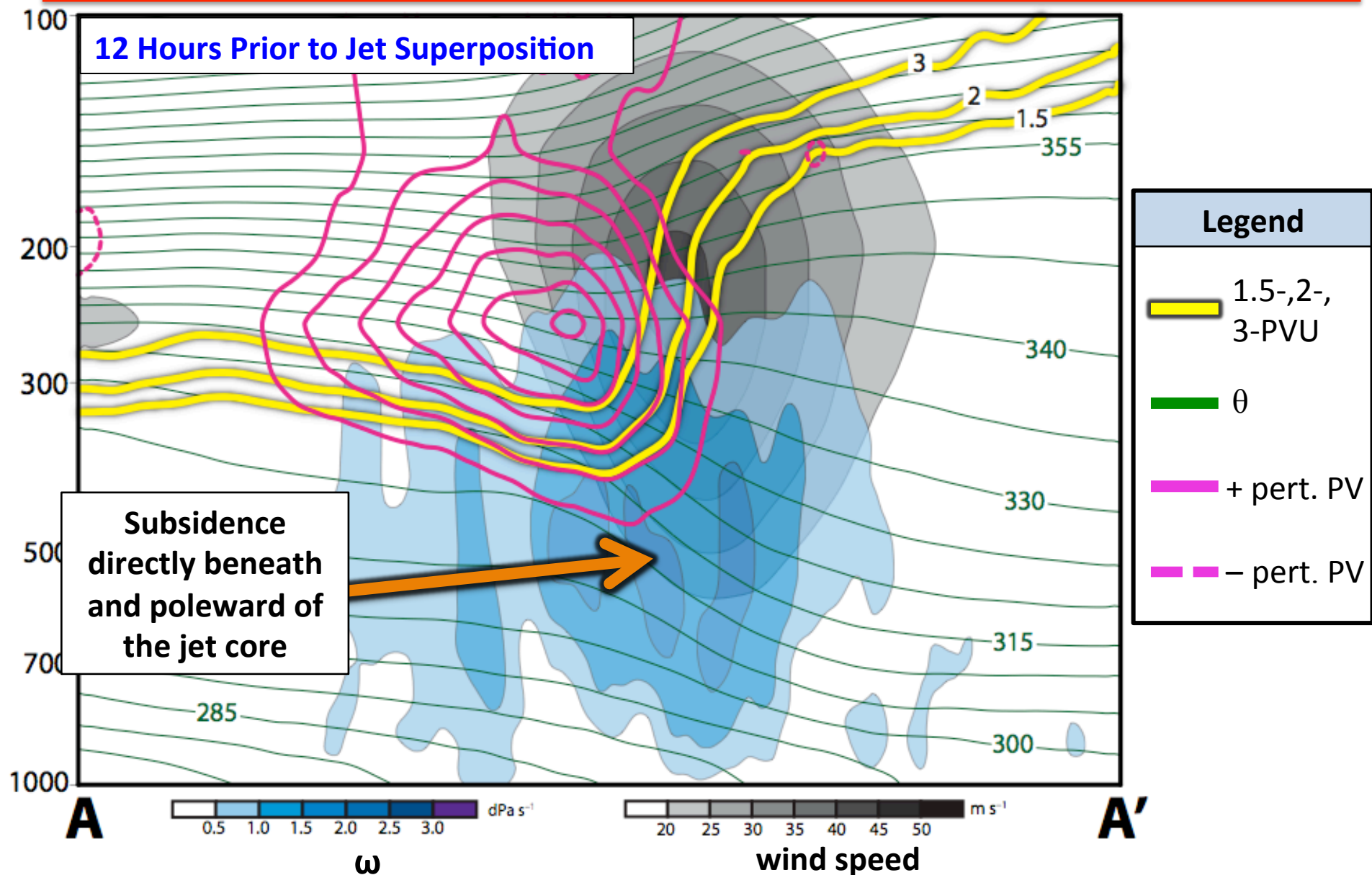
Polar Dominant Jet Superposition Events



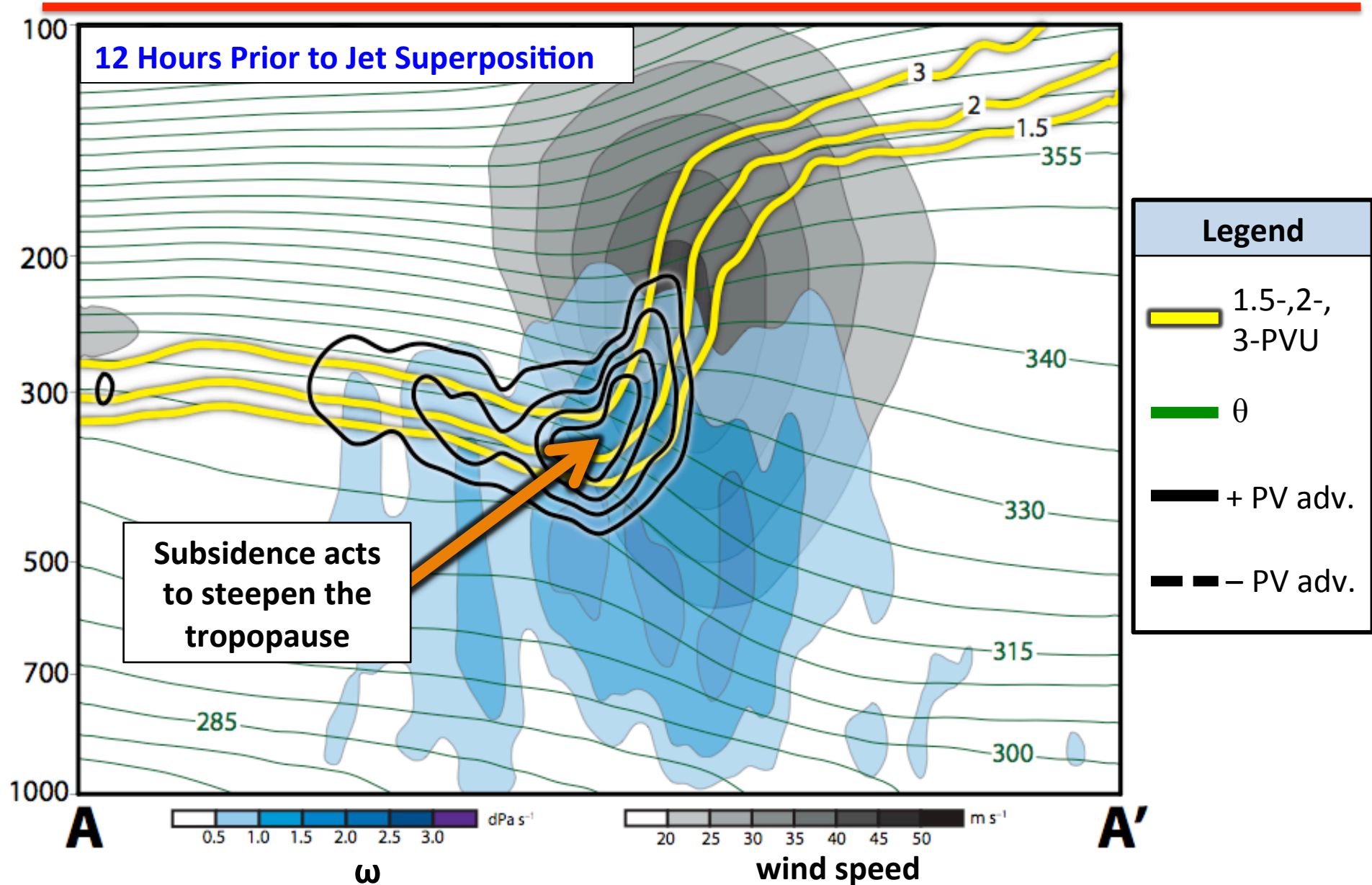
Polar Dominant Jet Superposition Events



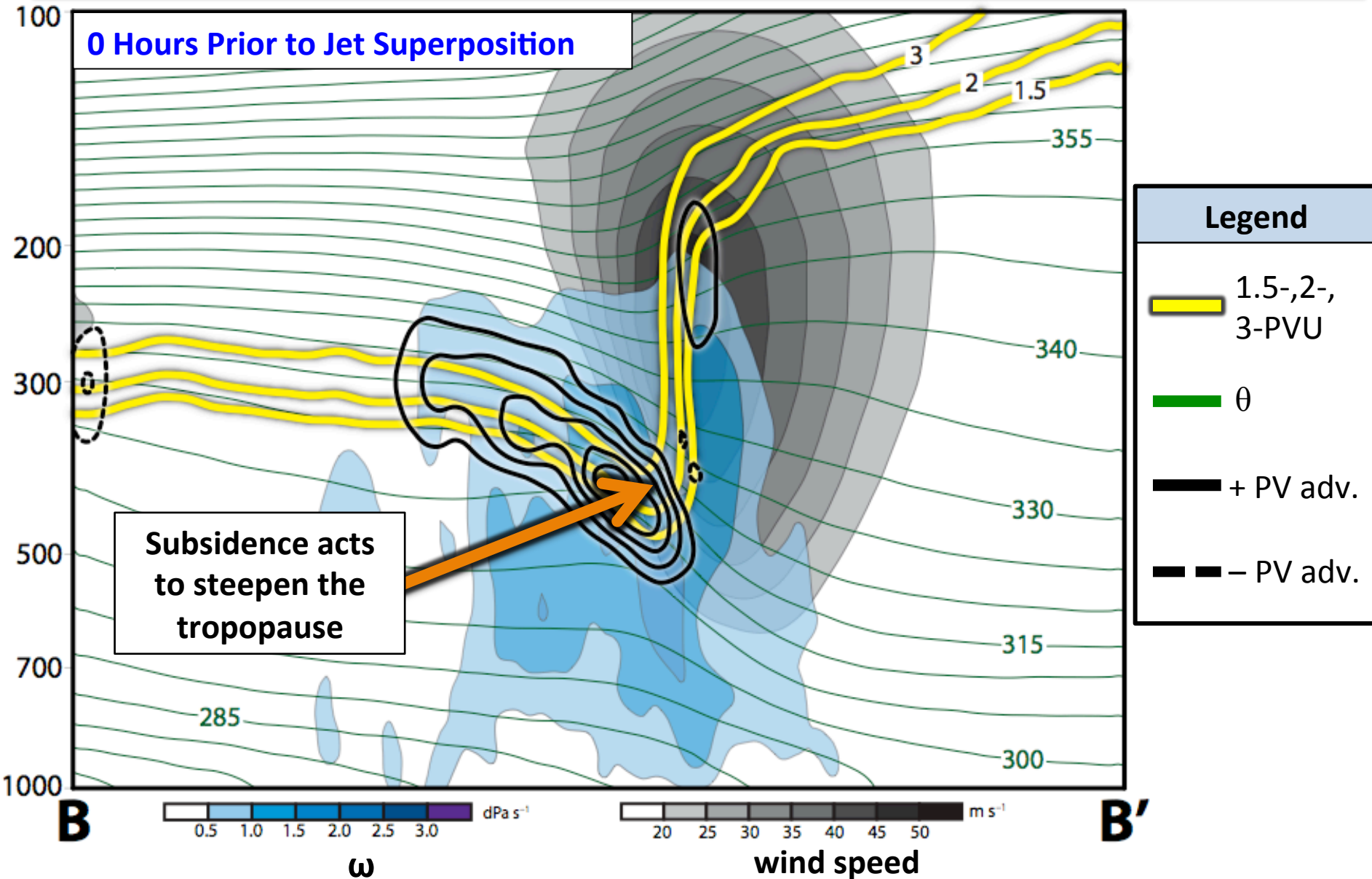
Polar Dominant Jet Superposition Events



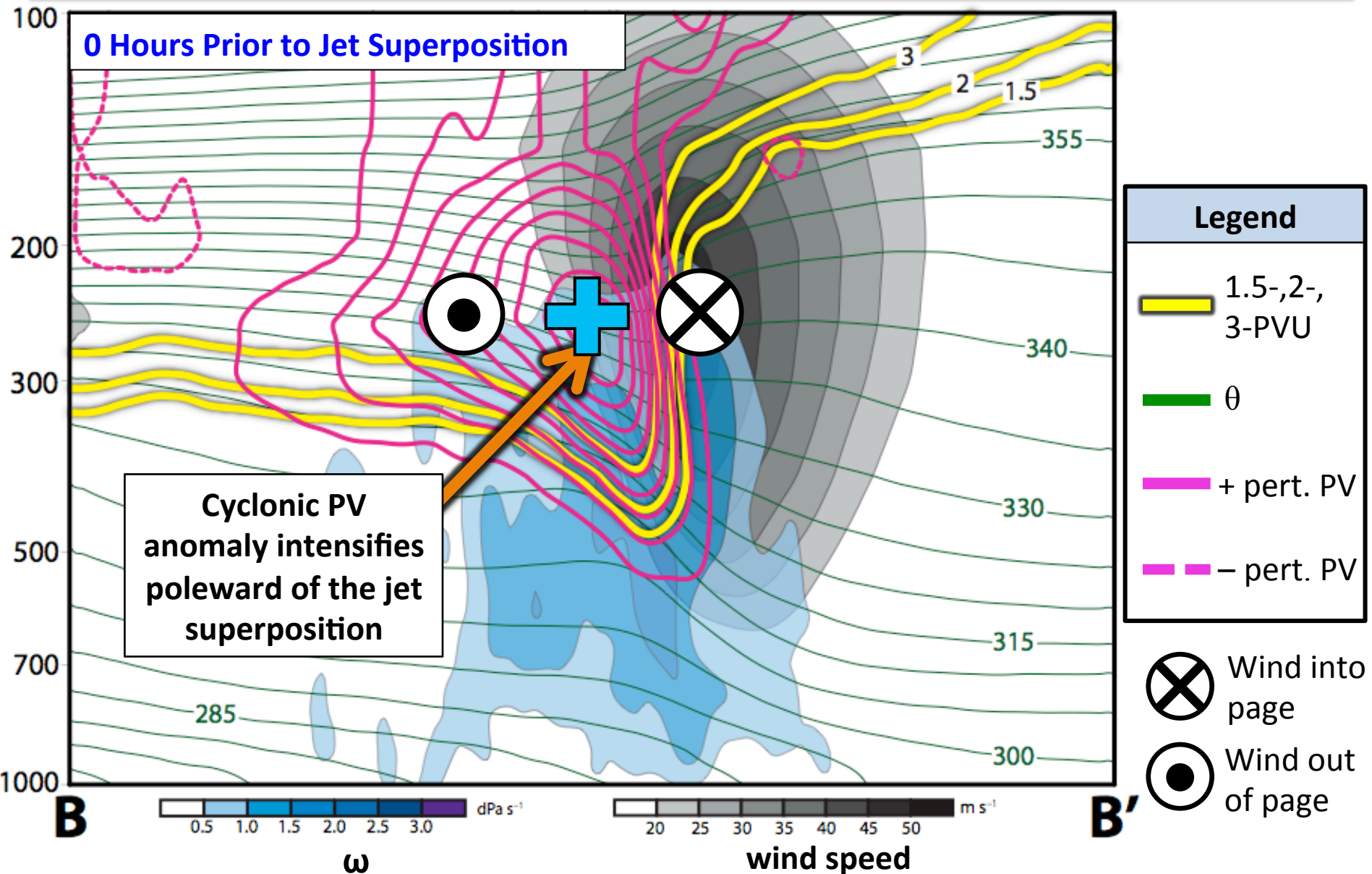
Polar Dominant Jet Superposition Events



Polar Dominant Jet Superposition Events

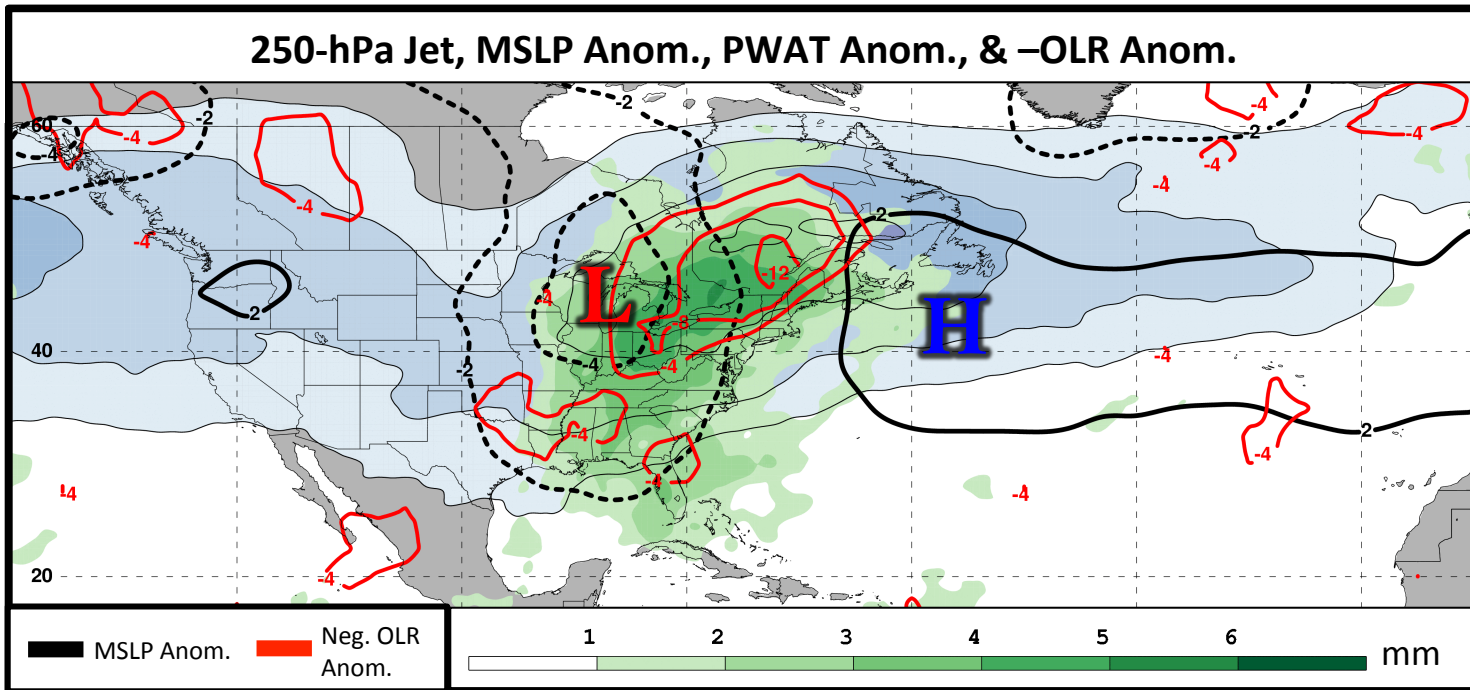
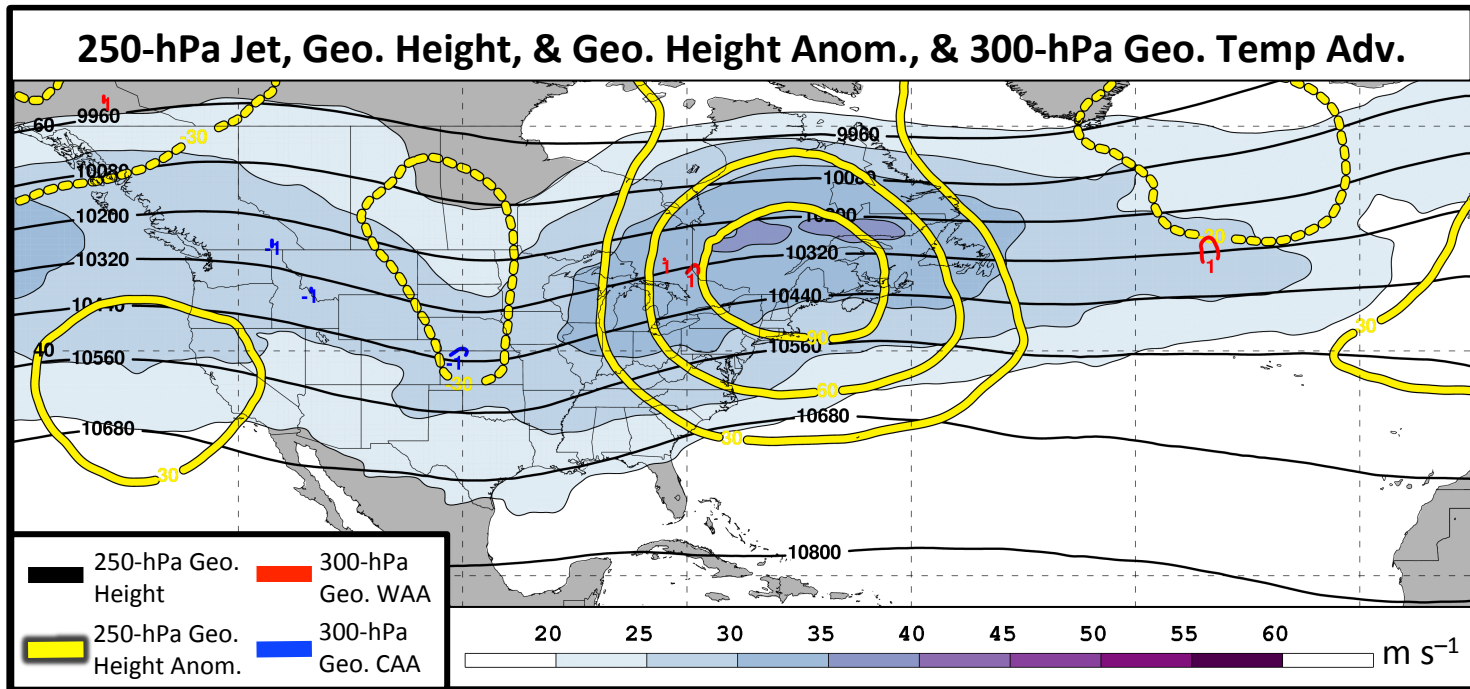


Polar Dominant Jet Superposition Events



E. Subtropical Dominant Jet Superposition Events

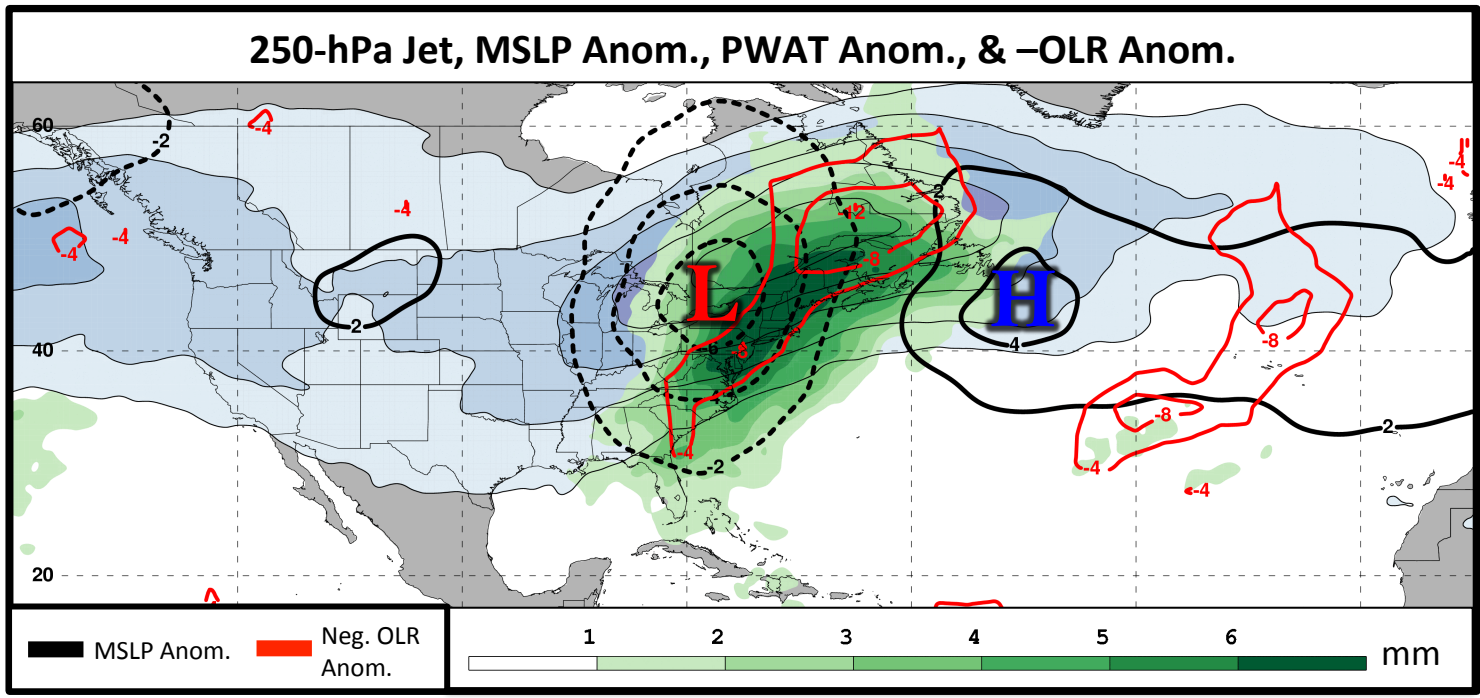
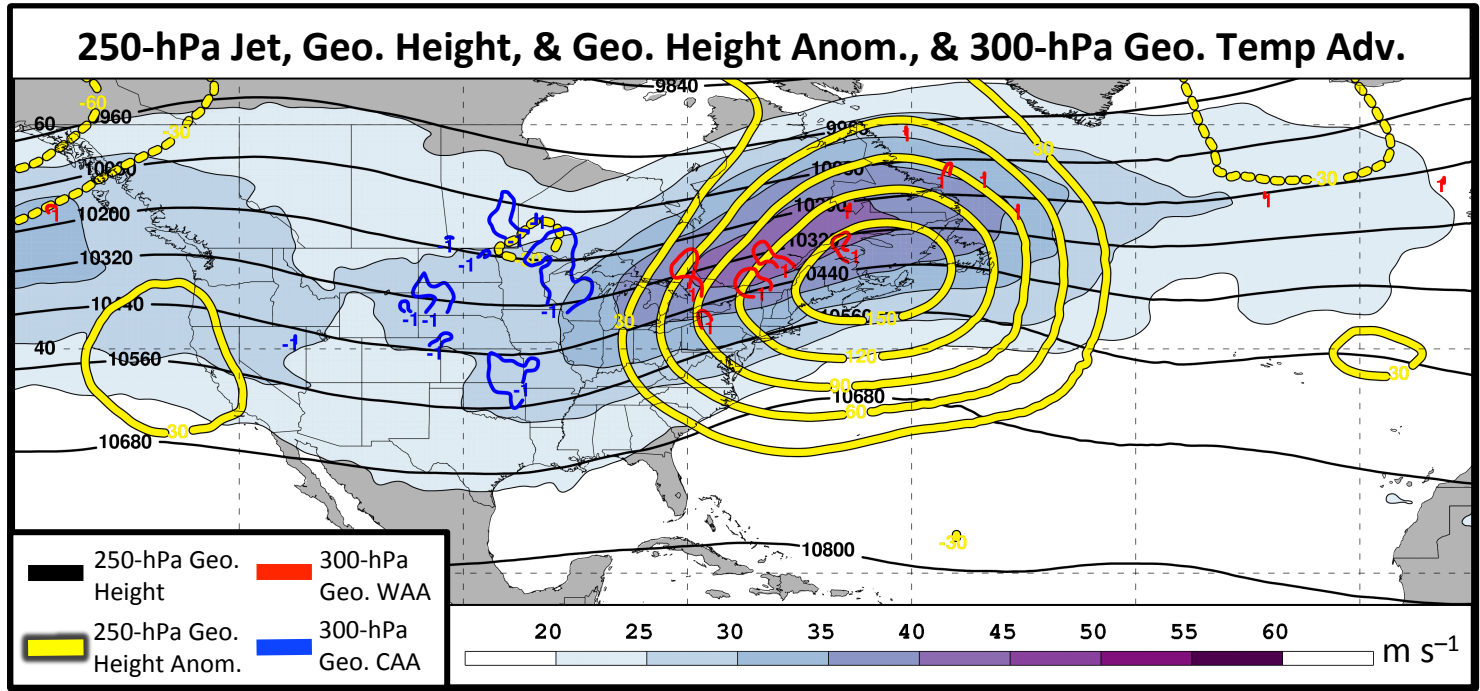
2 Days
Prior to Jet
Superposition



N=76

E. Subtropical Dominant Jet Superposition Events

1 Day Prior to Jet Superposition



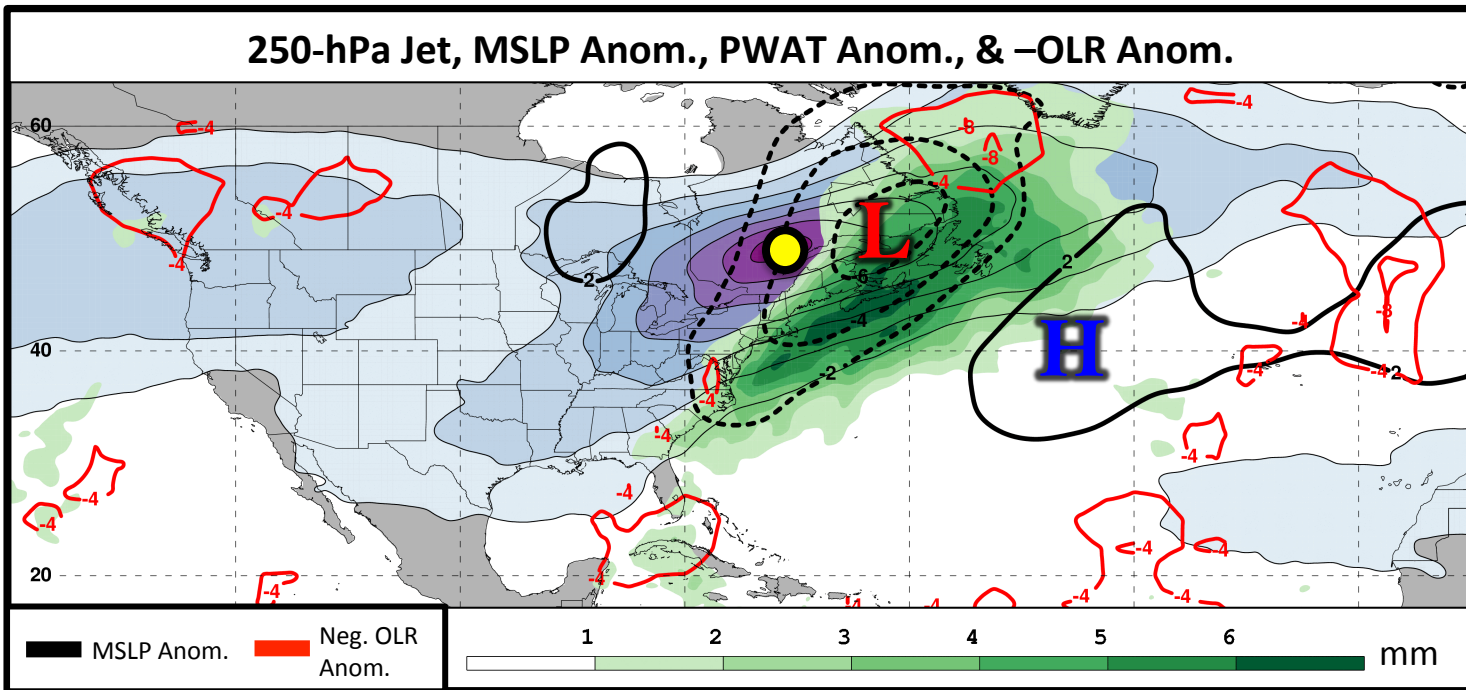
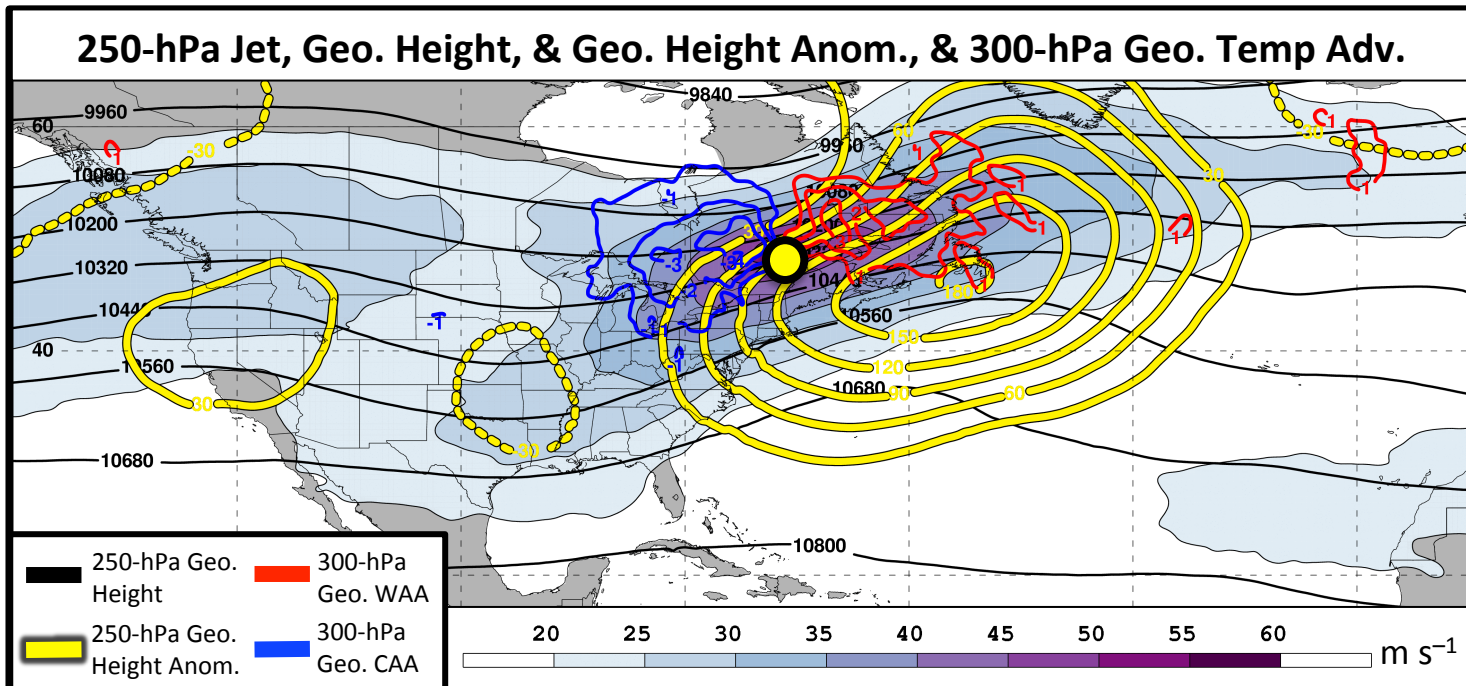
N=76

E. Subtropical Dominant Jet Superposition Events

0 Days
Prior to Jet
Superposition

Average
Location of
Superposition

N=76

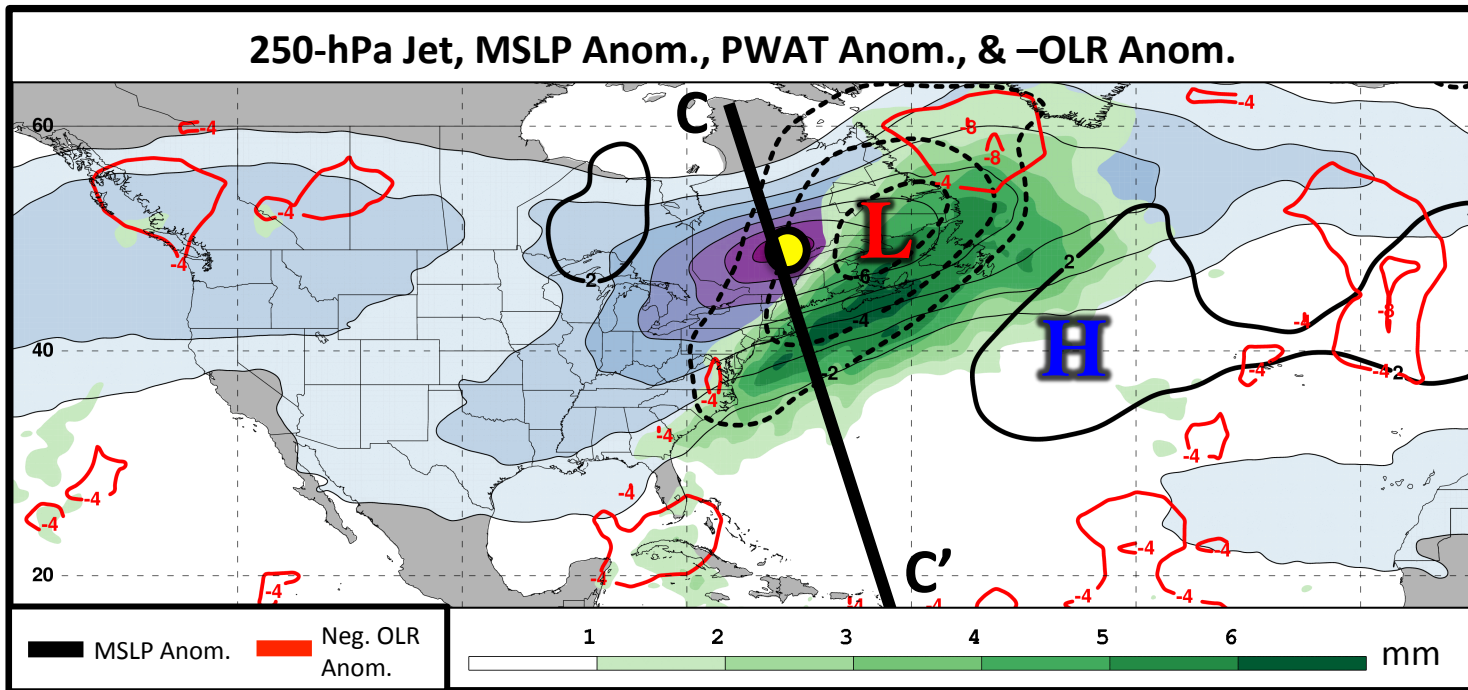
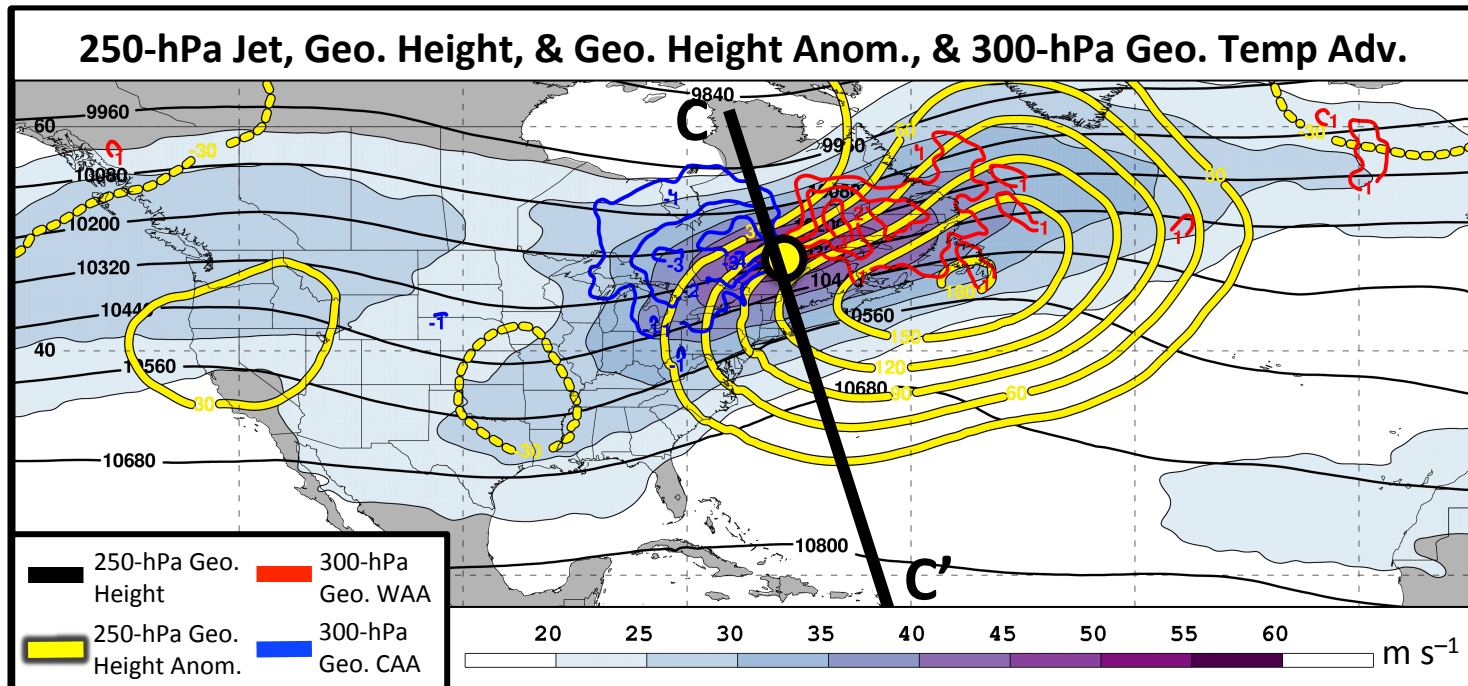


E. Subtropical Dominant Jet Superposition Events

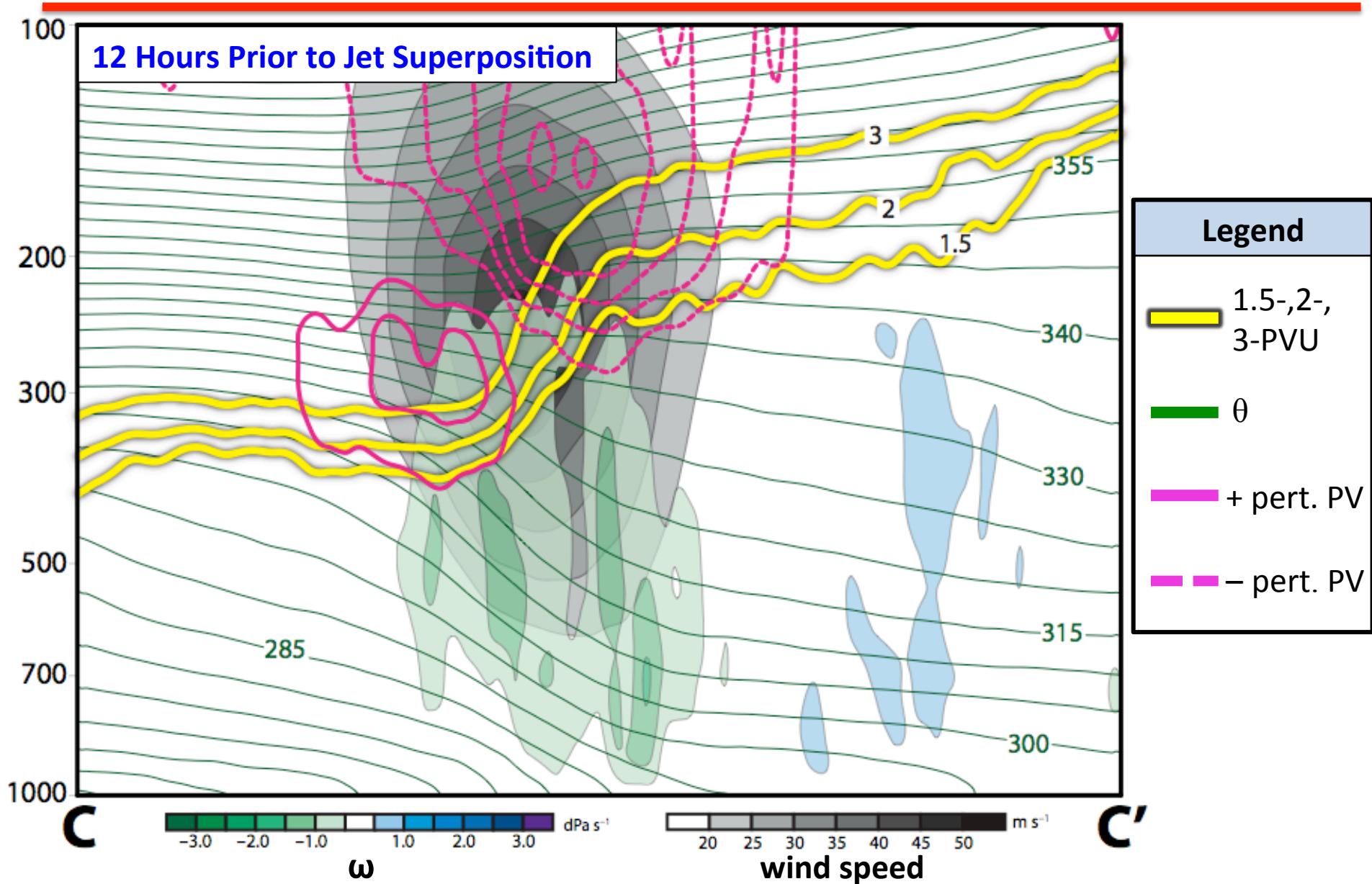
0 Days
Prior to Jet
Superposition

Average
Location of
Superposition

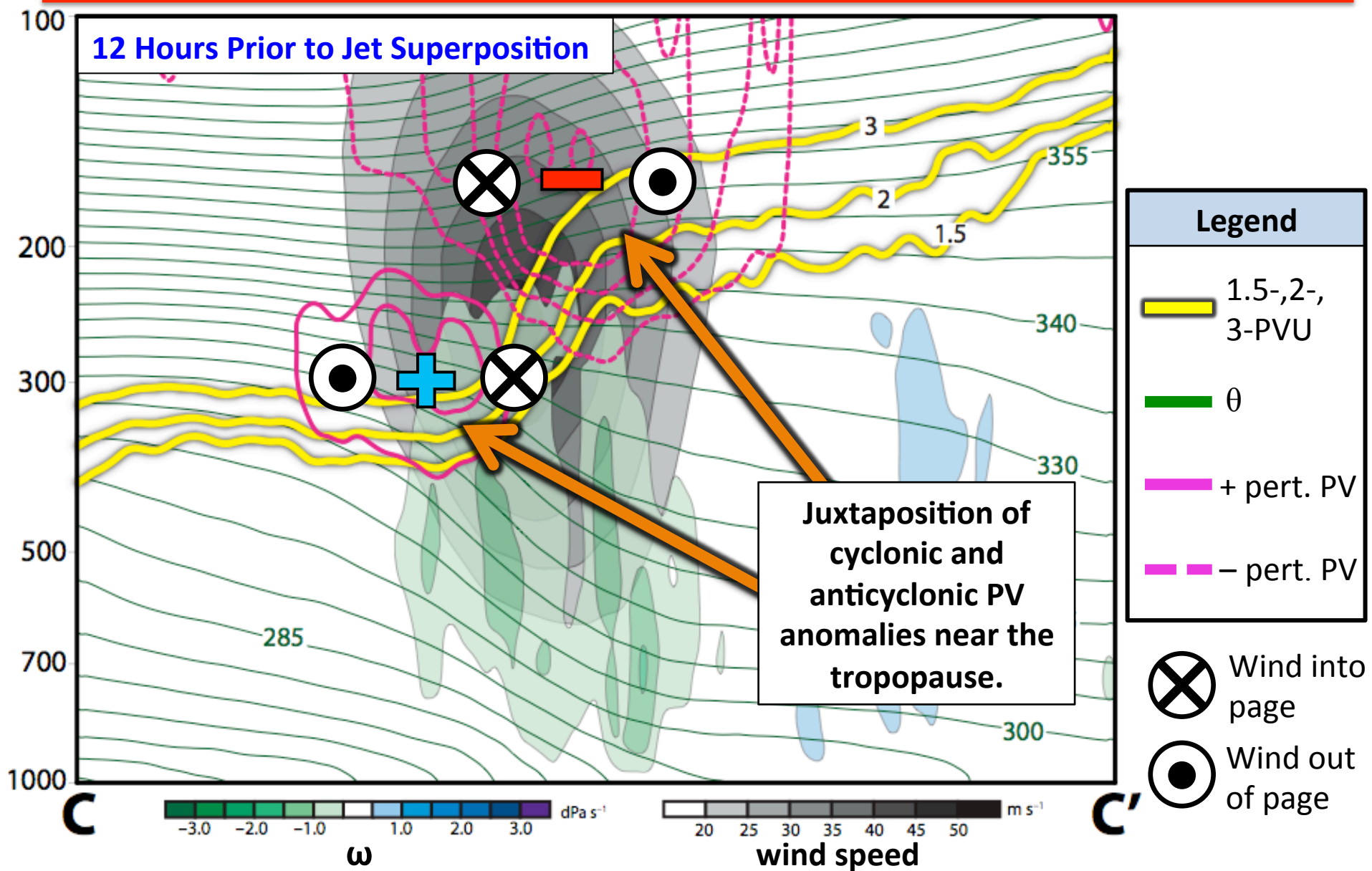
N=76



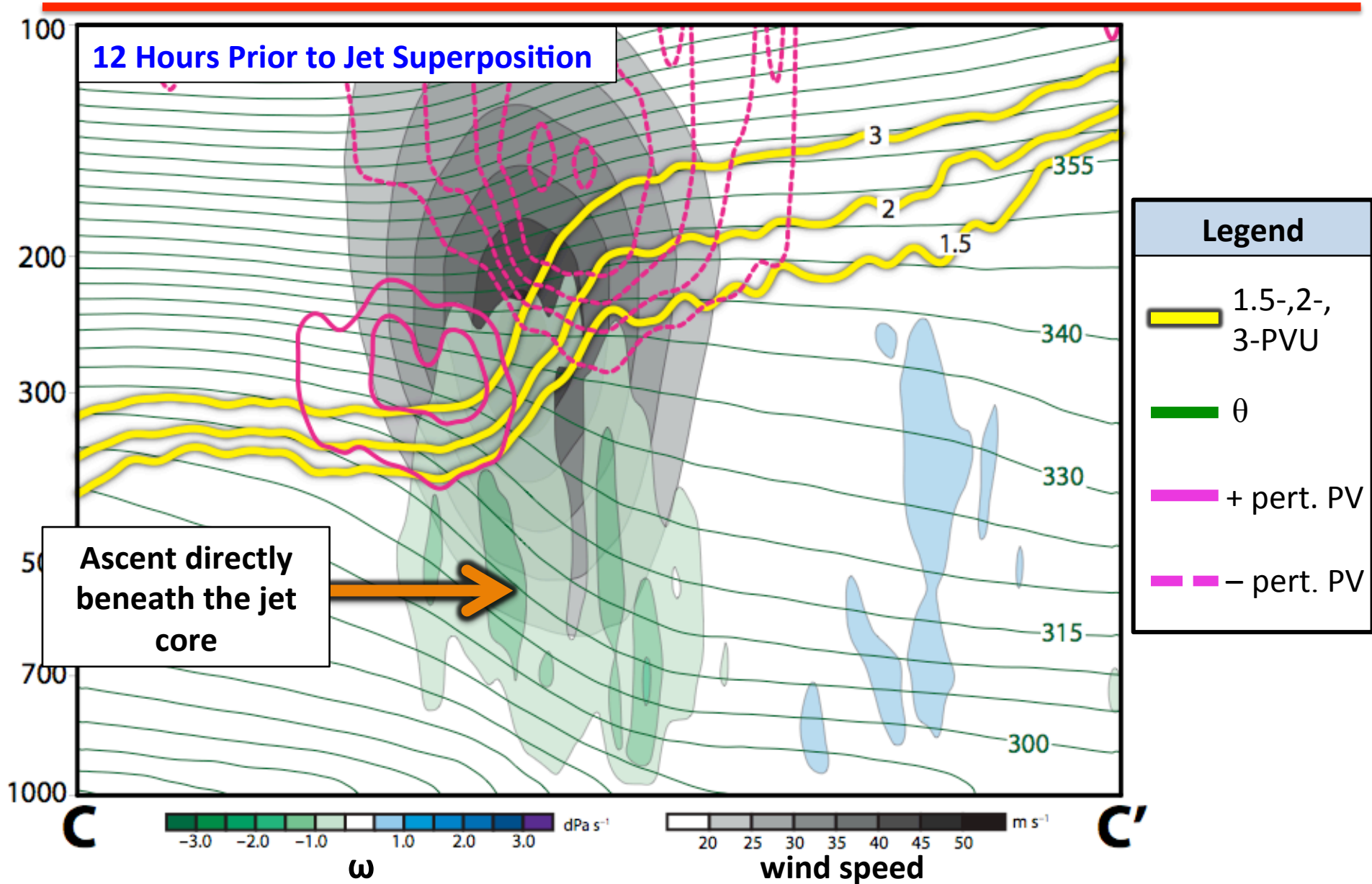
E. Subtropical Dominant Jet Superposition Events



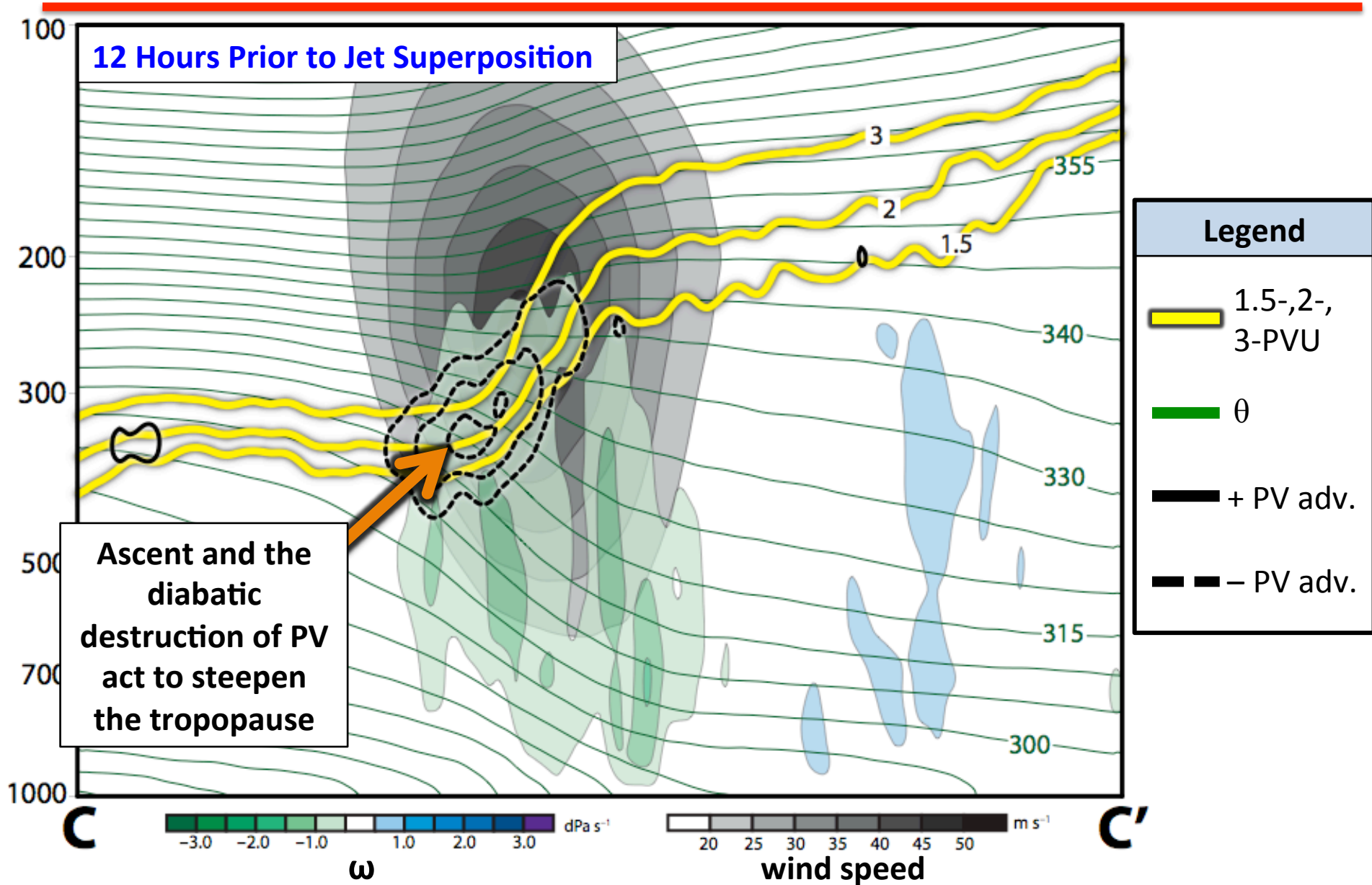
E. Subtropical Dominant Jet Superposition Events



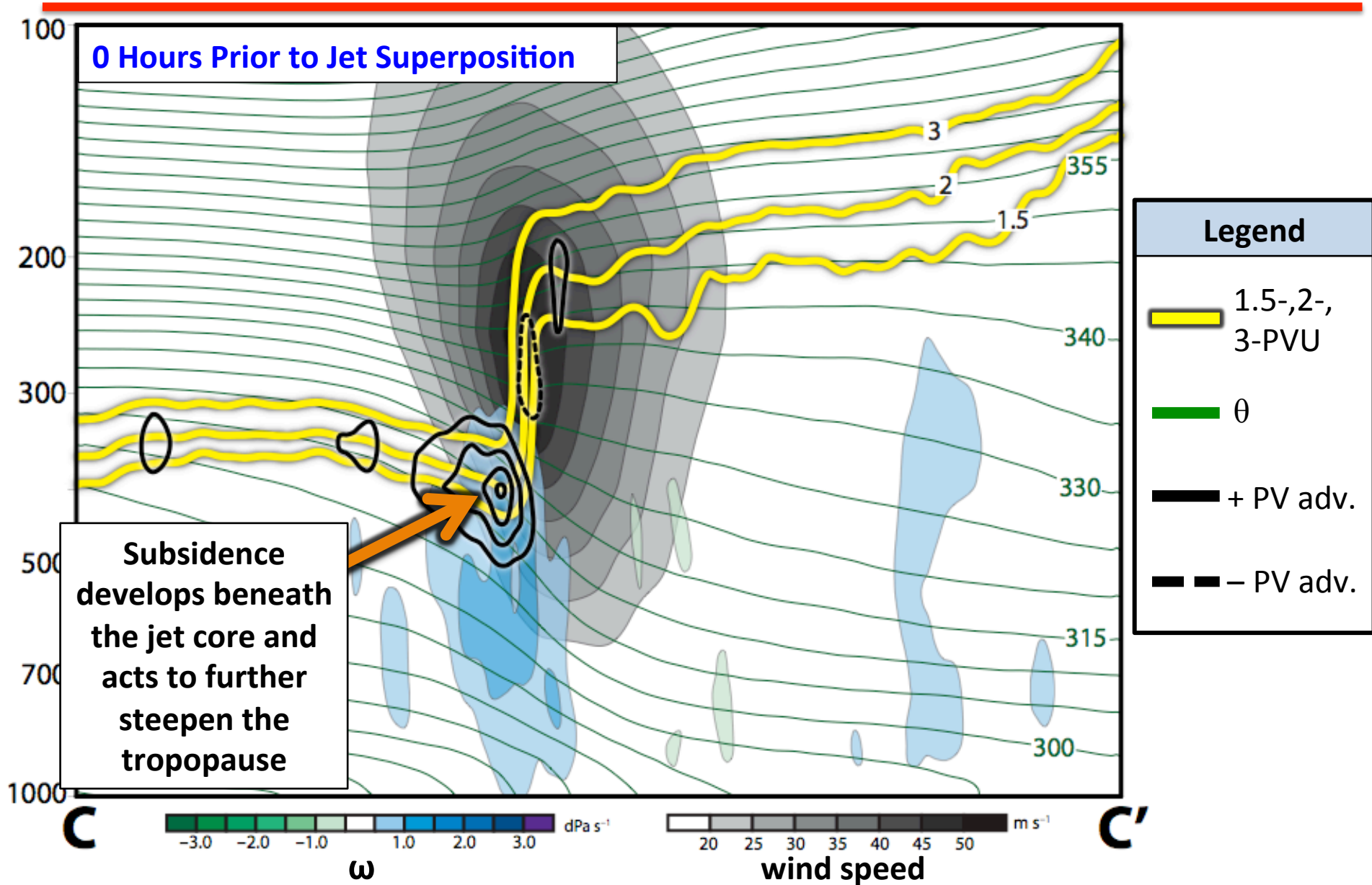
E. Subtropical Dominant Jet Superposition Events



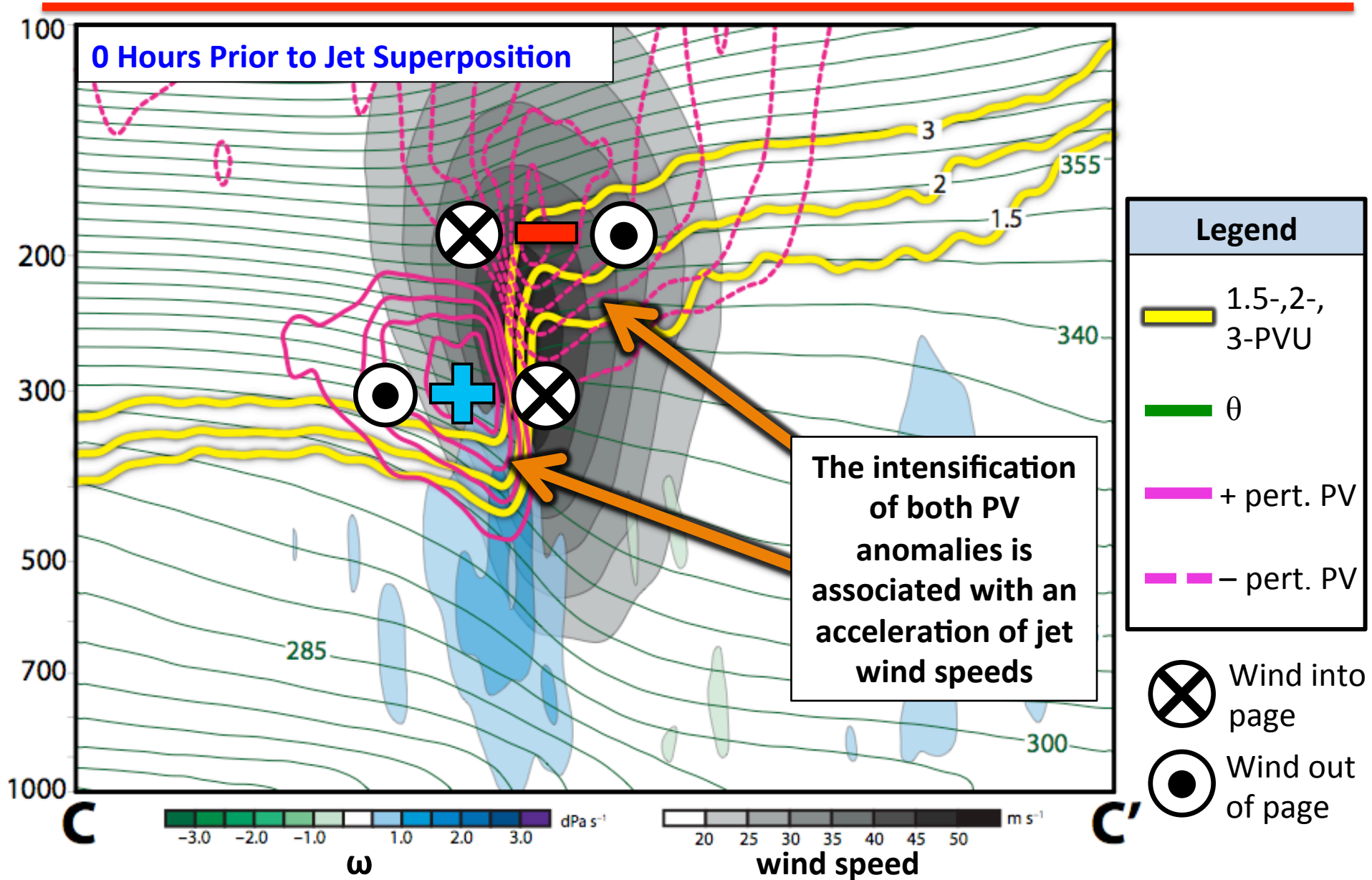
E. Subtropical Dominant Jet Superposition Events



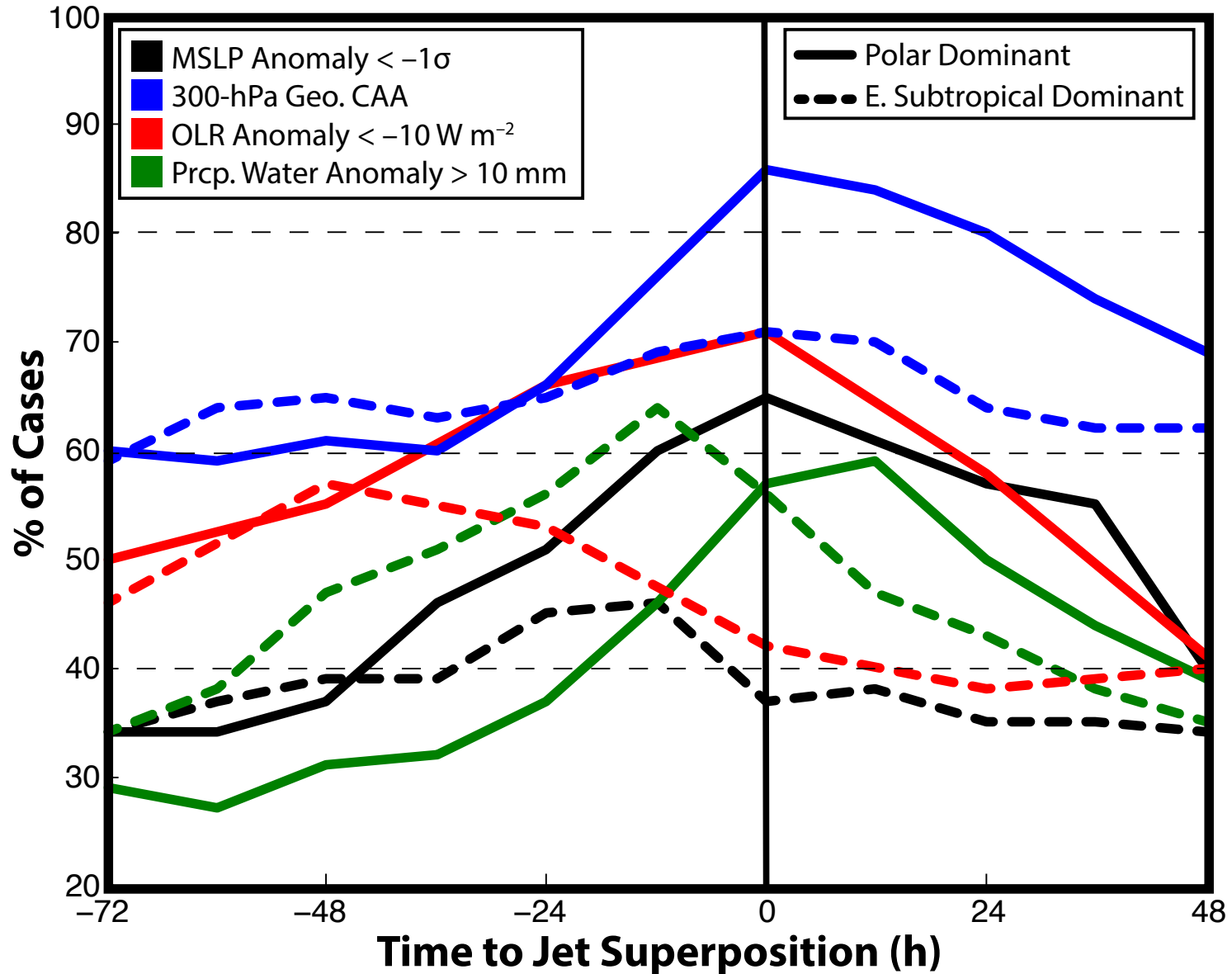
E. Subtropical Dominant Jet Superposition Events



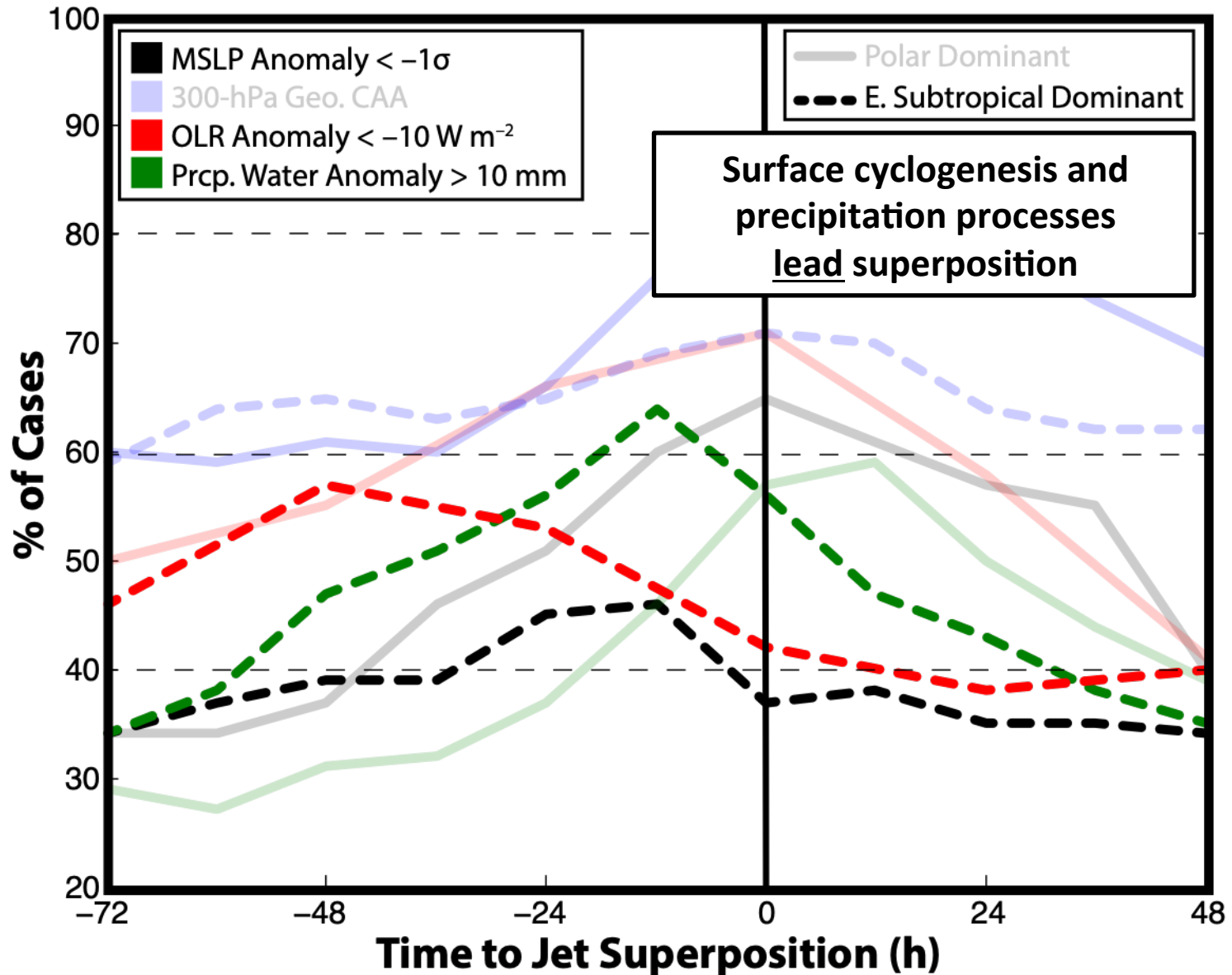
E. Subtropical Dominant Jet Superposition Events



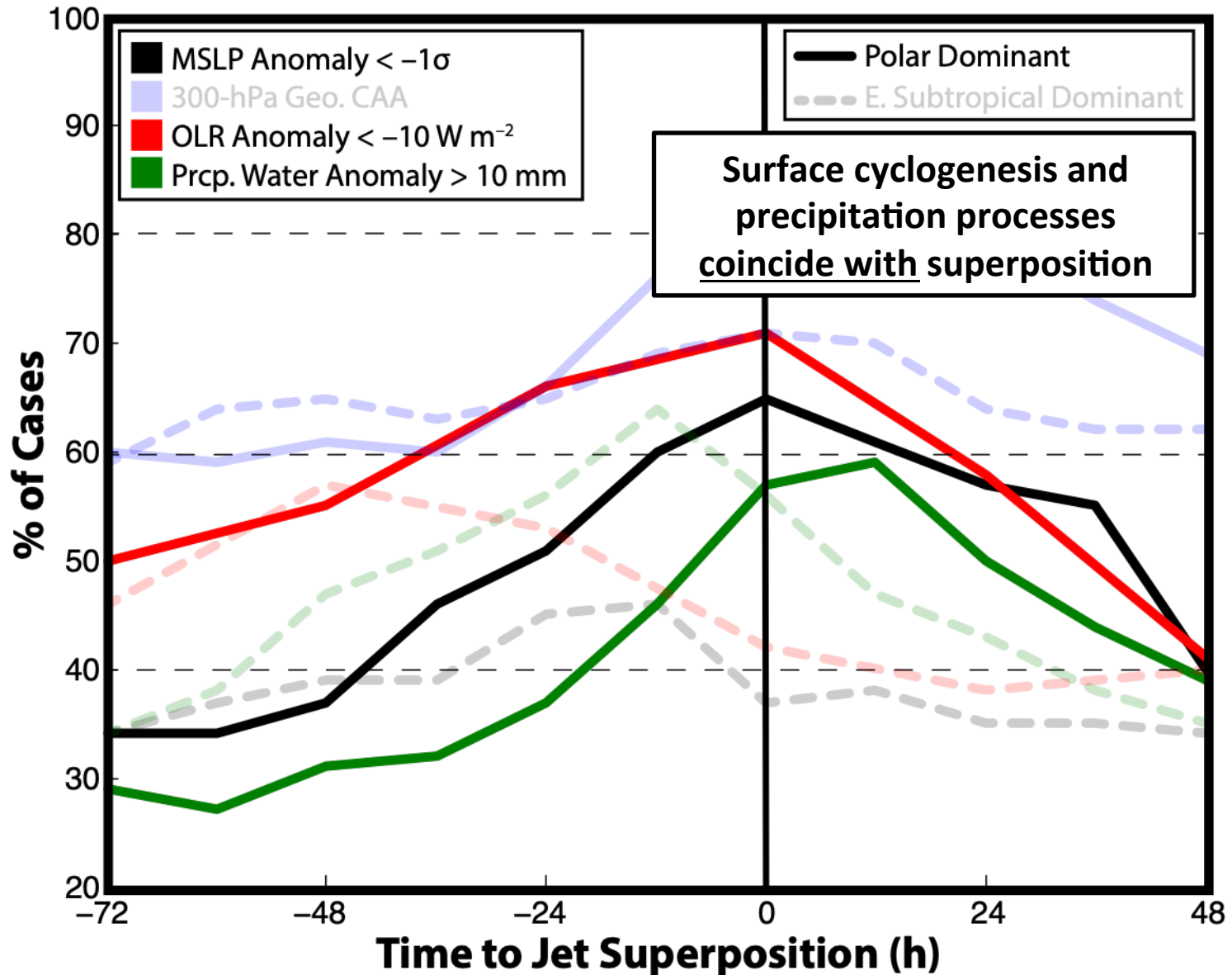
Jet Superposition Event Composites



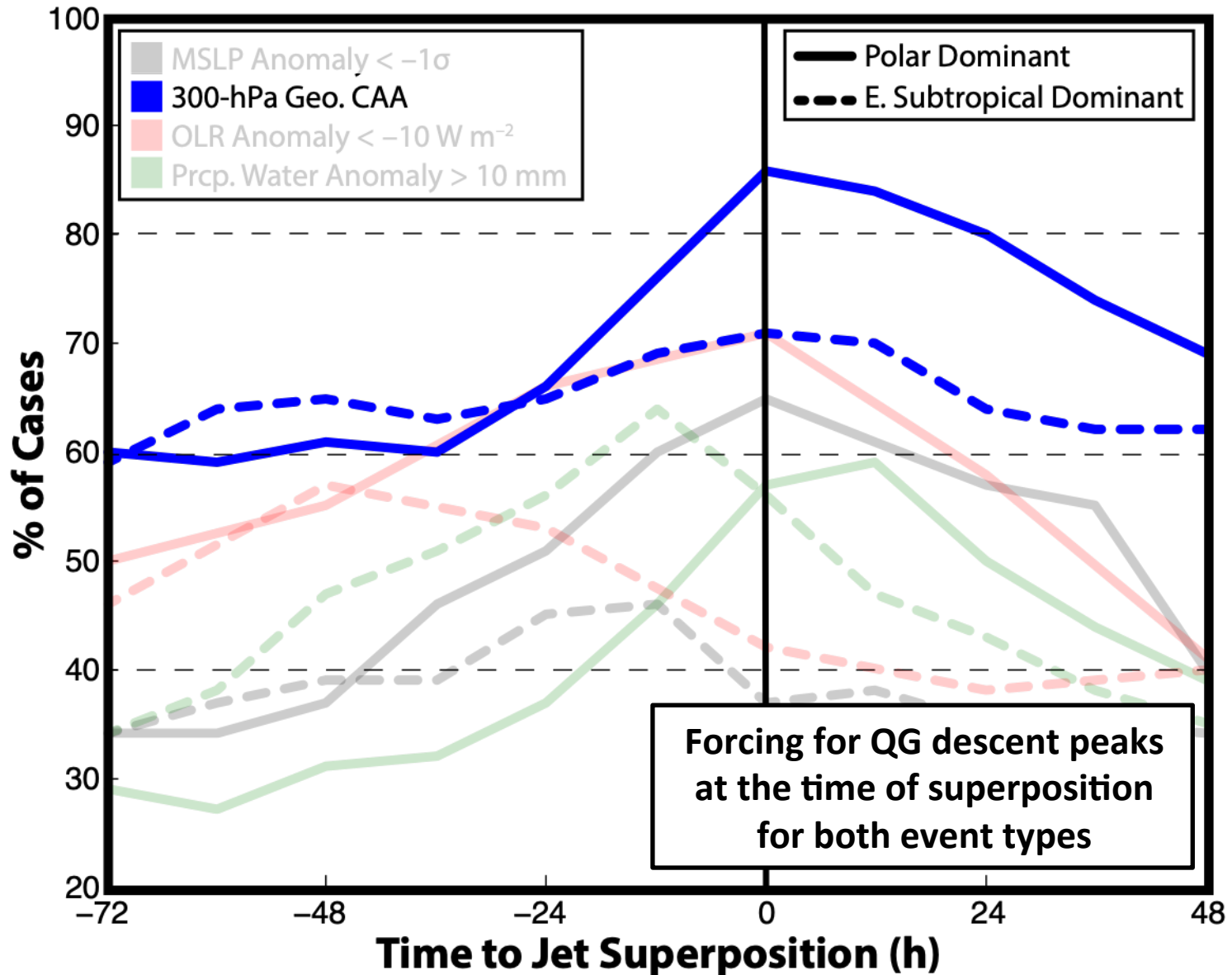
Jet Superposition Event Composites



Jet Superposition Event Composites

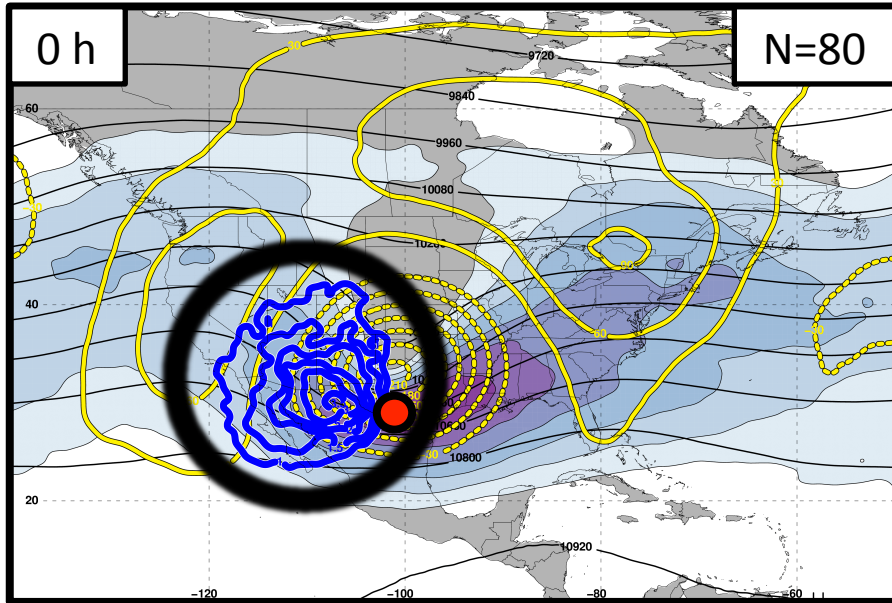


Jet Superposition Event Composites

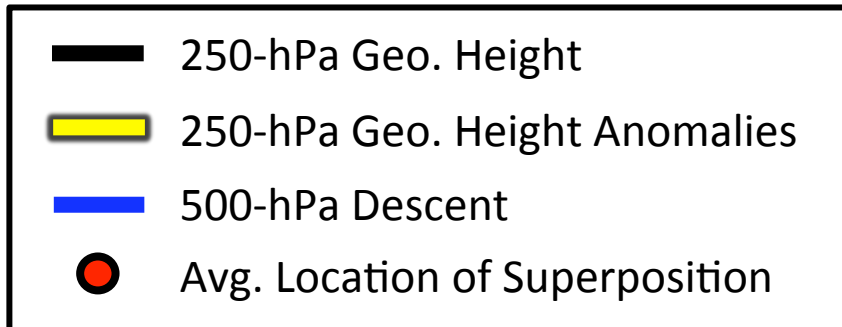
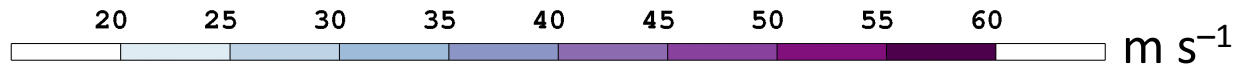
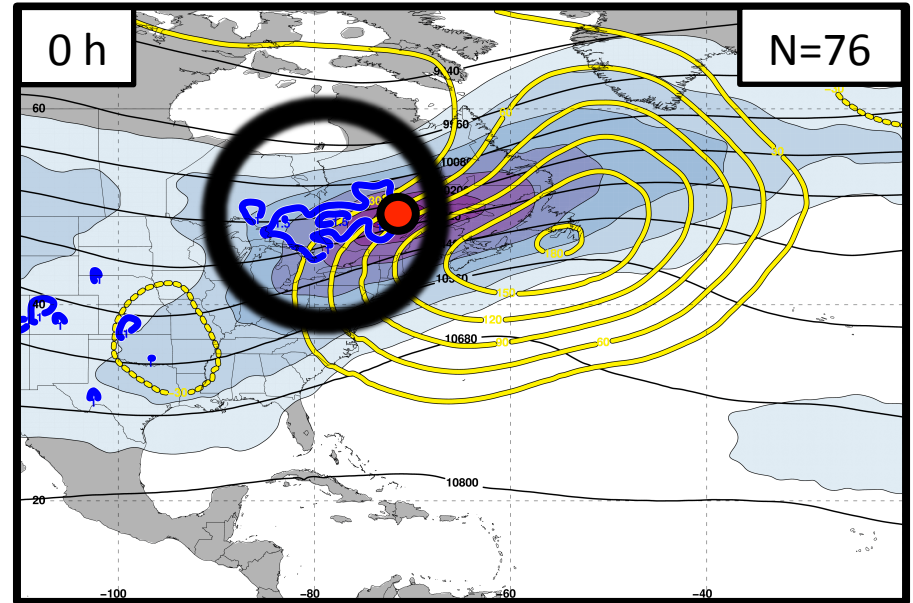


The Consistent Role of Descent

Polar Dominant Events



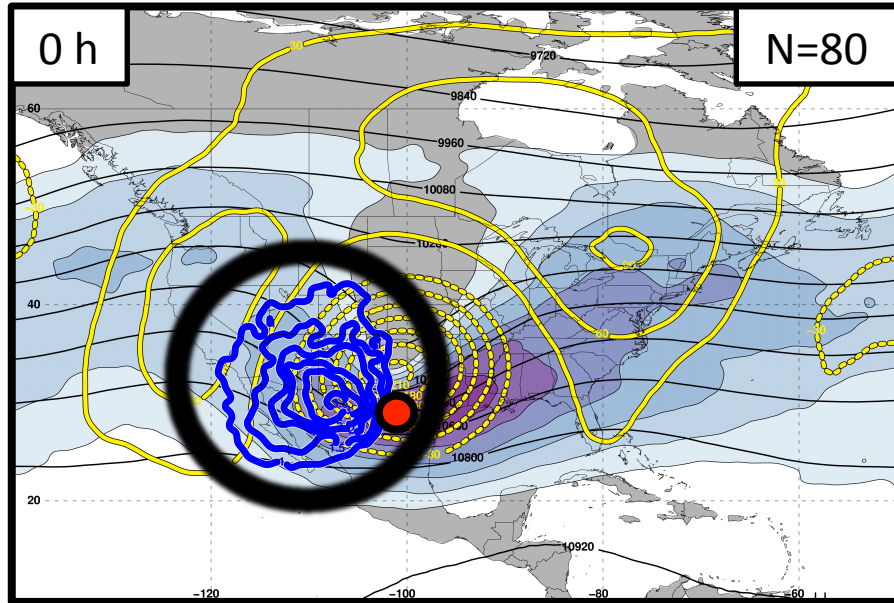
East Subtropical Dominant Events



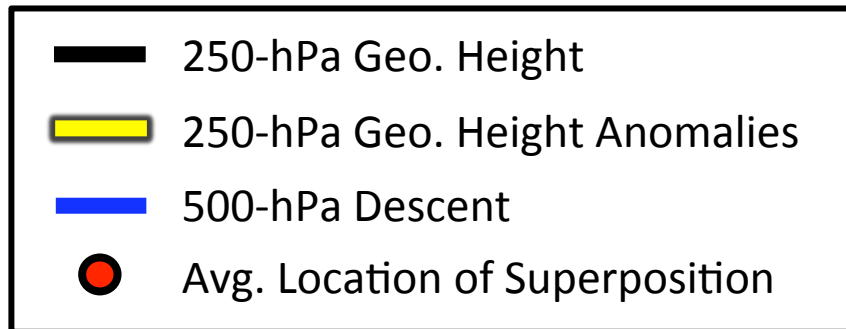
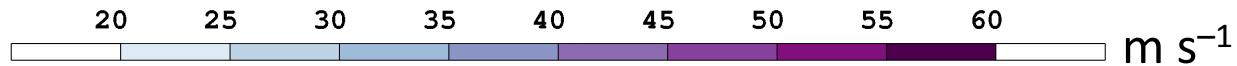
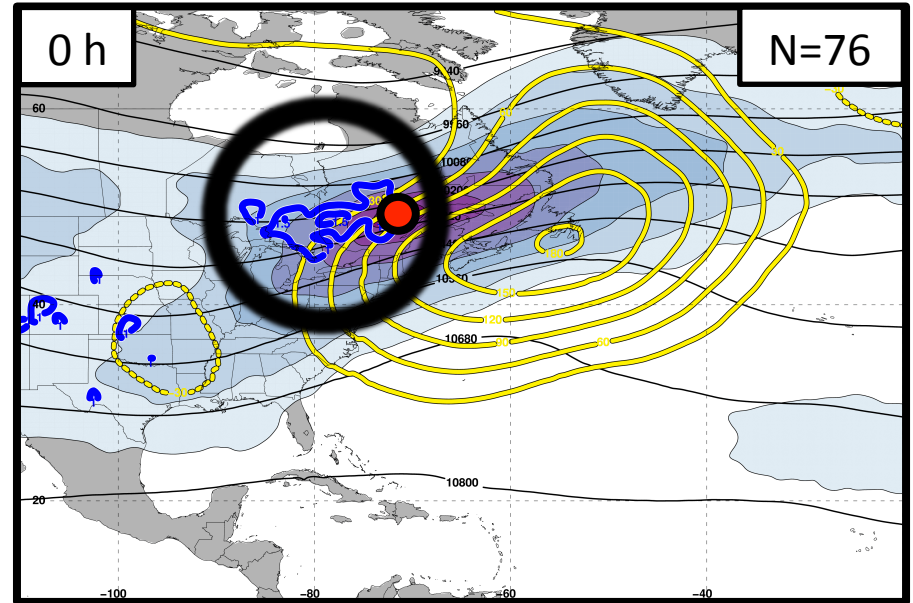
Descent within the jet-entrance region is a common element among the jet superposition event composites.

The Consistent Role of Descent

Polar Dominant Events



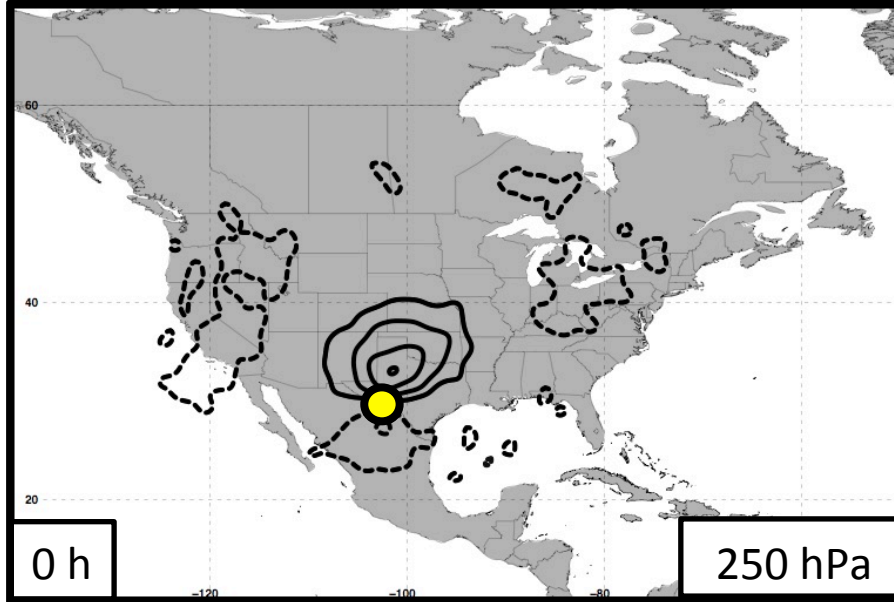
East Subtropical Dominant Events



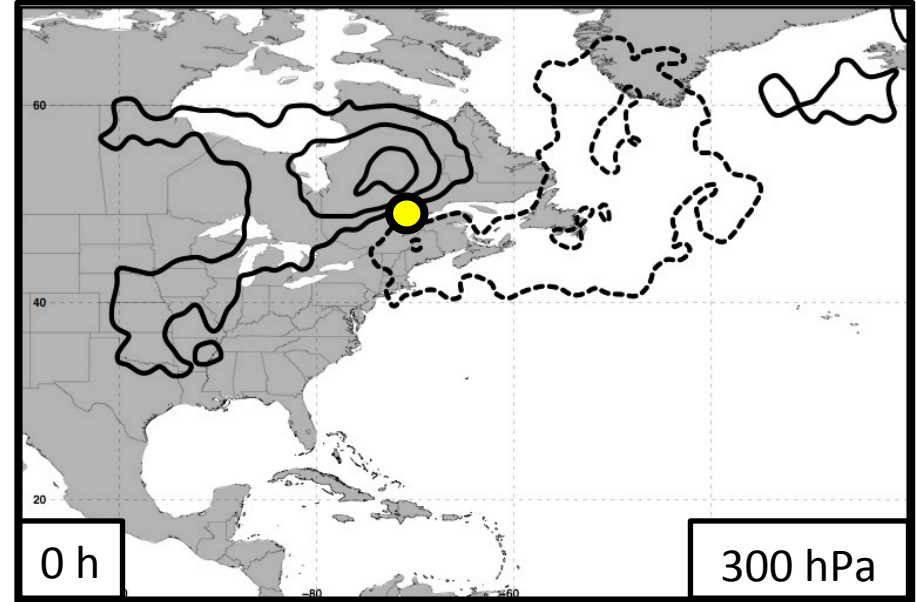
The consistent role of descent motivates further investigation of the dynamical structures responsible for the observed descent.

The Consistent Role of Descent

Polar Dominant Events



East Subtropical Dominant Events

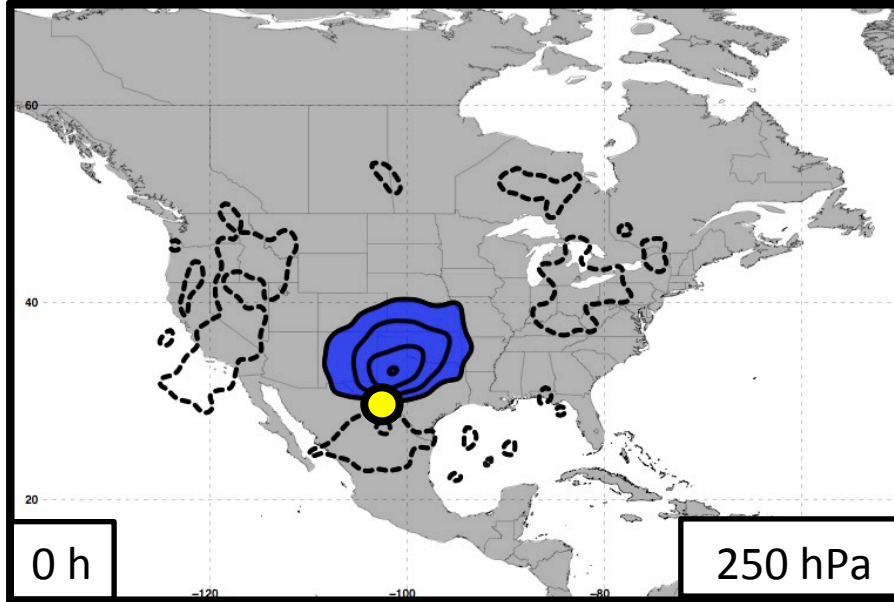


— + QGPV Anomalies - - - - - QGPV Anomalies ● Avg. Location of Superposition

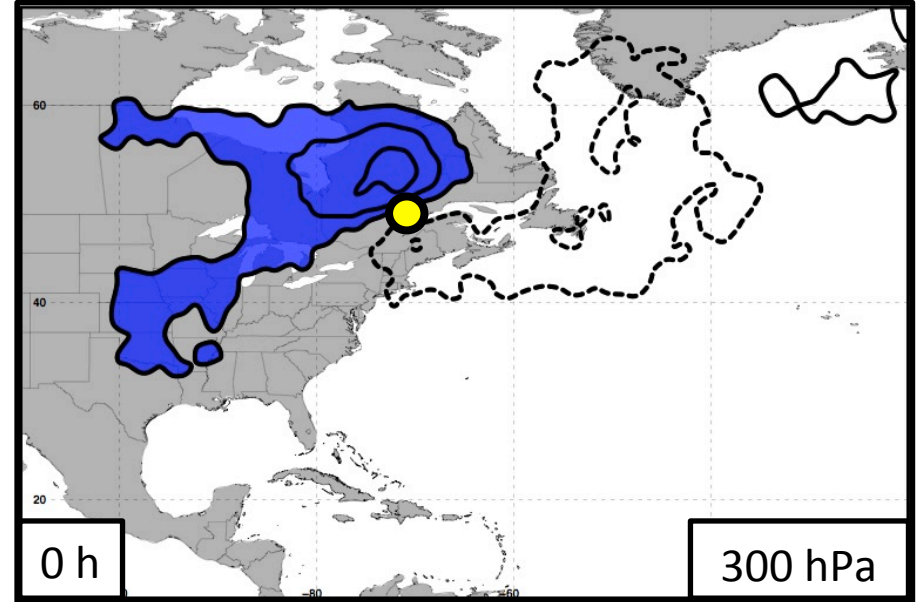
The descent characterizing each jet superposition event composite is examined further by isolating quasi-geostrophic (QG) PV anomalies in the vicinity of the jet superposition.

The Consistent Role of Descent


Polar Dominant Events



East Subtropical Dominant Events

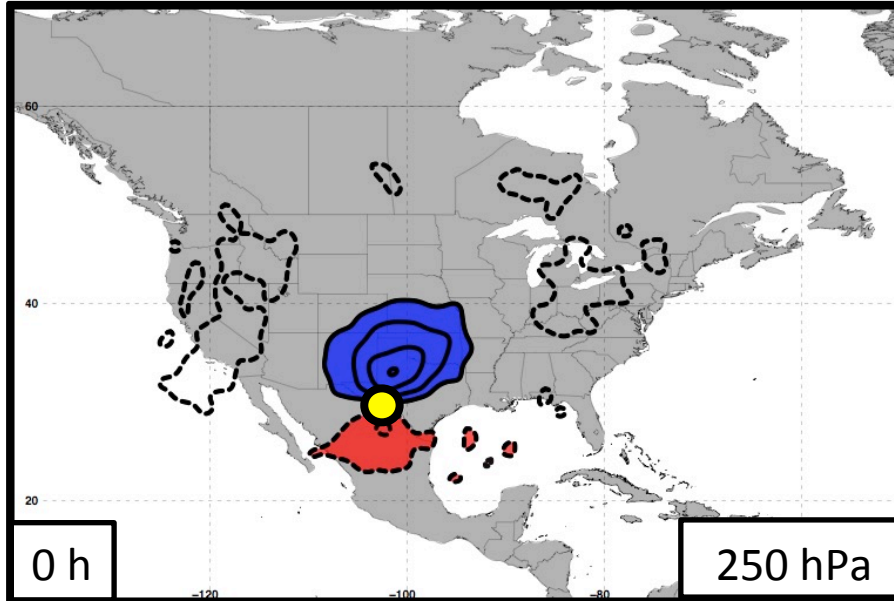


 Polar Cyclonic QGPV Anomalies

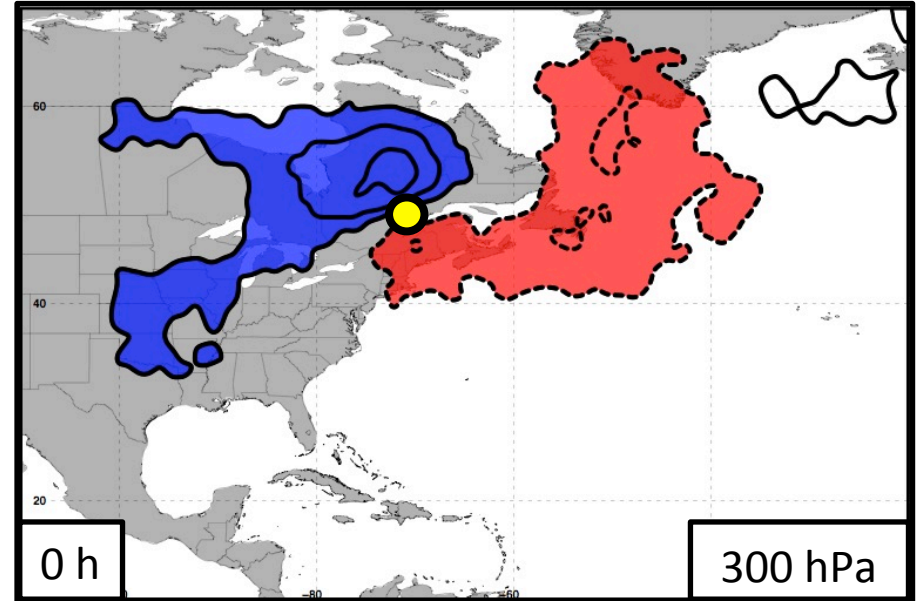
 Avg. Location of Superposition

The Consistent Role of Descent

Polar Dominant Events



East Subtropical Dominant Events

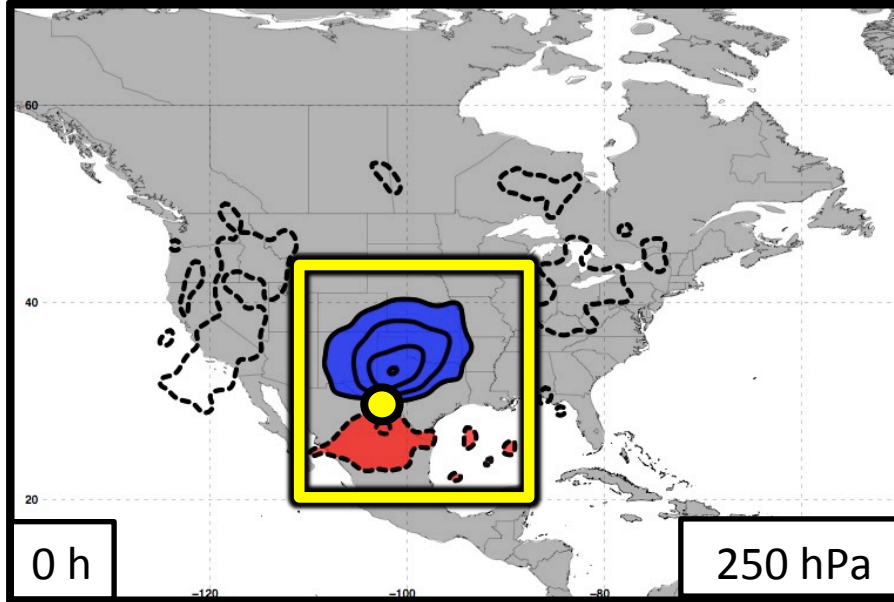


- Blue square: Polar Cyclonic QGPV Anomalies
- Red square: Tropical Anticyclonic QGPV Anomalies

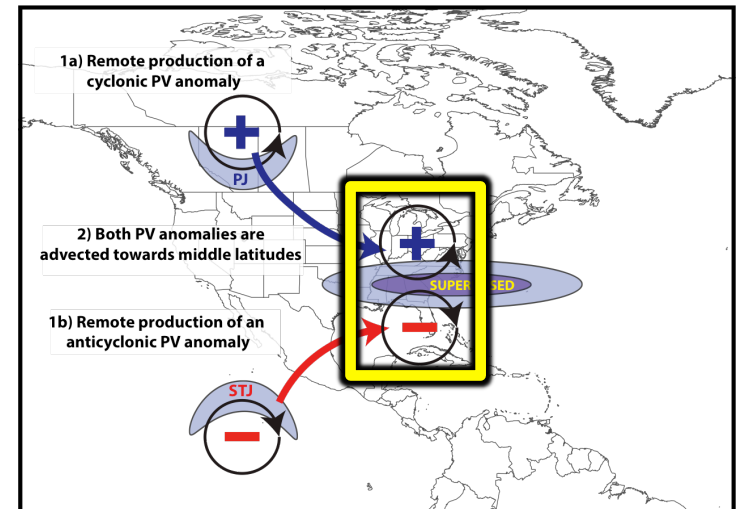
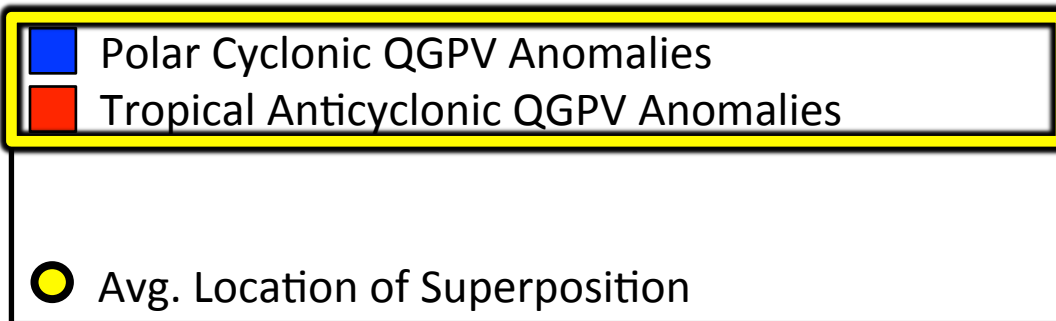
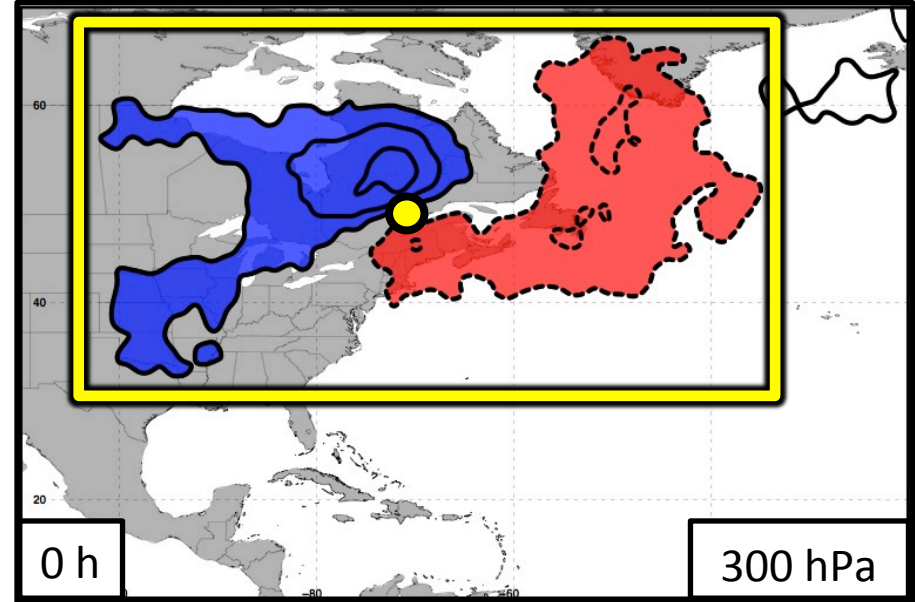
Yellow circle: Avg. Location of Superposition

The Consistent Role of Descent

Polar Dominant Events

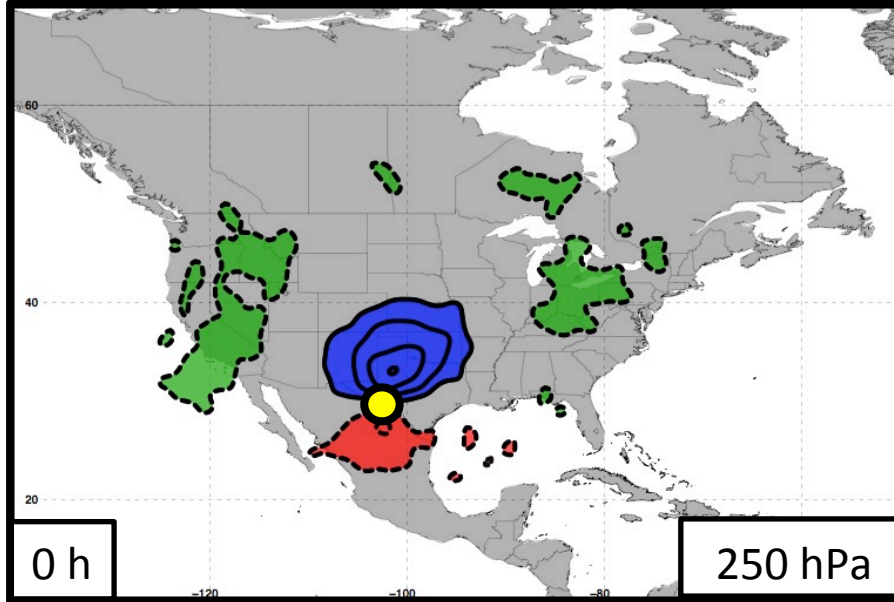


East Subtropical Dominant Events

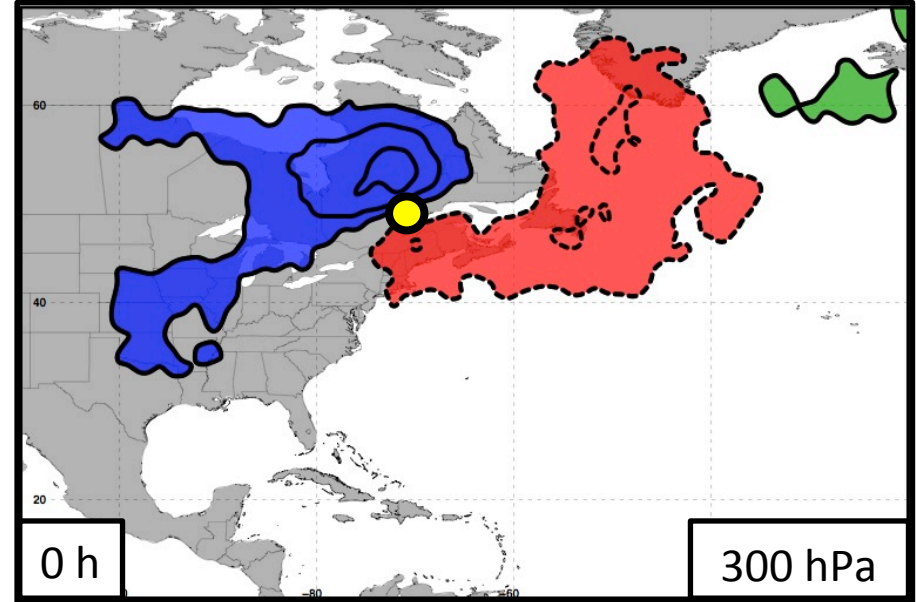


The Consistent Role of Descent

Polar Dominant Events



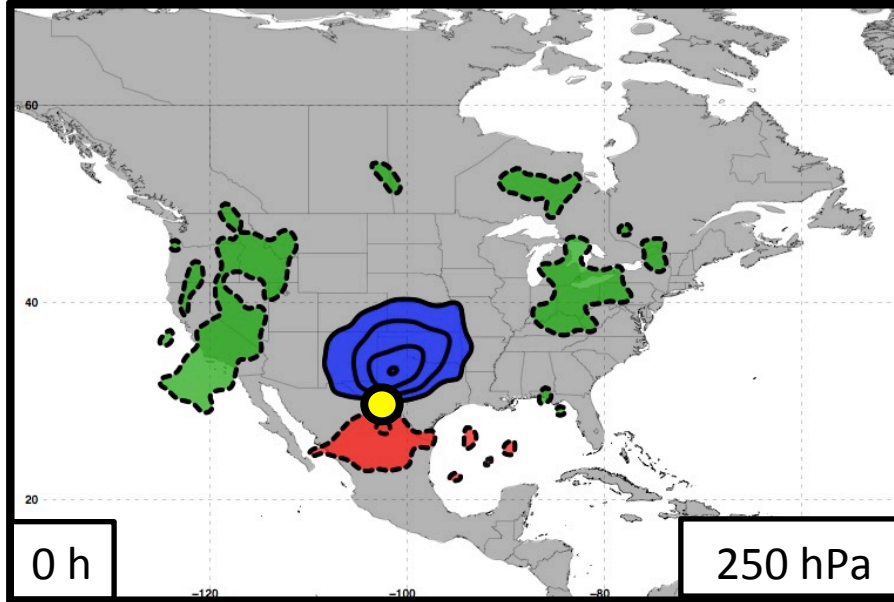
East Subtropical Dominant Events



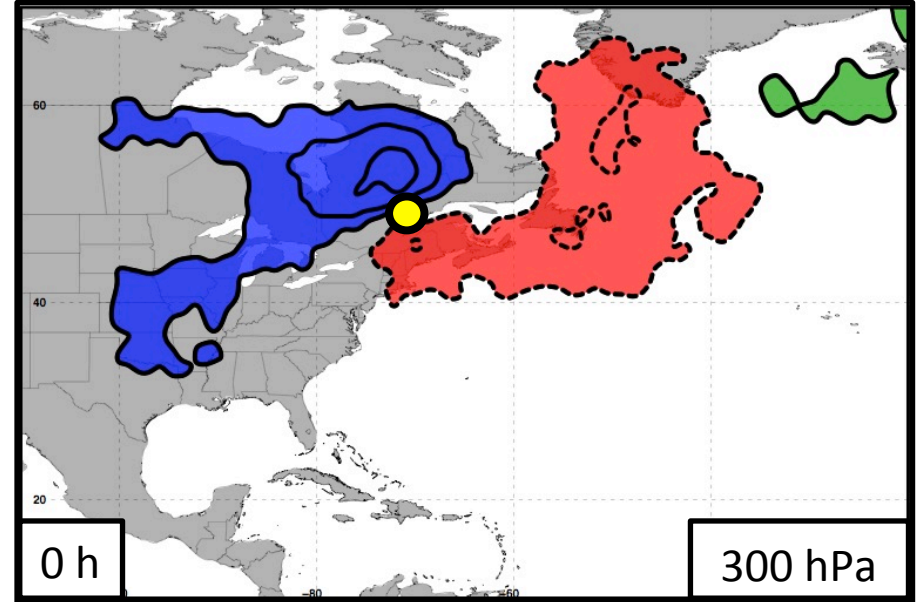
- Blue square: Polar Cyclonic QGPV Anomalies
- Red square: Tropical Anticyclonic QGPV Anomalies
- Green square: Residual Upper-Tropospheric QGPV Anomalies
- Yellow circle: Avg. Location of Superposition

The Consistent Role of Descent

Polar Dominant Events



East Subtropical Dominant Events



- Blue square: Polar Cyclonic QGPV Anomalies
- Red square: Tropical Anticyclonic QGPV Anomalies
- Green square: Residual Upper-Tropospheric QGPV Anomalies
- Pink square: Lower-Tropospheric QGPV Anomalies
- Yellow circle: Avg. Location of Superposition

The Consistent Role of Descent

Each category of QGPV anomalies (q') is inverted to determine its associated geopotential (ϕ') field:

$$q' = \frac{1}{f_0} \nabla^2 \phi' + f_0 \frac{\partial}{\partial p} \left(\frac{1}{\sigma_r} \frac{\partial \phi'}{\partial p} \right) \quad \text{where} \quad \begin{array}{l} f_0 = \text{Reference Coriolis Parameter} \\ \sigma_r = \text{Static Stability of the U.S. Std. Atm.} \end{array}$$

The Consistent Role of Descent

Each category of QGPV anomalies (q') is inverted to determine its associated geopotential (ϕ') field:

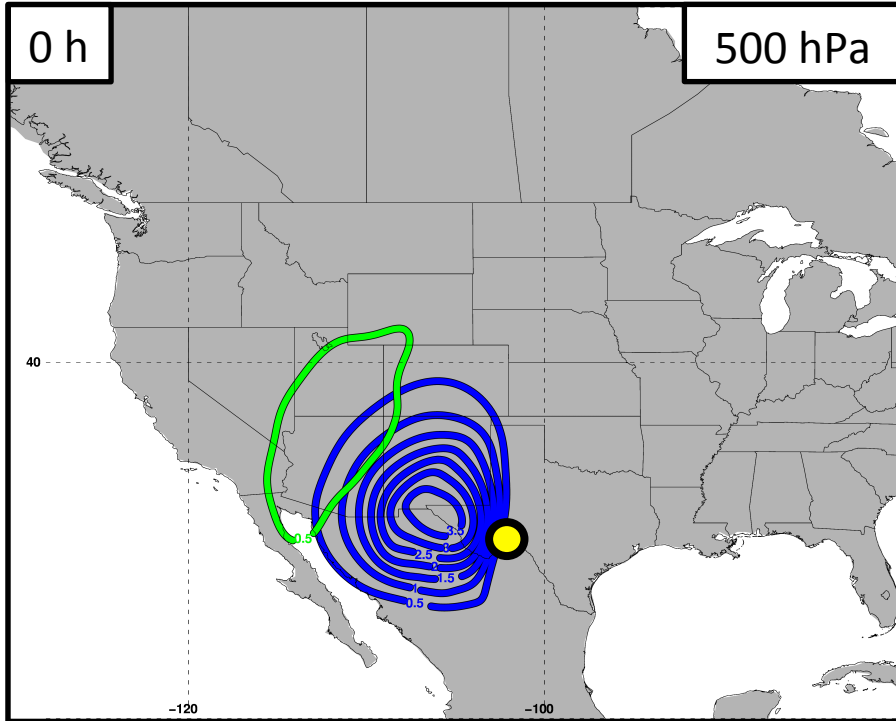
$$q' = \frac{1}{f_0} \nabla^2 \phi' + f_0 \frac{\partial}{\partial p} \left(\frac{1}{\sigma_r} \frac{\partial \phi'}{\partial p} \right) \quad \text{where} \quad \begin{array}{l} f_0 = \text{Reference Coriolis Parameter} \\ \sigma_r = \text{Static Stability of the U.S. Std. Atm.} \end{array}$$

The geopotential fields and the composite temperature (T) field are used to determine the QG vertical motion (ω) associated with each category of QGPV:

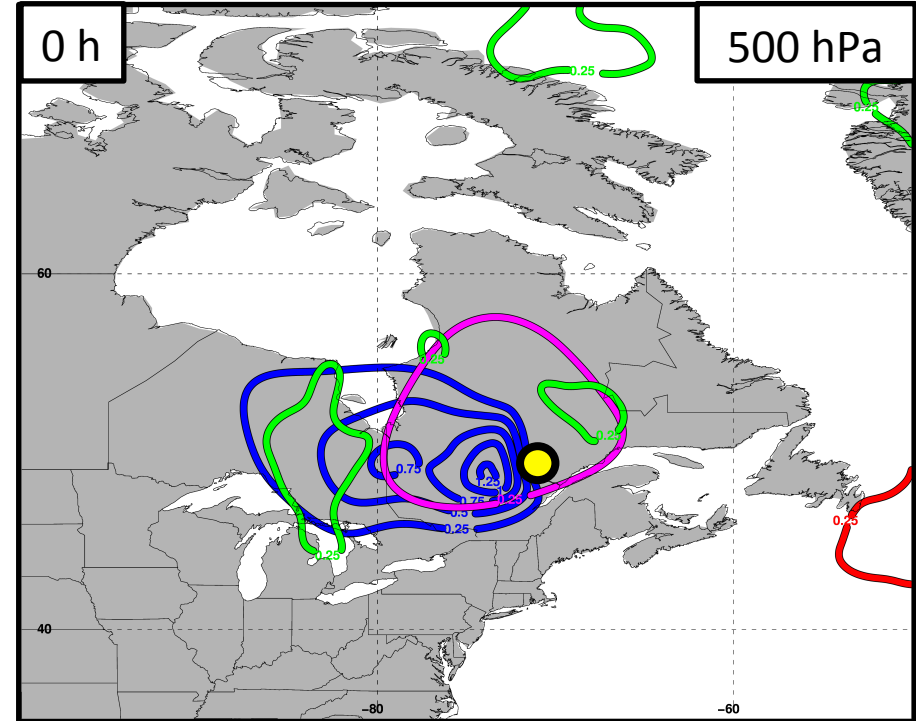
$$\sigma_r \nabla^2 \omega + f_0^2 \frac{\partial^2 \omega}{\partial p^2} = -2 \nabla \cdot \vec{Q} \quad \text{where} \quad \begin{array}{l} \vec{V}_g' = -(1/f_0)(\hat{k} \times \nabla \phi') \\ \vec{Q} = -\frac{R}{p} \left[\left(\frac{\partial \vec{V}_g'}{\partial x} \cdot \nabla T \right), \left(\frac{\partial \vec{V}_g'}{\partial y} \cdot \nabla T \right) \right] \end{array}$$

The Consistent Role of Descent

Polar Dominant Events



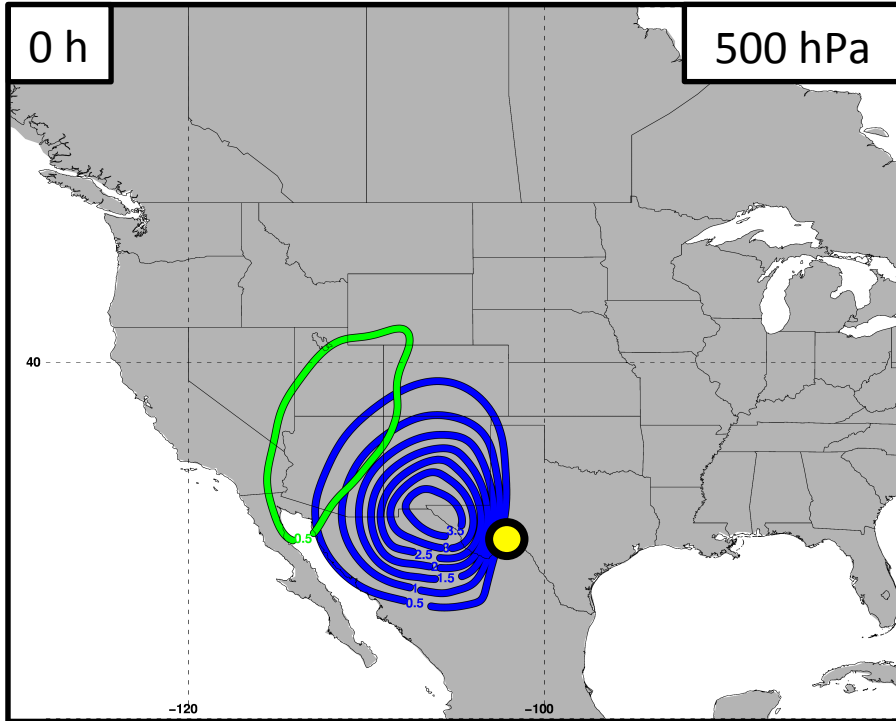
East Subtropical Dominant Events



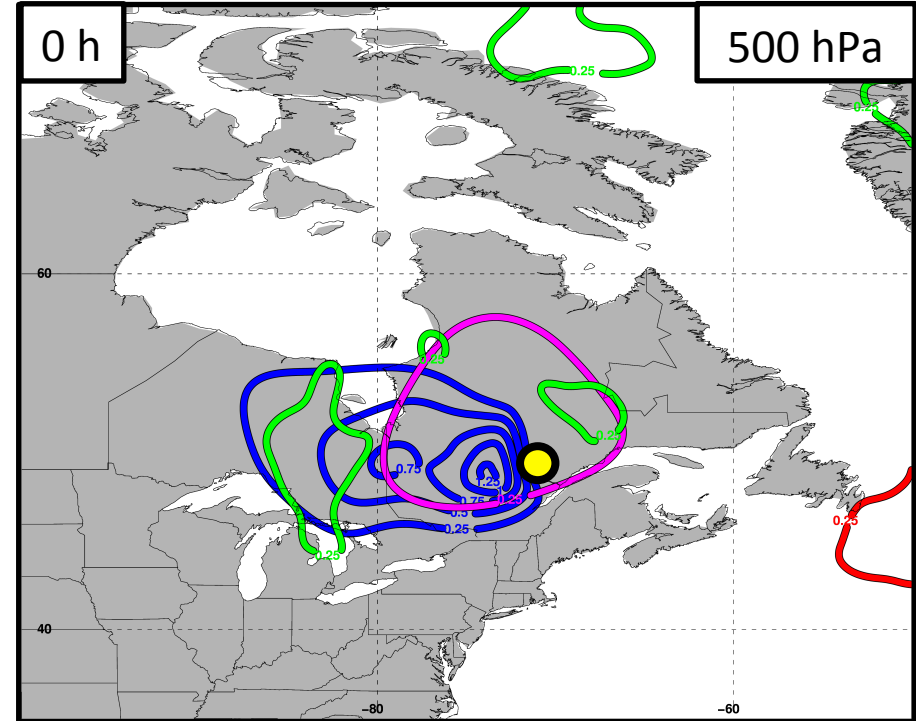
- Blue Polar Cyclonic QGPV Anomalies
- Red Tropical Anticyclonic QGPV Anomalies
- Green Residual Upper-Tropospheric QGPV Anomalies
- Magenta Lower-Tropospheric QGPV Anomalies
- Yellow Avg. Location of Superposition




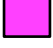

The Consistent Role of Descent

Polar Dominant Events



East Subtropical Dominant Events

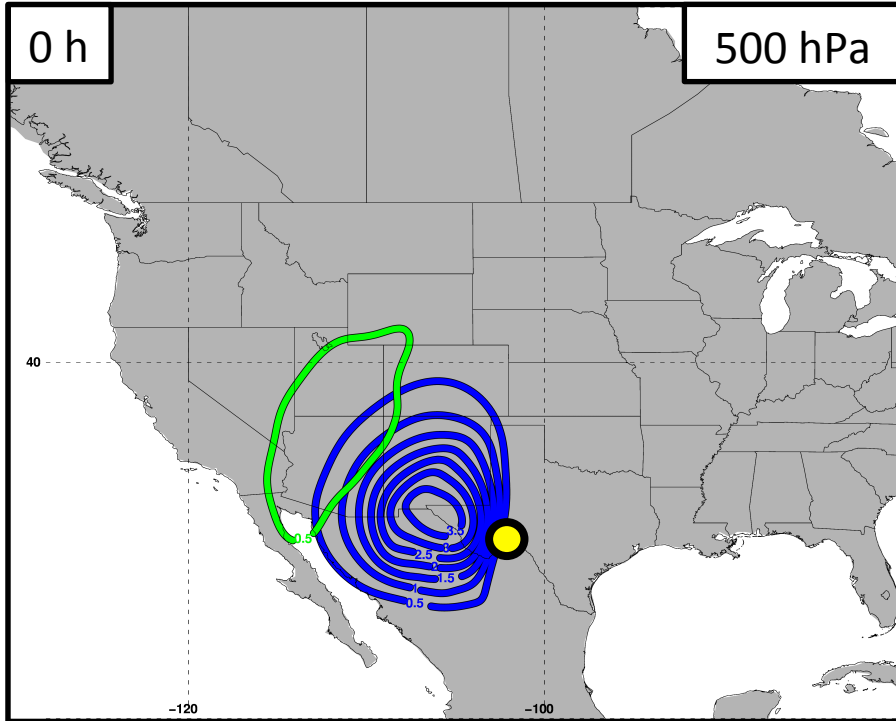


-  Polar Cyclonic QGPV Anomalies
-  Tropical Anticyclonic QGPV Anomalies
-  Residual Upper-Tropospheric QGPV Anomalies
-  Lower-Tropospheric QGPV Anomalies
-  Avg. Location of Superposition

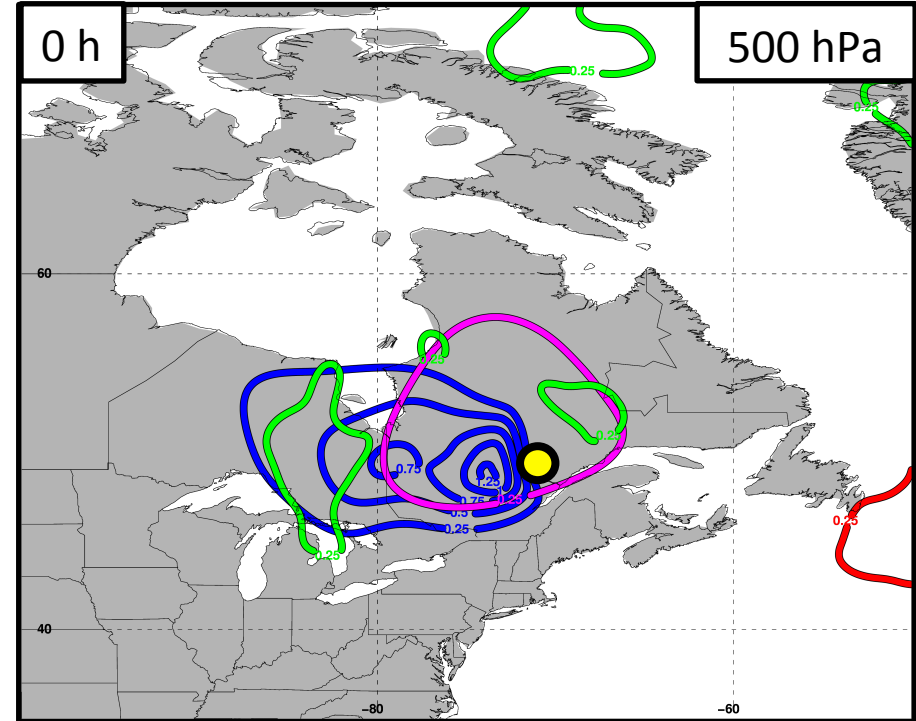
Descent is primarily associated with polar cyclonic QGPV anomalies.

The Consistent Role of Descent

Polar Dominant Events



East Subtropical Dominant Events



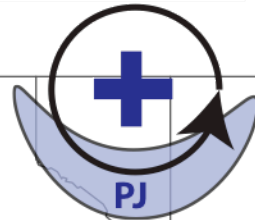
- Blue Polar Cyclonic QGPV Anomalies
- Red Tropical Anticyclonic QGPV Anomalies
- Green Residual Upper-Tropospheric QGPV Anomalies
- Pink Lower-Tropospheric QGPV Anomalies
- Yellow Avg. Location of Superposition

Polar cyclonic QGPV anomalies play a critical role during jet superpositions.

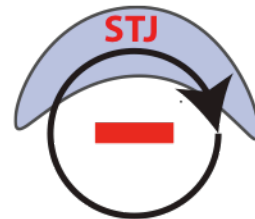
Summary

Polar Dominant Events:

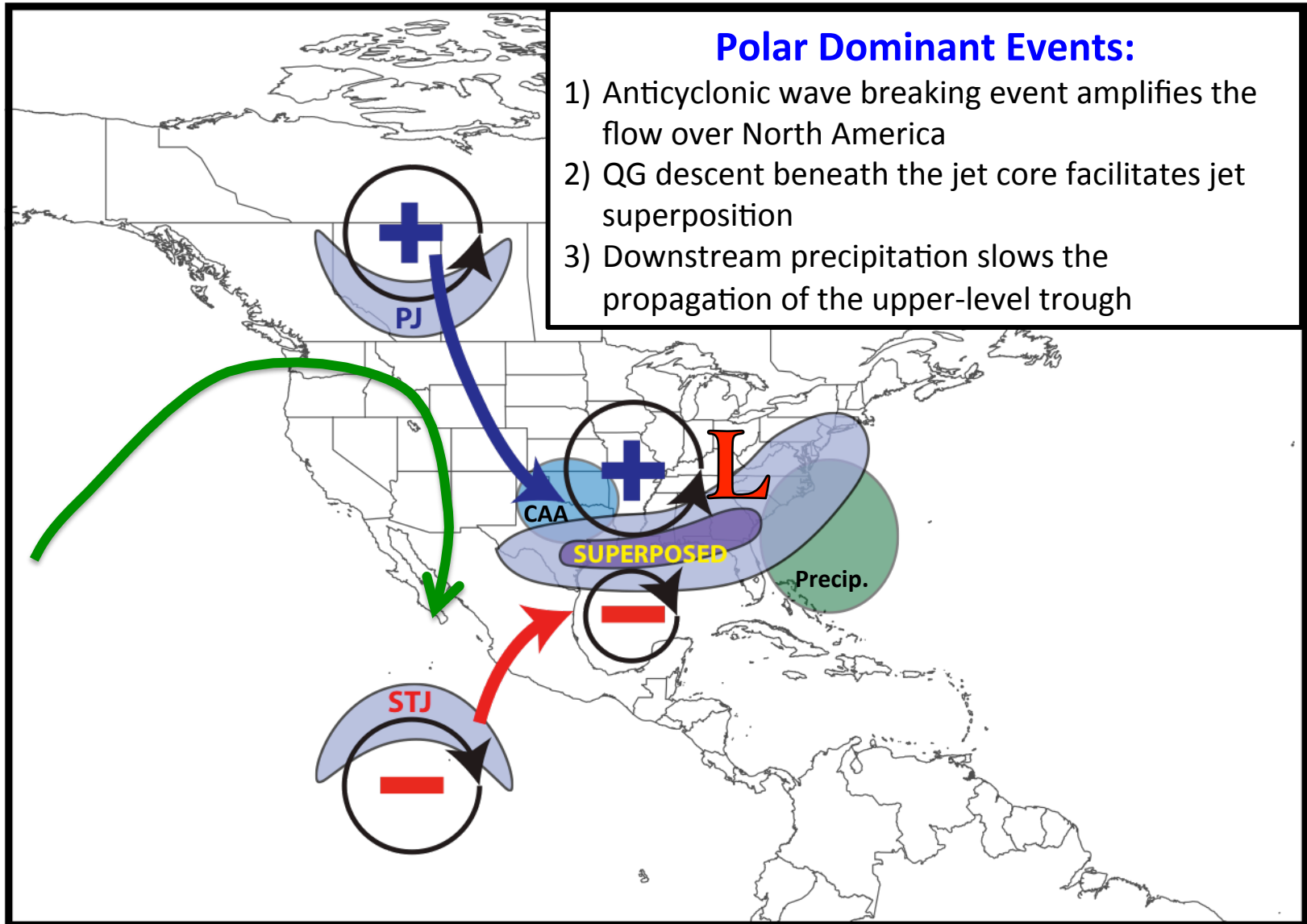
1a) Remote production of a cyclonic PV anomaly



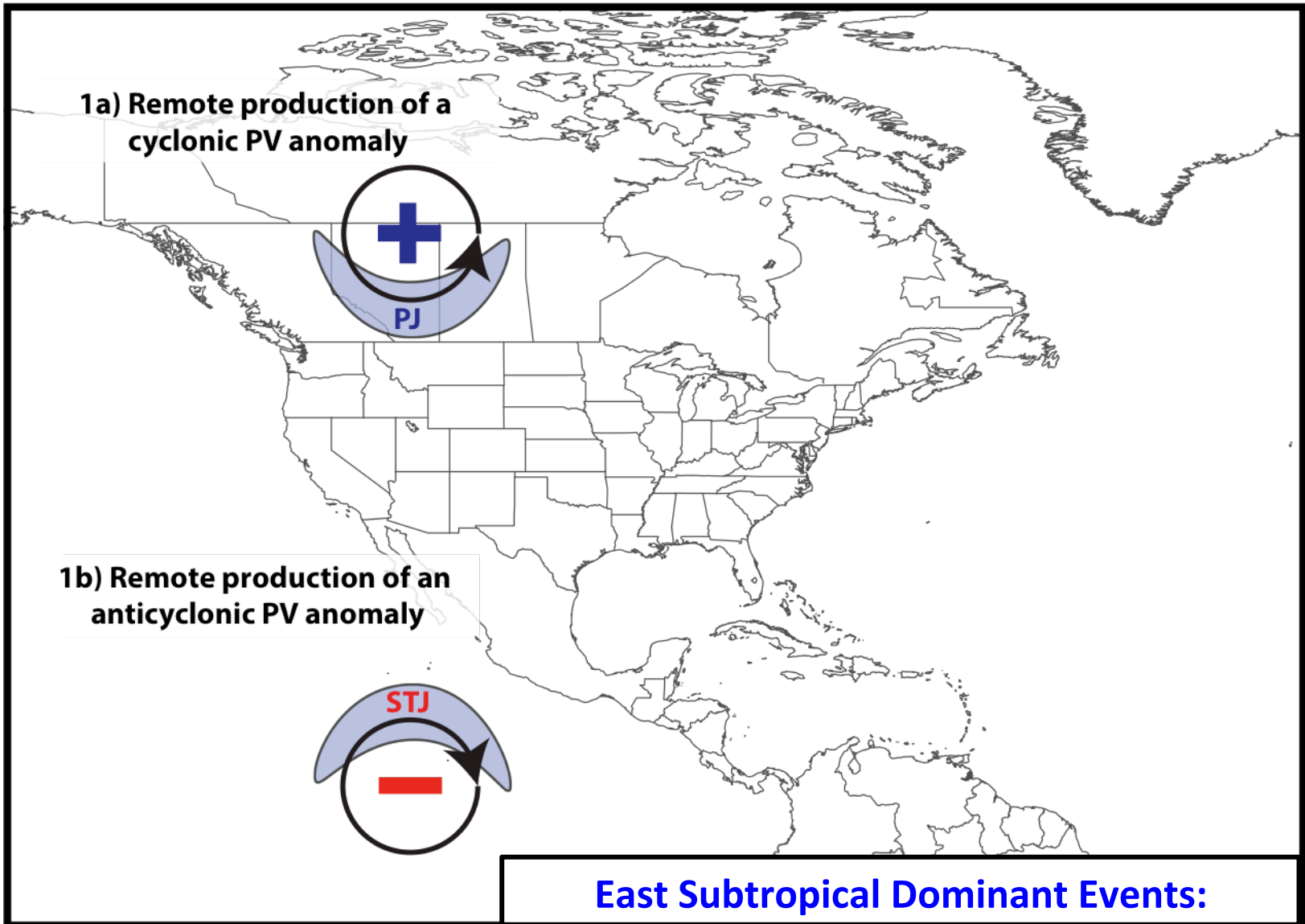
1b) Remote production of an anticyclonic PV anomaly



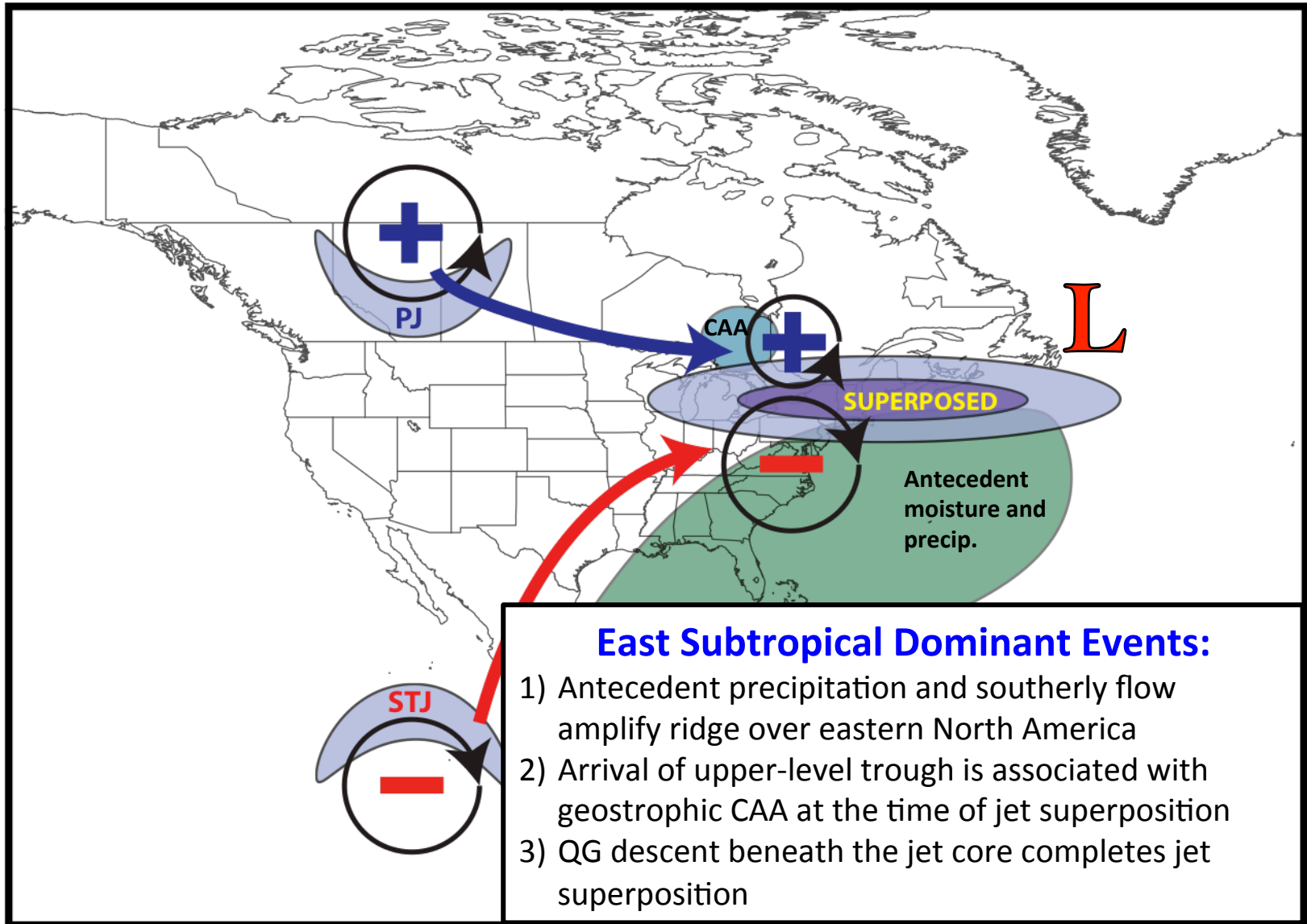
Summary



Summary



Summary



Future Work

- Examine the impact that each type of jet superposition event has on the evolution of the downstream large-scale flow pattern.
- Decipher the relationship between each type of jet superposition and the development of high-impact weather.
- Utilize numerical simulations of jet superposition events to examine the sensitivity of jet superposition to diabatic processes.
- Examine the frequency and characteristics of jet superposition events within future climate scenarios.

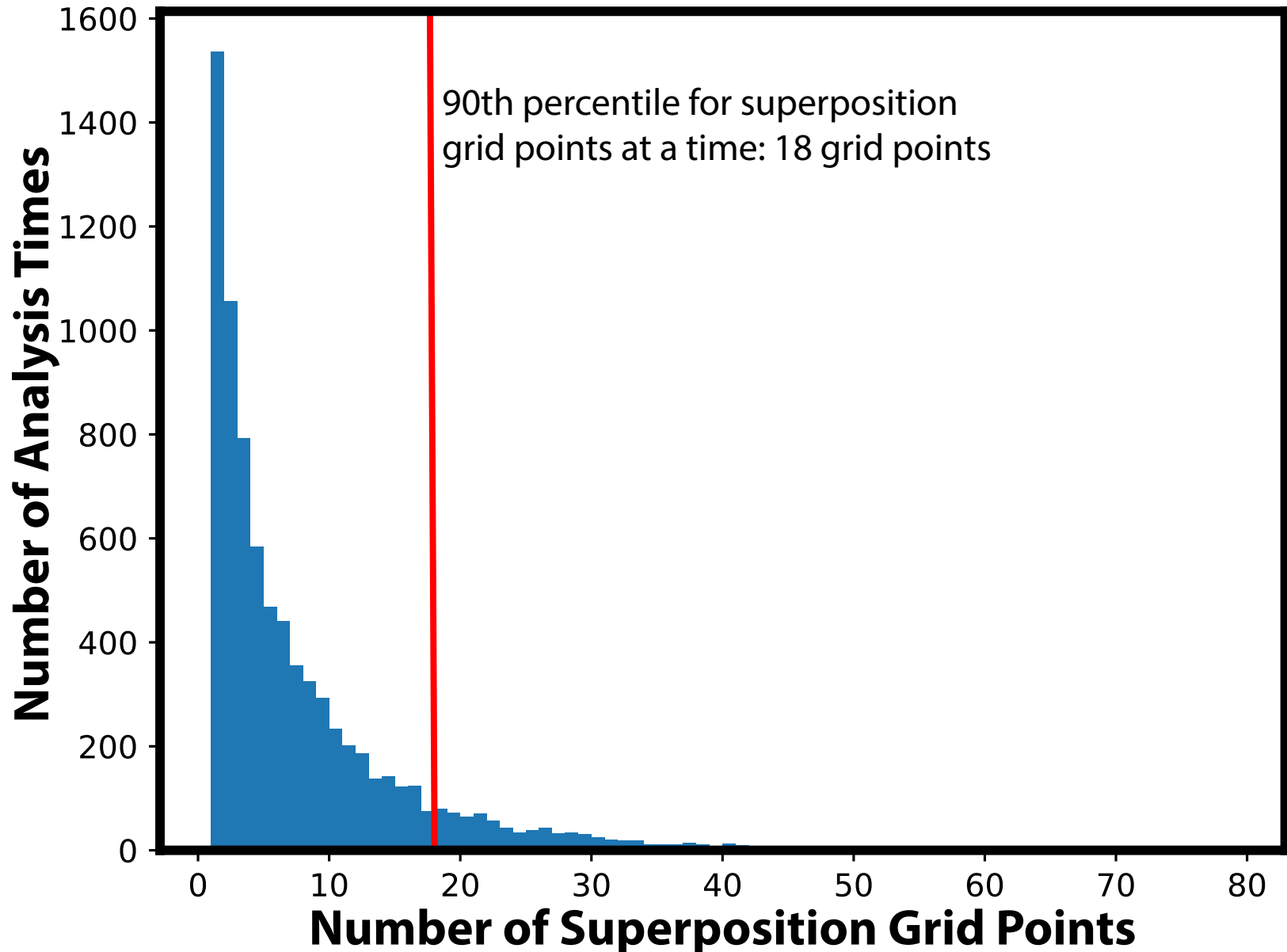
Contact: acwinters@albany.edu

Supplementary Slides

References

- Cavallo, S. M., and G. J. Hakim, 2010: Composite structure of tropopause polar cyclones. *Mon. Wea. Rev.*, **138**, 3840-3857.
- Christenson, C. E., and J. E. Martin, 2012: The large-scale environment associated with the 25-28 April 2011 severe weather outbreak. *16th NWA Severe Storms and Doppler Radar Conference*, Des Moines, IA, National Weather Association, 31 March 2012.
- Christenson, C. E., J. E. Martin, and Z. J. Handlos, 2017: A synoptic-climatology of Northern Hemisphere, cold season polar and subtropical jet superposition events. *J. Climate*, **30**, 7231-7246.
- Defant, F., and H. Taba, 1957: The threefold structure of the atmosphere and the characteristics of the tropopause. *Tellus*, **9**, 259-275.
- Lang, A. A., and J. E. Martin, 2012: The structure and evolution of lower stratospheric frontal zones. Part I: Examples in northwesterly and southwesterly flow. *Quart. J. Roy. Meteor. Soc.*, **138**, 1350-1365.
- Handlos, Z. J. and J. E. Martin, 2016: Composite analysis of large-scale environments conducive to west Pacific polar/subtropical jet superposition. *J. Climate*, **29**, 7145–7165.
- Knupp, K. R., T. A. Murphy, T. A. Coleman, R. A. Wade, S. A. Mullins, C. J. Schultz, E. V. Schultz, L. Carey, A. Sherrer, E. W. McCaul Jr., B. Carcione, S. Latimer, A. Kula, K. Laws, P. T. Marsh, and K. Klockow, 2014: Meteorological overview of the devastating 27 April 2011 Tornado Outbreak. *Bull. Amer. Meteor. Soc.*, **95**, 1041-1062.
- Moore, B. J., P. J. Neiman, F. M. Ralph, and F. E. Barthold, 2012: Physical processes associated with heavy flooding rainfall in Nashville, Tennessee, and vicinity during 1-2 May 2010: The role of an atmospheric river and mesoscale convective systems. *Mon. Wea. Rev.*, **140**, 358-378.
- Pyle, M. E., D. Keyser, and L. F. Bosart, 2004: A diagnostic study of jet streaks: Kinematic signatures and relationship to coherent tropopause disturbances. *Mon. Wea. Rev.*, **132**, 297-319.
- Saha, S. and co-authors, 2014: The NCEP Climate Forecast System Version 2. *J. Climate*, **27**, 2185-2208.
- Winters, A. C., and J. E. Martin, 2014: The role of a polar/subtropical jet superposition in the May 2010 Nashville Flood. *Wea. Forecasting*, **29**, 954–974.
- Winters, A. C. and J. E. Martin, 2016: Synoptic and mesoscale processes supporting vertical superposition of the polar and subtropical jets in two contrasting cases. *Quart. J. Roy. Meteor. Soc.*, **142**, 1133–1149.
- Winters, A. C., and J. E. Martin, 2017: Diagnosis of a North American polar/subtropical jet superposition employing piecewise potential vorticity inversion. *Mon. Wea. Rev.*, **145**, 1853-1873.

Jet Superposition Event Identification

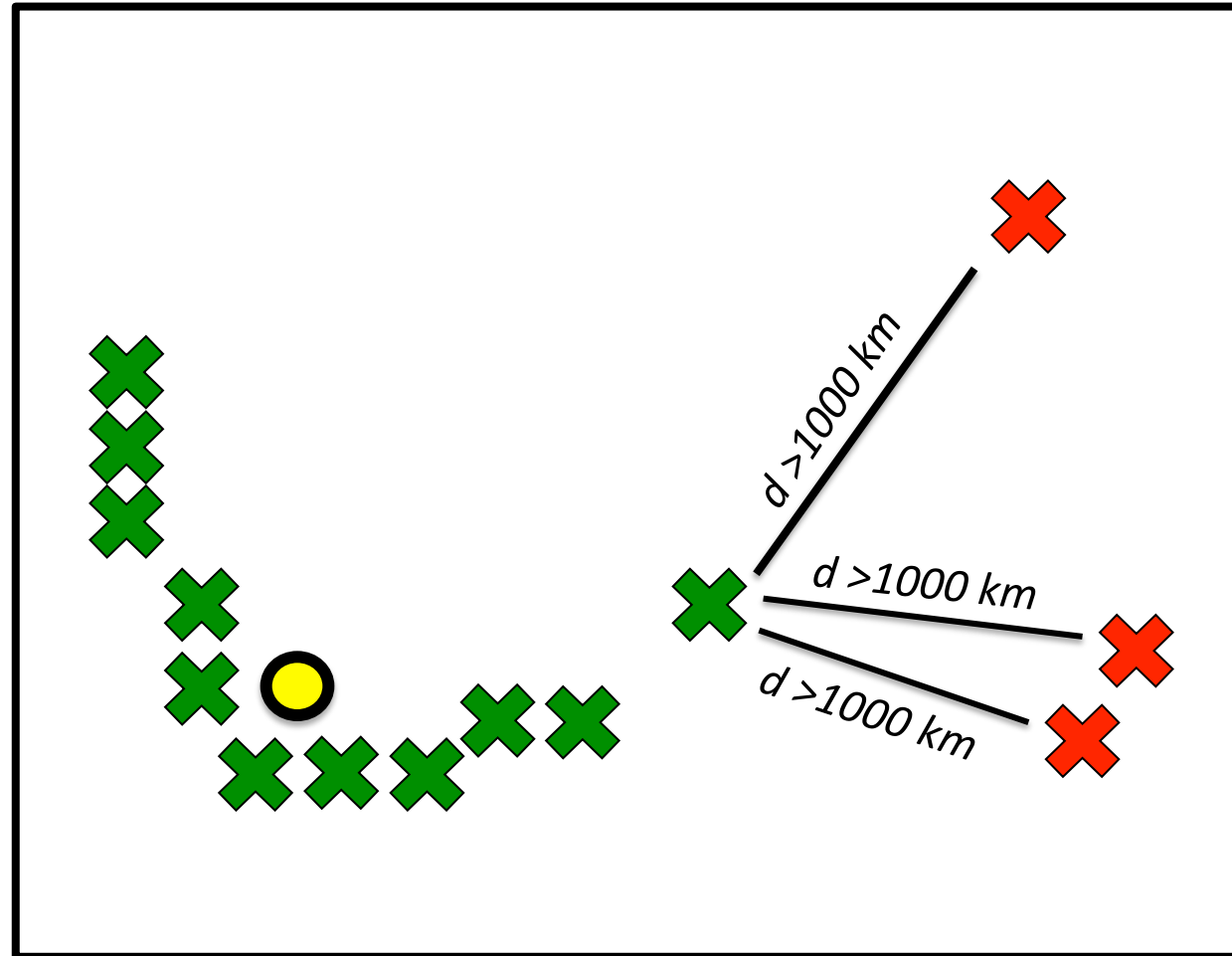


Jet Superposition Event Identification

Sample Jet Superposition Centroid Calculation

Calculated the centroid of each jet superposition based on all valid grid points at a particular analysis time.

To calculate the centroid, there must exist a group of 18 superposition grid points, of which no superposition grid point is >1000 km away from another superposition grid point.

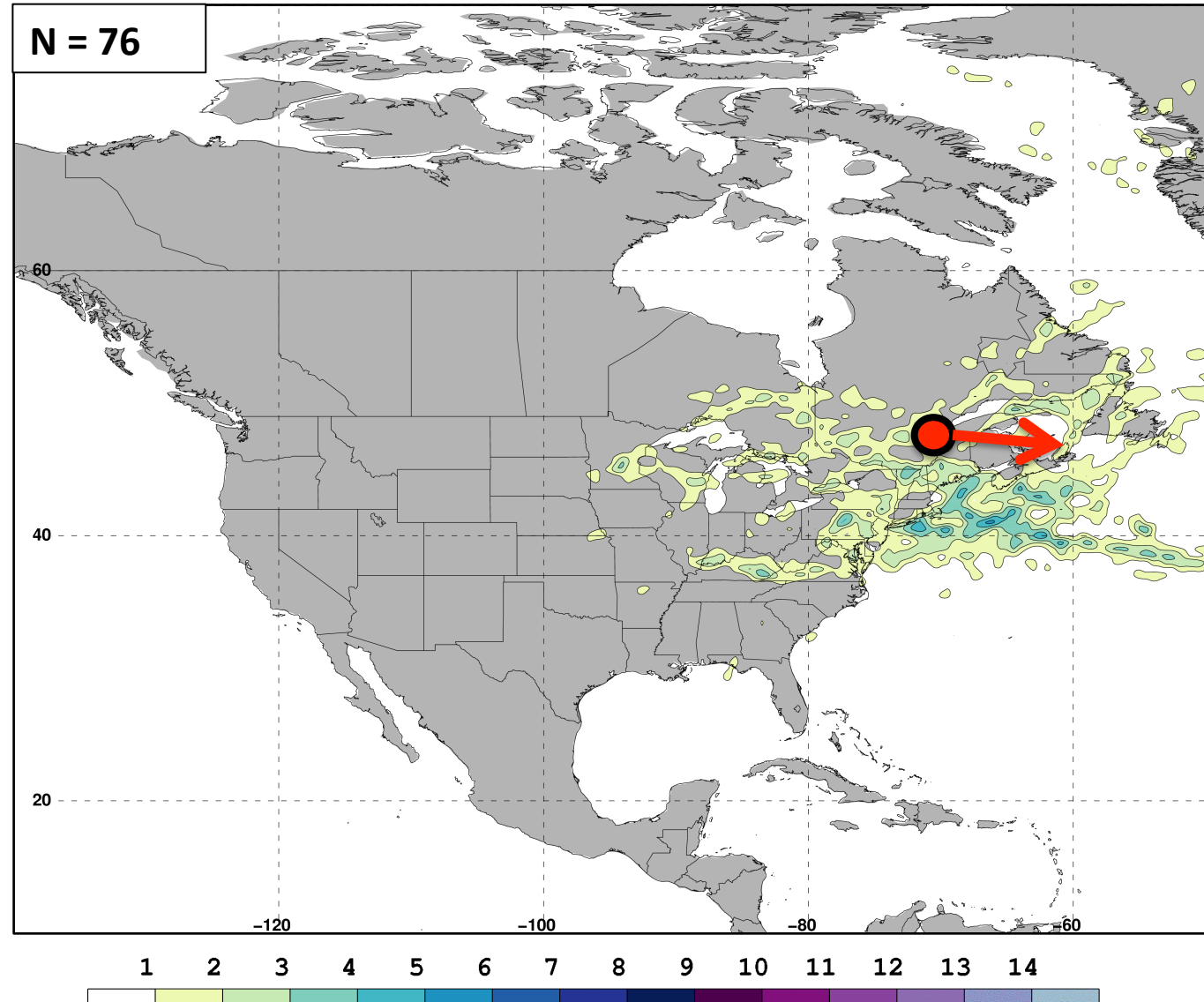


- ✕ Used for calculation
- ✕ Not used for calculation

● Jet superposition centroid

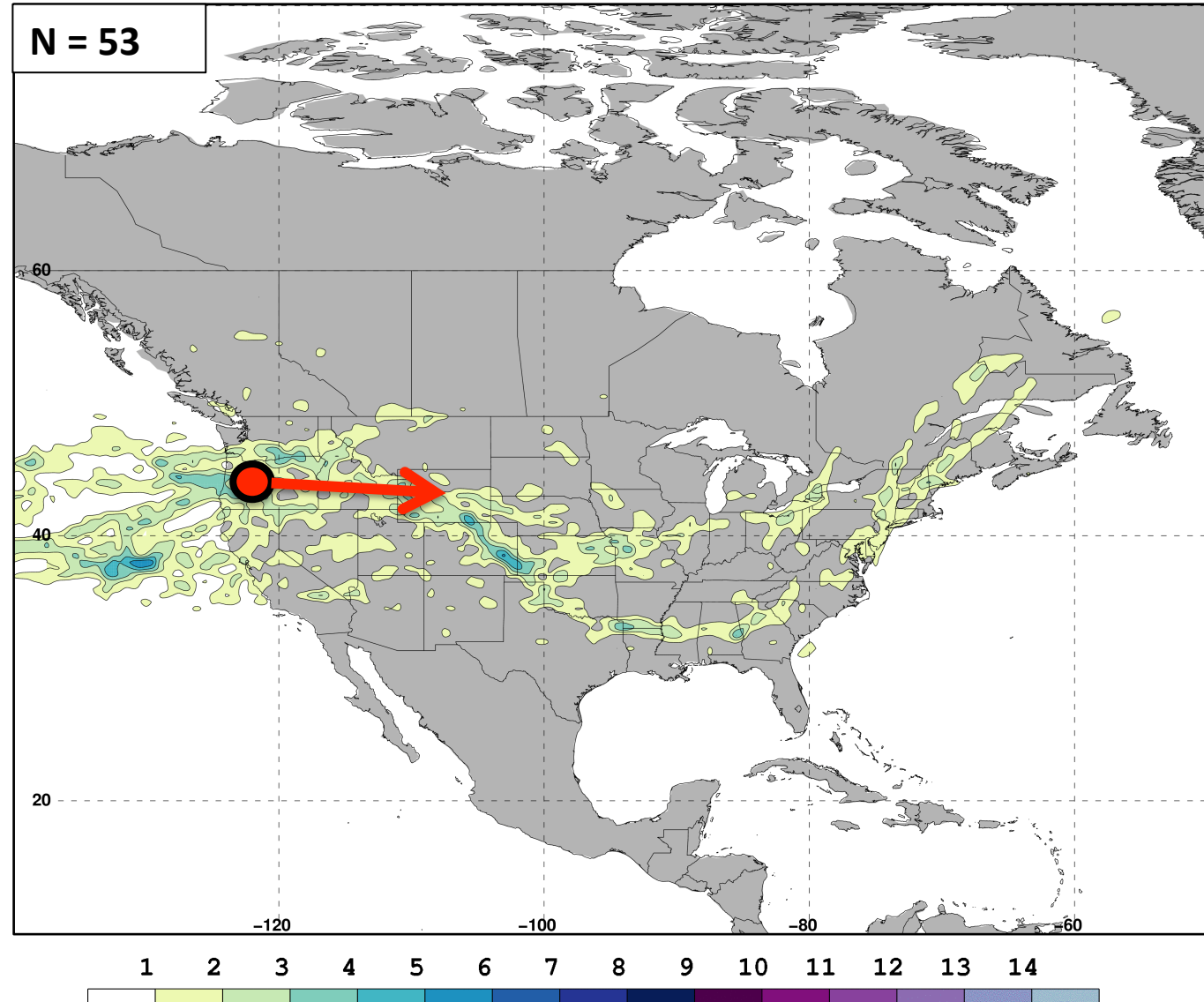
Jet Superposition Event Identification

Frequency of East Subtropical Dominant Jet Superposition Events

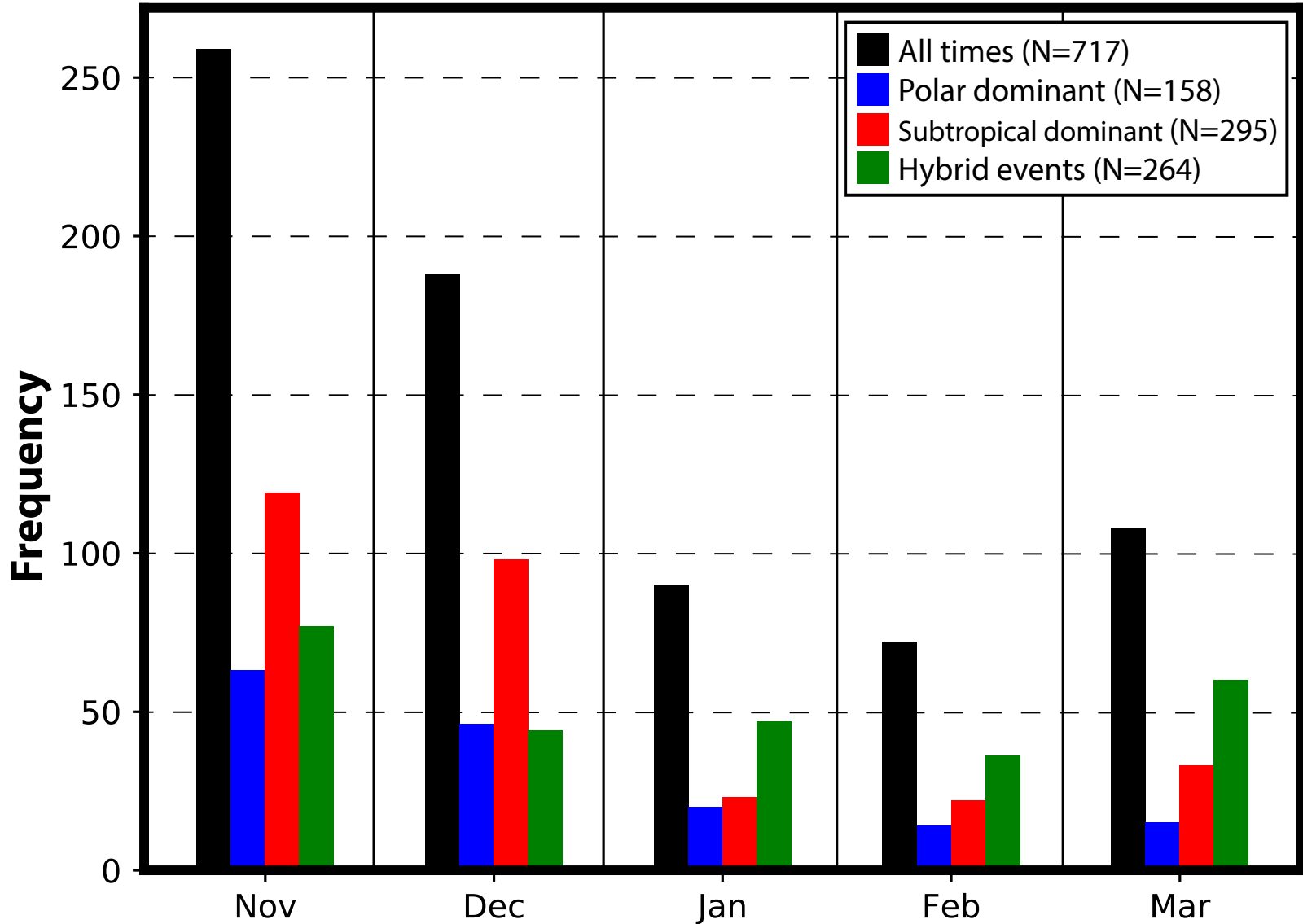


Jet Superposition Event Identification

Frequency of West Subtropical Dominant Jet Superposition Events

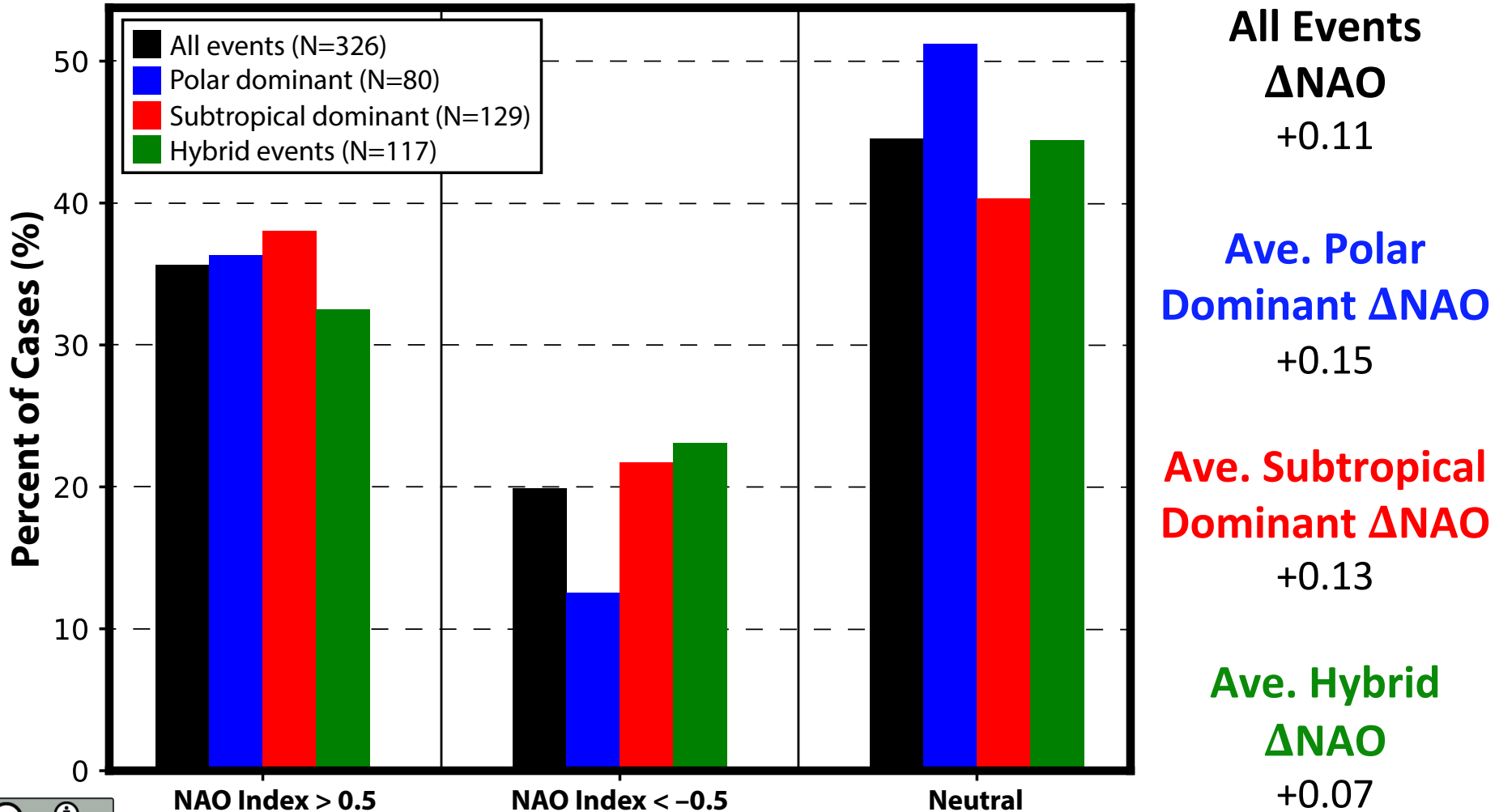


Jet Superposition Event Classification



Downstream Consequences

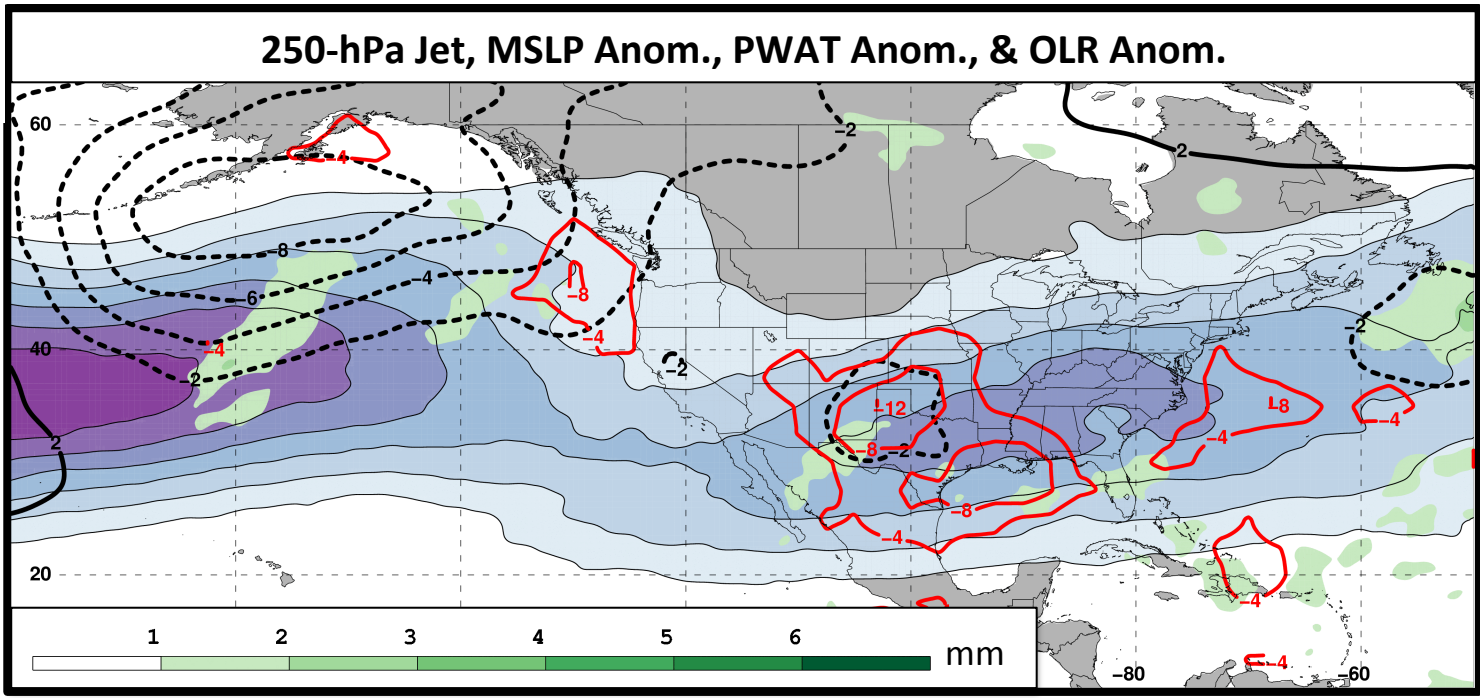
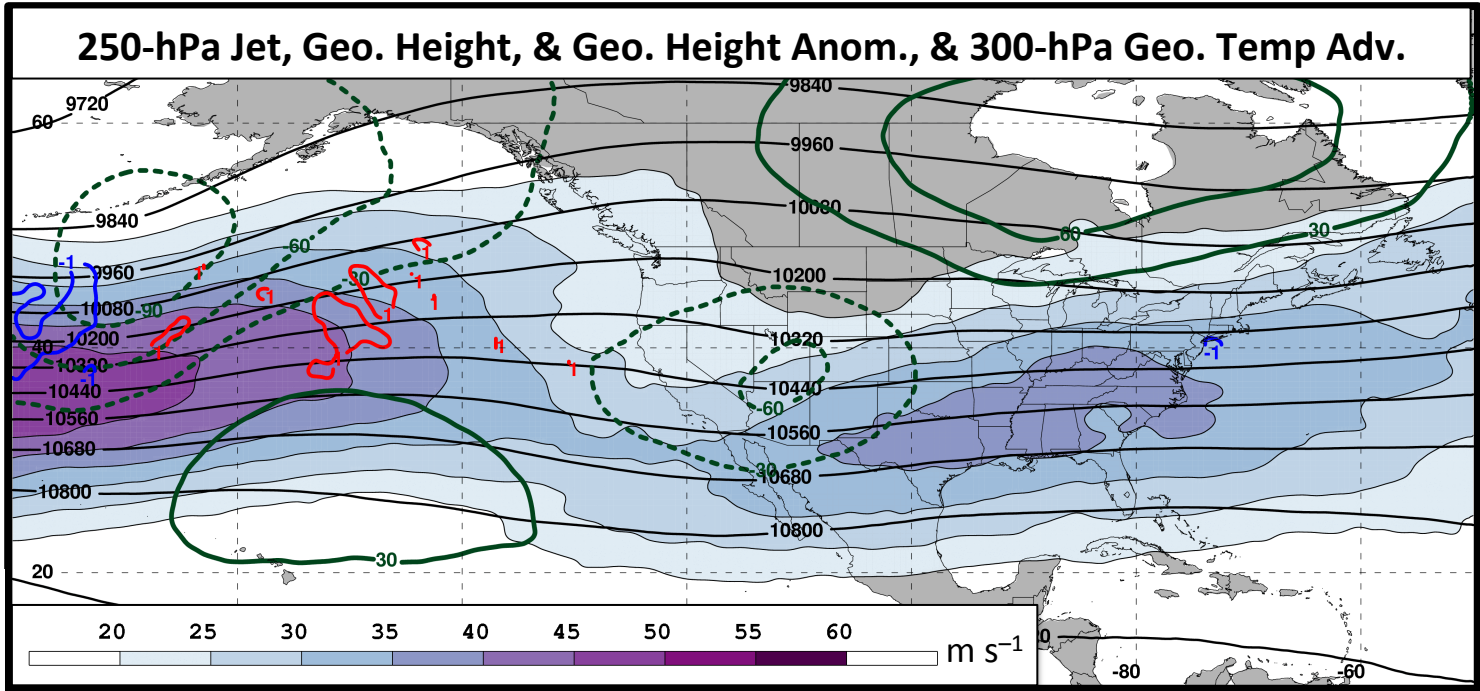
North Atlantic Oscillation: 5 Days After Jet Superposition



Polar Dominant Jet Superposition Events

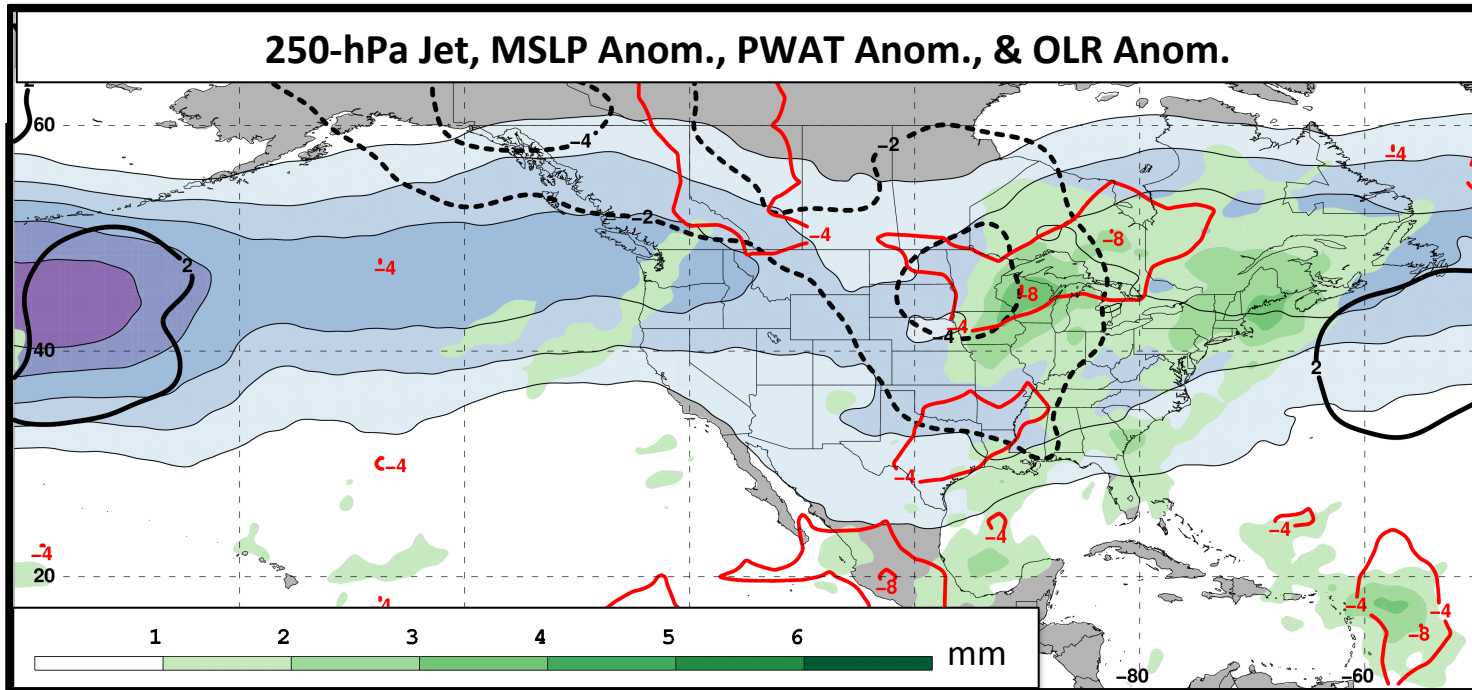
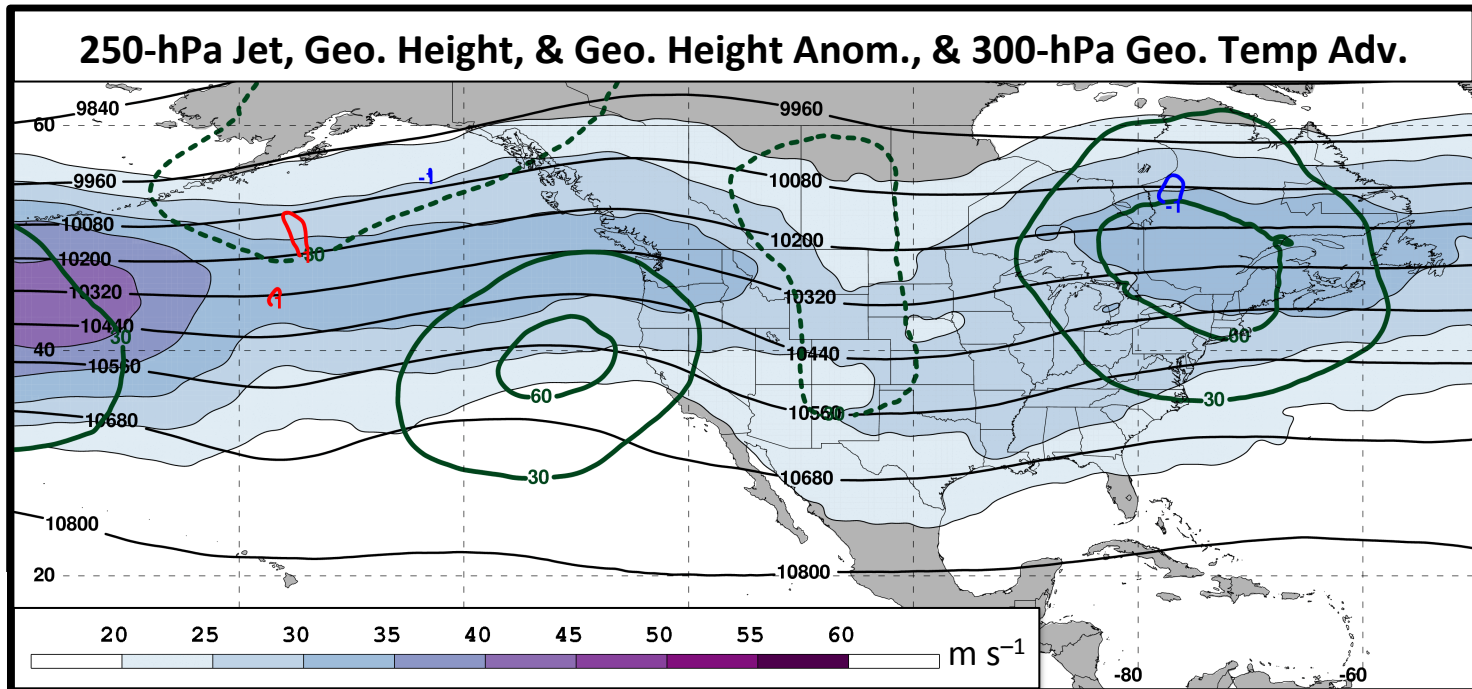
3 Days
Prior to Jet
Superposition

N=80



E. Subtropical Dominant Jet Superposition Events

3 Days
Prior to Jet
Superposition

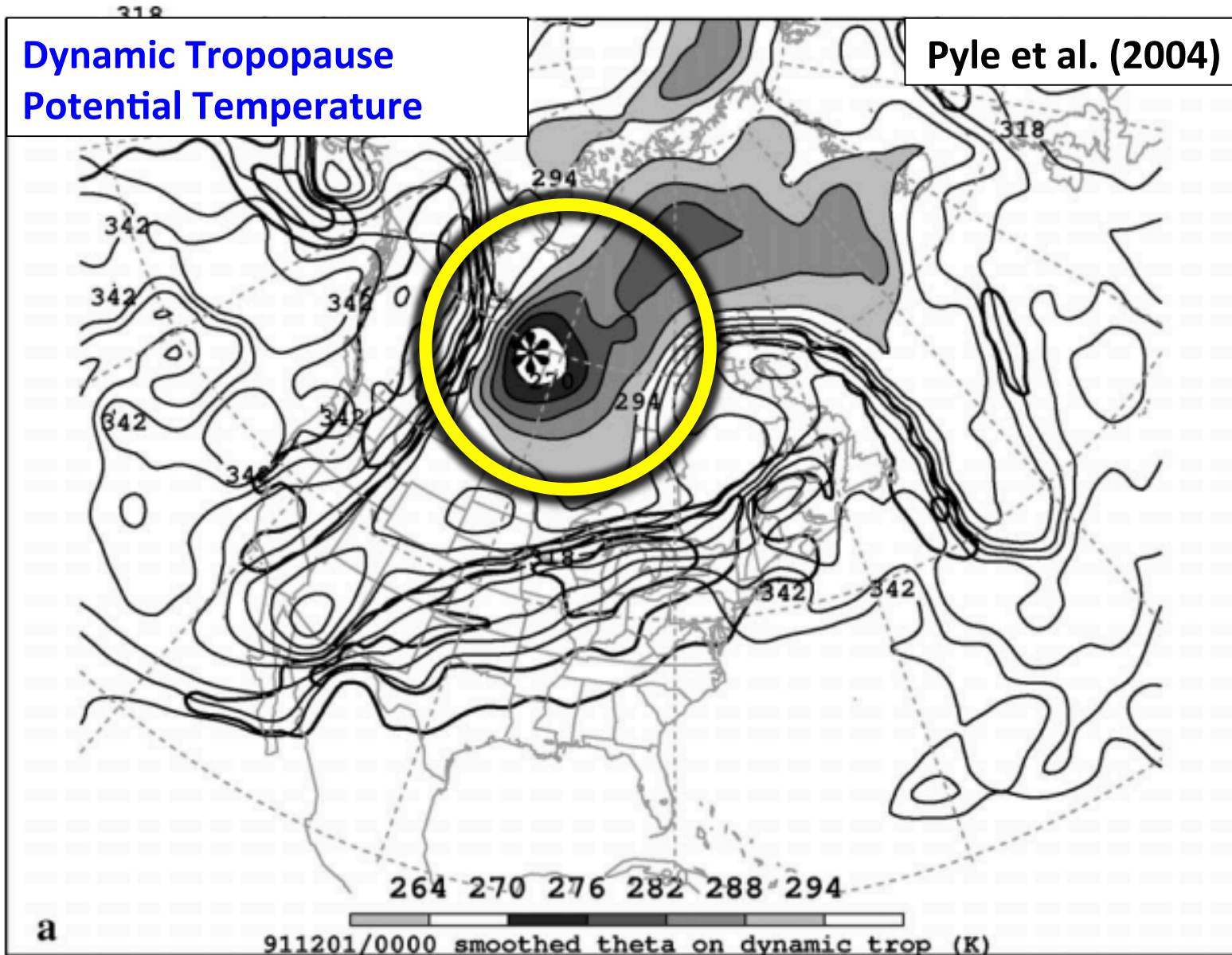


N=76

Jet Superposition Conceptual Model

Dynamic Tropopause
Potential Temperature

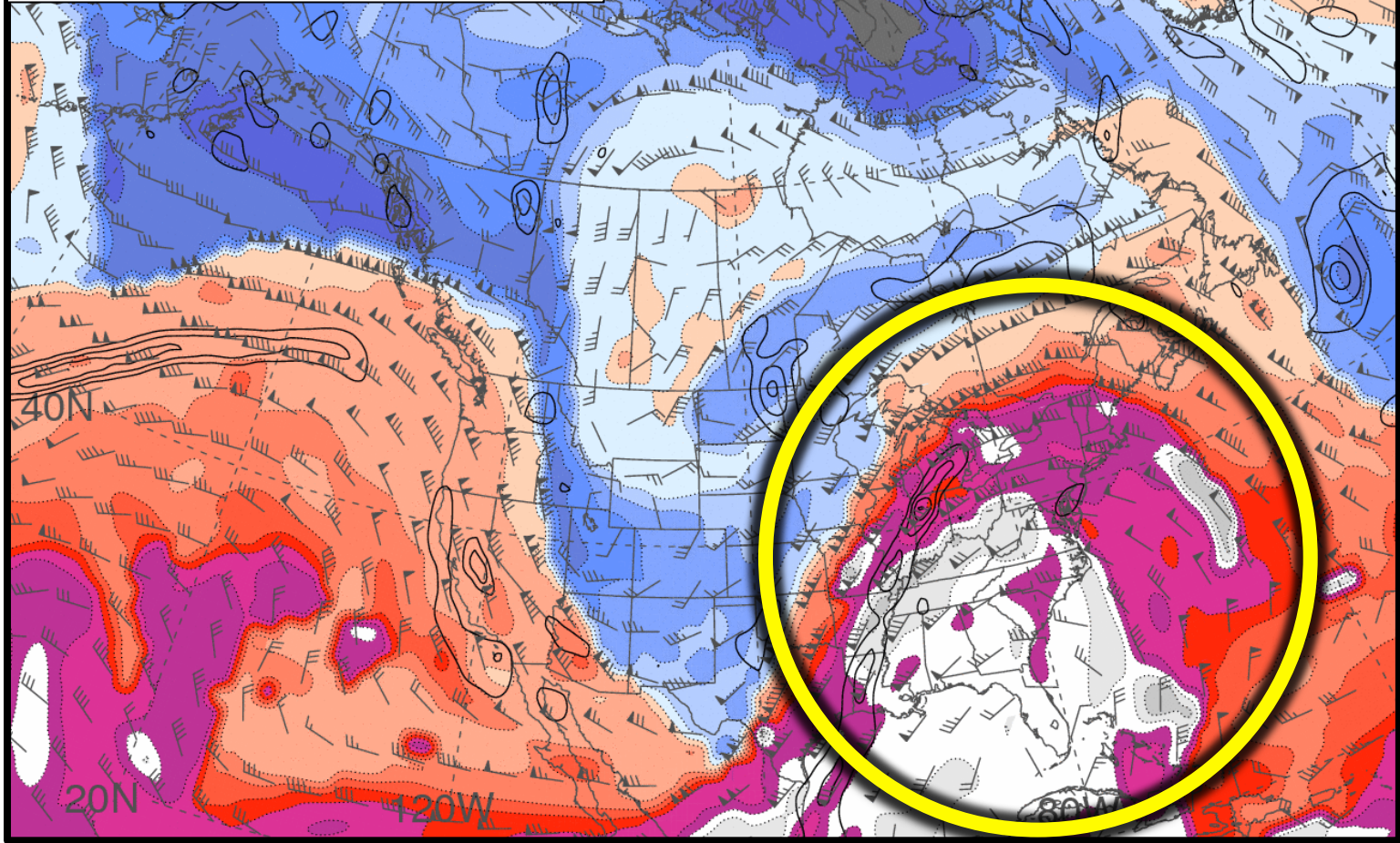
Pyle et al. (2004)



Jet Superposition Conceptual Model

Dynamic Tropopause
Potential Temperature

Heather Archambault



264 270 276 282 288 294 306 312 318 324 330 336 342 348 354 360 366 372 378

DT THTA & WND; LL REL VORT 100502/1200

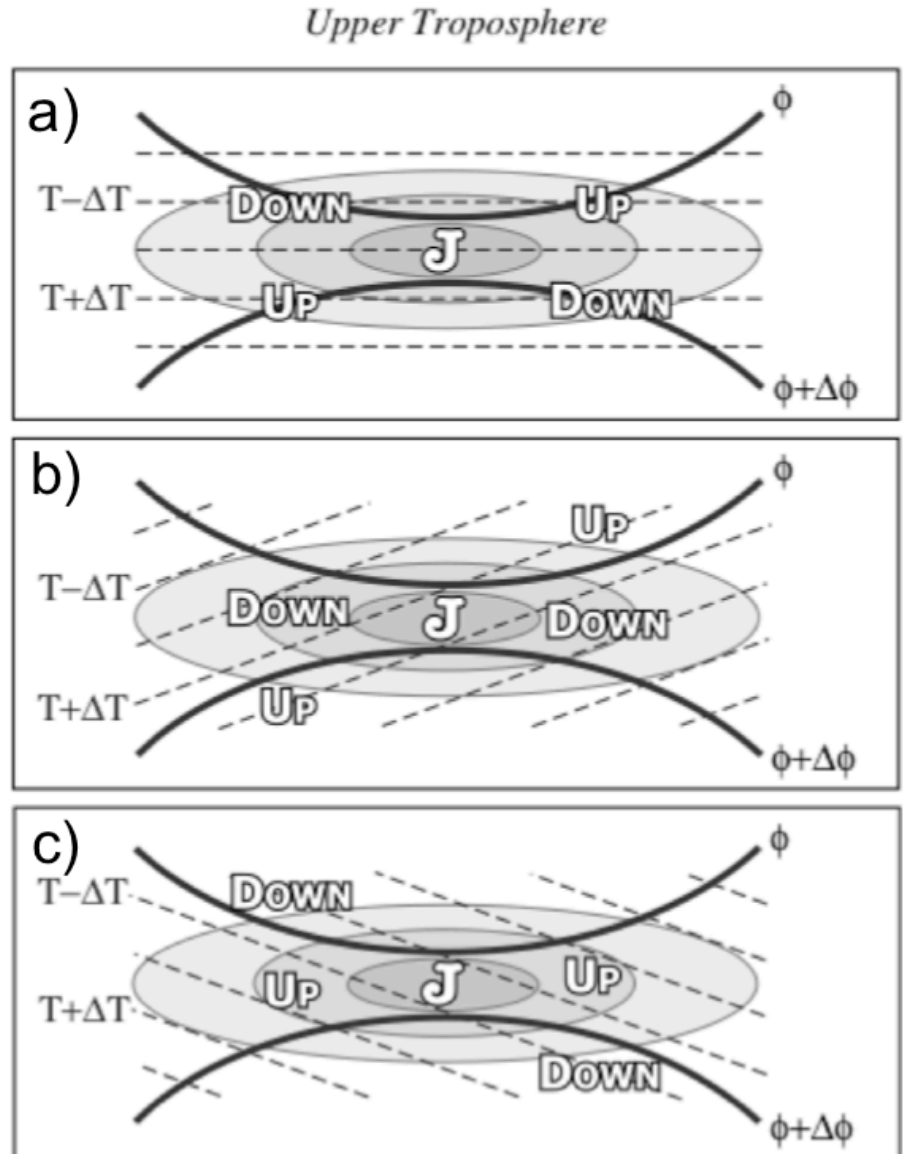
Ageostrophic Transverse Jet Circulations

Traditional four-quadrant model

Geo. cold-air advection (CAA)
along the jet axis promotes
subsidence through the jet core

Geo. warm-air advection (WAA)
along the jet axis promotes
ascent through the jet core

Lang and Martin (2012)

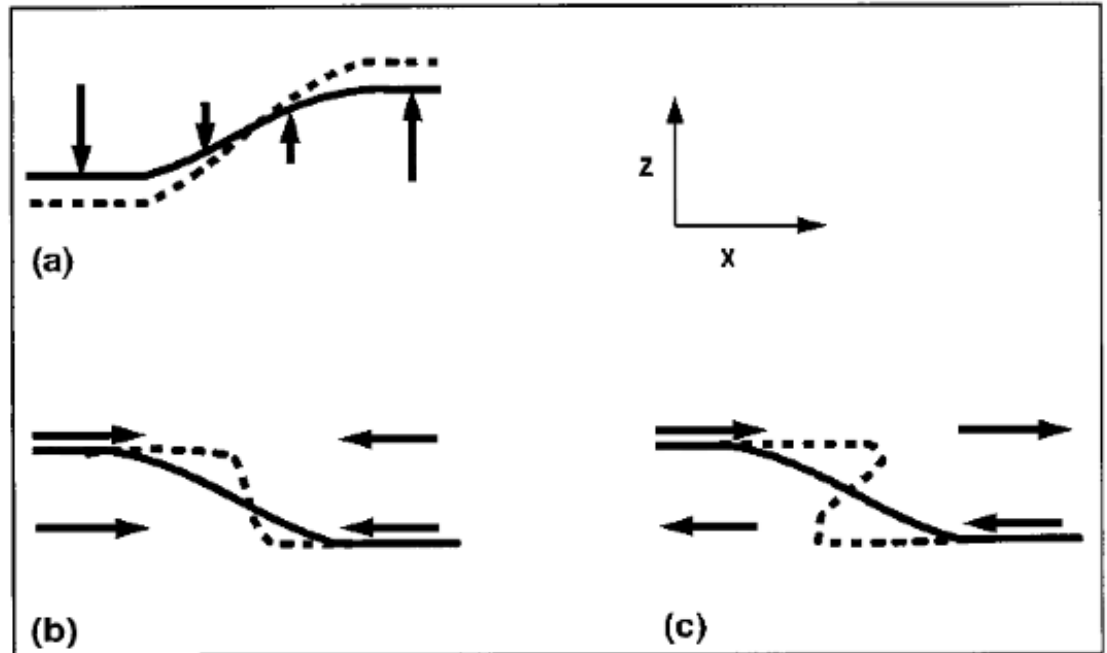


Background

Insight into how the tropopause can be restructured from a PV perspective can be found by consulting Wandishin et al. (2000)

Two processes can account for “foldogenesis”:

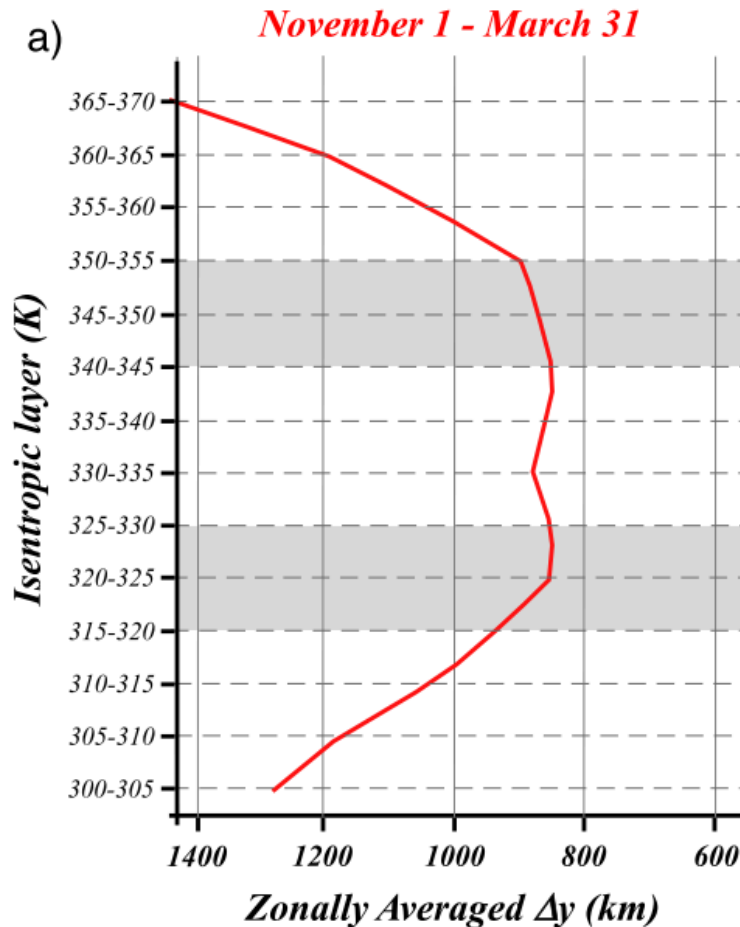
- 1) **Differential vertical motions** can vertically steepen the tropopause.
- 2) **Convergence or a vertical shear** can produce a differential horizontal advection of the tropopause surface.



Wandishin et al. 2000

These same mechanisms are also likely to play an important role in superpositions.

Background



Christenson et al. (2017)

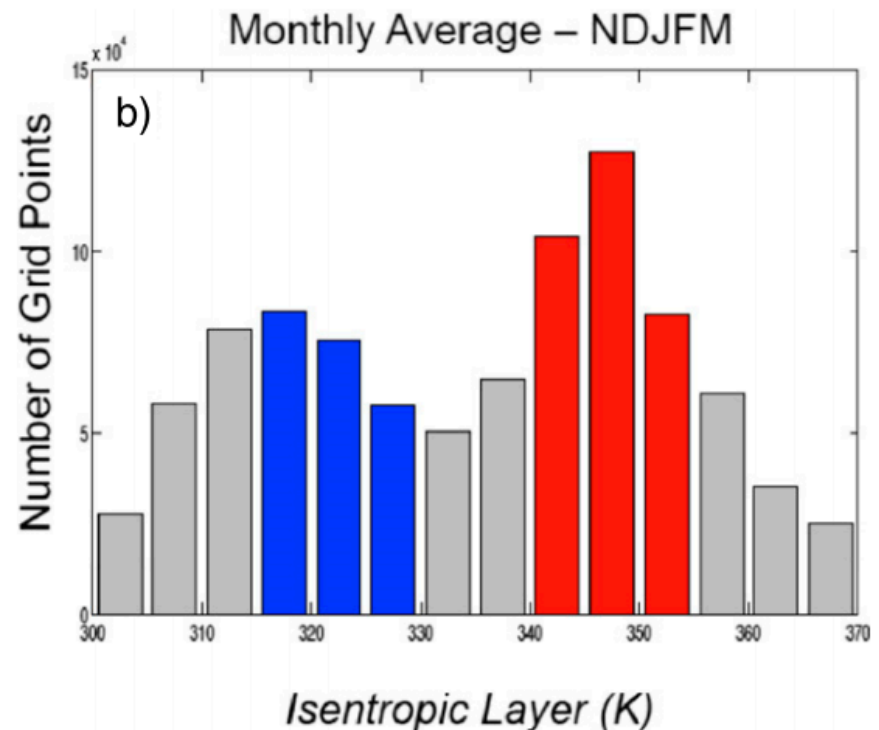


FIG. 2. (a) Cold season average of zonally averaged Δy (km) for 5-K isentropic layers ranging from 300–305 to 365–370 K. The 315–330- and 340–355-K layers are highlighted in light gray shading. (b) The average frequency of occurrence of grid points with a maximum wind speed value within the 5-K isentropic layers along the abscissa per cold season. The 315–330- and 340–355-K layers are shaded in blue and red, respectively.